Transboundary Transport of Atmospheric Aerosols and POPs from Ukraine, Adsorption Thermodynamics and Reaction Kinetics of VOCs on the Surface of the Aerosol' Components

Vladimir Bogillo

Department of Antarctic Geology and Geoecology

Institute of Geological Sciences

National Academy of Sciences of Ukraine,Kiev

e-mail: vbog@carrier.kiev.ua

Transboundary transport of aerosols from Ukraine after Chernobyl' incident (^{137}Cs)

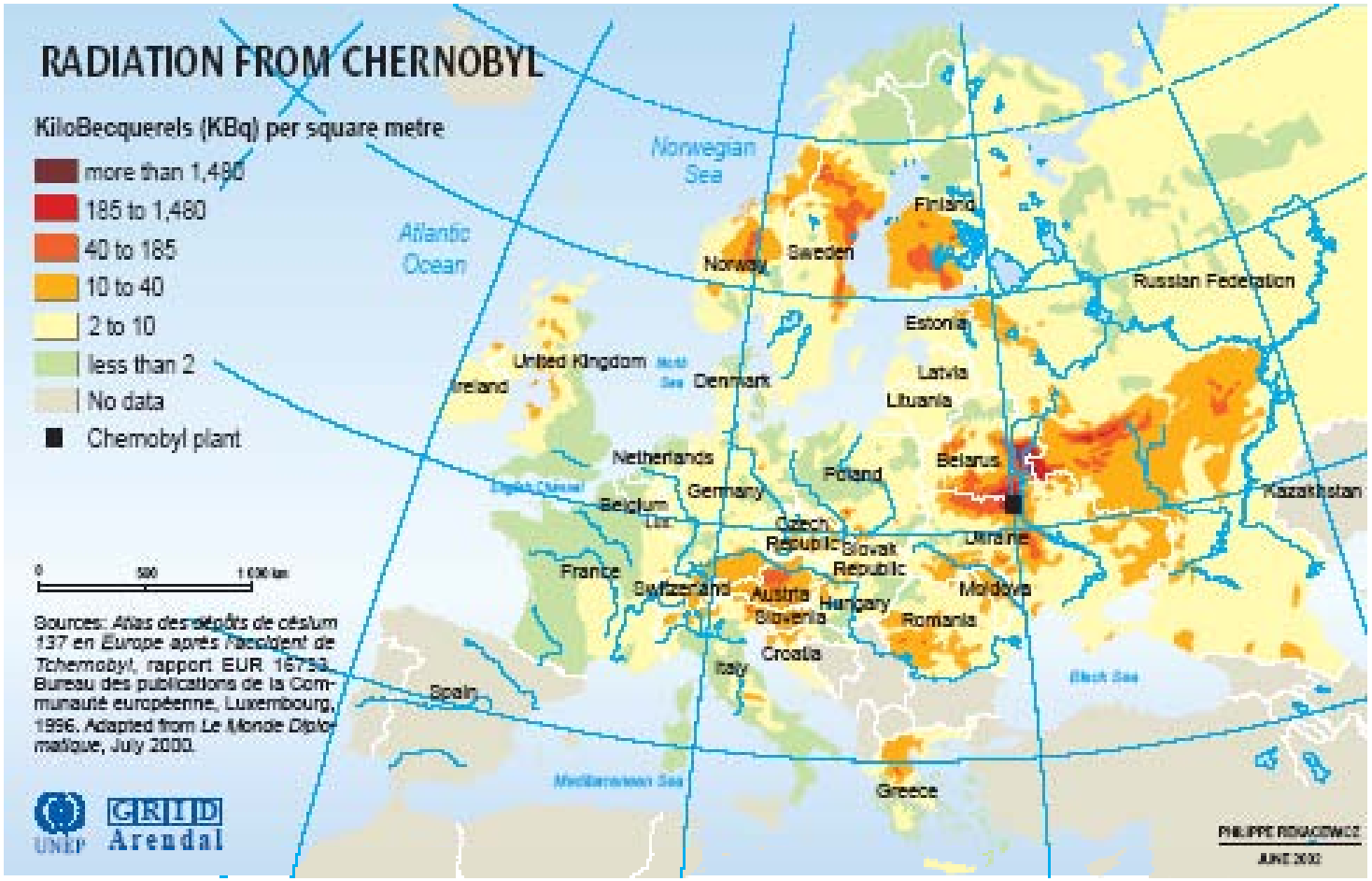

Content of first part

- **Transport of dust to Central Europe**
  (W. Birmili et al., Atmos. Chem. Phys., 8, 997–1016, 2008; Hladil, J., Bulletin of Geosciences 83(2), 175–206, 2008)
- **Transport of fine particles to Southern Finland**
  (J. V. Niemi et al., Atmos. Chem. Phys., 6, 5049–5066, 2006)
- **Transport of combustion aerosols to Crete Island**
  (J. Sciare et al, Atmos. Chem. Phys. Discuss., 8, 6949–6982, 2008)
- **Transport of industrial aerosols to Israel**
  (Y. Erel et al, Environ. Sci. Technol.41, 5198-5203, 2007)
- **Transport of PM_{10} to Istanbul**
  (T. Kindap et al, Atmos. Environ. 40, 3536–3547, 2006)
- **Transboundary transport of POPs in Europe**
  (EMEP Status Report 2/2007)
- **Influence of aerosols and air temperature on transboundary transport of POPs**

Hydromet's network of air-quality monitoring stations in Ukraine

Air pollutions in Ukraine

- **Ukraine has declared *air pollution* a priority area for international cooperation**
- **Since the early 1990s, the long-term trend in air pollution in Ukraine has been positive. During 1995–2002, air emissions from stationary sources decreased by a factor of 1.4**
- **An inventory in 2002–2003 of the POPs stored on Ukrainian territory revealed that 19,341 t of obsolete pesticides were stored at 4,983 storage sites and of these sites, only 499 are well maintained, 2,871 have satisfactory storage conditions, and the rest are not maintained properly**
- **In 2004, air emissions from leading industrial sectors were distributed as follows: 62% from manufacturing, 37% from mining and quarrying and 1% from construction materials**
- **In 2005, air emission from industrial sources runs up to 4449300 t (96.5% from heavy industry and 3.5% from transport)**
- **Emissions from mining of metals, minerals and energy-producing materials totaled 991400 t in 2004**
- **Donetsk oblast alone accounts for about 40% of total air emissions in Ukraine, followed by Dnipropetrovsk (21%) and Zaporizhzhia (6%) oblasts. The city of Mariupol, in the Donetsk oblast, has accounted for about 5% of total emissions in Ukraine**
- **The cities with the highest air pollution are located in the Donetsko-Prydniprivskyy industrial area**

Emissions of SO_2, NO_x and dust from power plants and electricity production

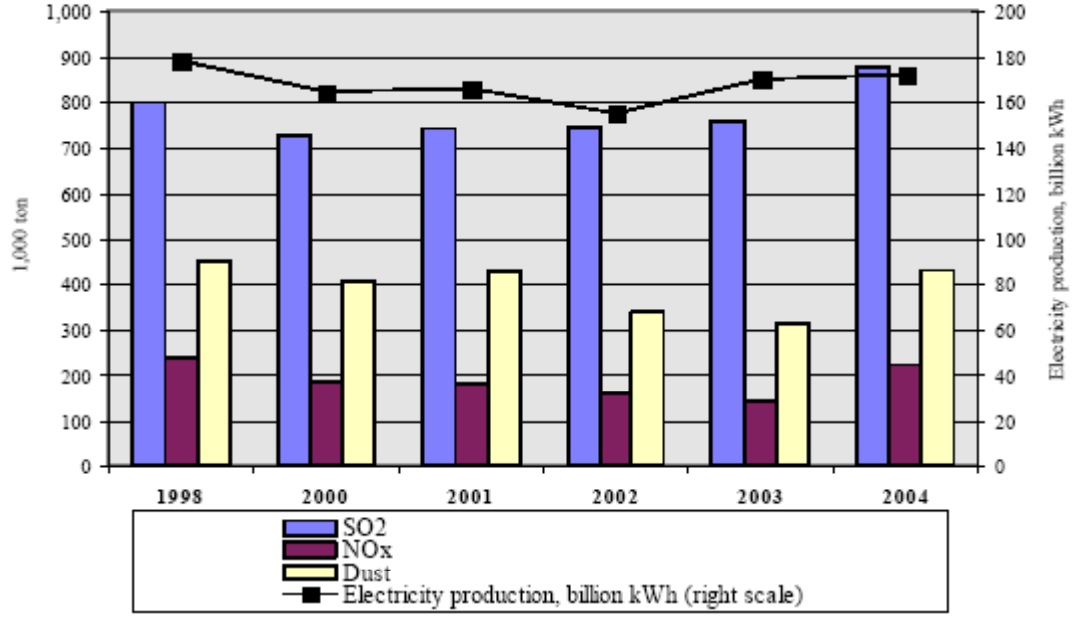

Industrial air emissions of main pollutants, 2000–2003

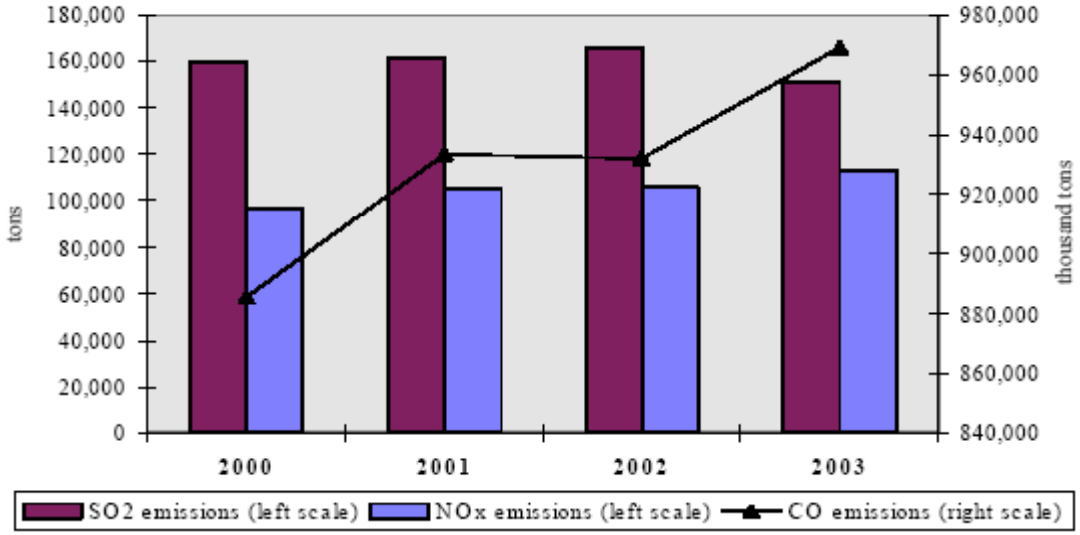

Soils degradation and contamination in Ukraine

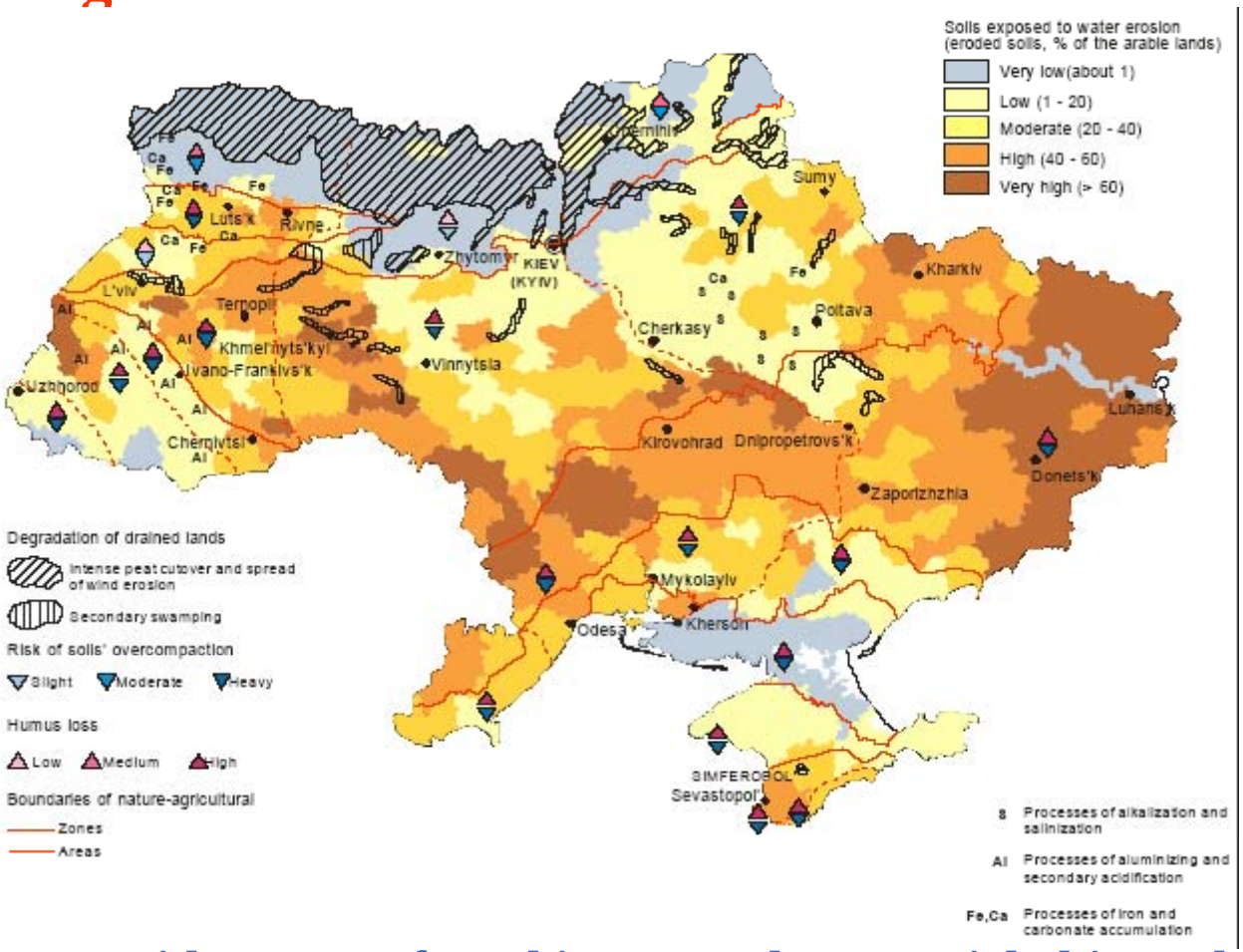

Still, in 2004, DDT residues were found in Donetsk, Zaporizhzhia and Kherson oblasts. A still unsolved problem is the contamination risk from more than 19,000 tons of often improperly stored obsolete pesticides.

A total of 5 million hectares are contaminated.

43 military sites are registered as potentially contaminated by toxic waste.

Hotspot fire maps (FIRMS data) for the year 2004

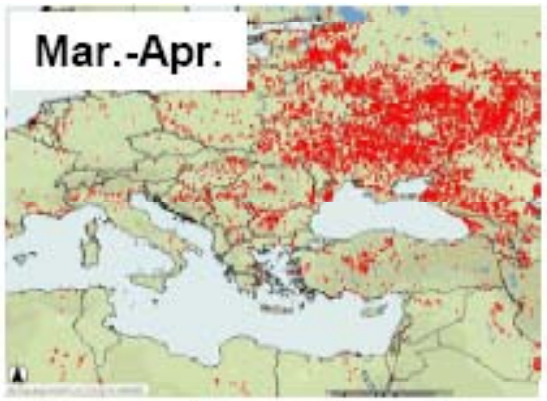

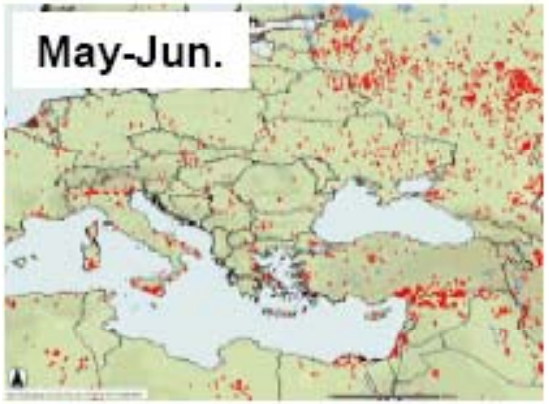

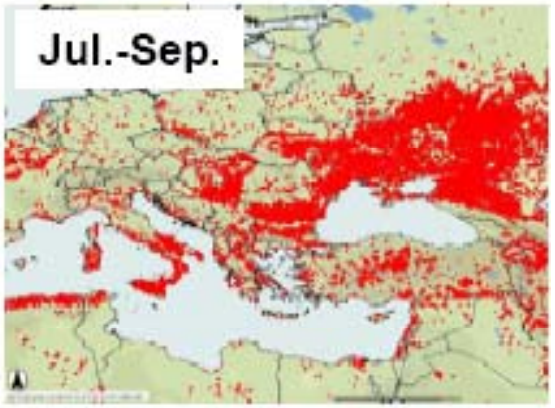

Main sources of aerosols in Ukraine

- **Wind-blown dust particles emitted from eroded dry soil surfaces of farm lands (423000 km^2)**
- **Combustion particles from biomass burning on the farm lands and forest fires**
- **Mixed particulates (mineral, carbonaceous, sulphate and organic, enriched by heavy metals (Pb, Cd, Hg, Zn, Fe, Sn, Cr, Mn, Cu) from various industrial sources (mining, quarrying, power plants, coke, metallurgy, chemical, petrochemical, construction materials, asphalt, woodworking industry, arms production and transport**
- **Sea-salt particles emitted from Black, Azov Seas and from numerous saline lakes in Southern Ukraine**
- **Biogenic and secondary particles from Carpathian, Polessya, Crimea**

Transport of dust to Central Europe

- **Wind-blown dust particles emitted from dry soil surfaces contribute considerably to the global aerosol mass and optical thickness, as well as to particle concentrations near the surface**
- **Current estimates of annual global emission of dust particles that are available for long-range transport vary between 1000 and 2000 Tg (Zender et al., 2004)**
- **Frequent transport of dust plumes from the Sahara, the largest dust source worldwide, towards Europe can be observed frequently within the free troposphere**
- **Other sources of mineral dust aerosol include the Arabian Peninsula, the Gobi and Taklamakan deserts in Asia, and the Australian and South American deserts**

- **Human activities can modify dust emissions from soils by changing the availability of fine particles, e.g., through destruction of soil crusts and removal of vegetation in semi-arid regions. The total amount of soil dust emission from such anthropogenic influence are currently estimated to contribute up to 20% of the total dust emissions (Solomon et al., 2007)**
- **The total area of the Ukraine is 603 700 km^2, 70% of which are used as farm lands. The Southern Ukraine has been characterized as a "steppe" zone. The human impact has almost completely removed the former native forests and steppe lands, and created large-scale agricultural units. In the wide "loess" plains the very fertile black earth (Chernozem) has formed, which belongs to the most fertile soils worldwide. Due to the intensive agricultural development, the soil has become prone to wind erosion and in fact, wind has been found to have eroded Ukrainian soils over an area of 220 000 km^2**

- **A comparison of the climate of the past (ca. 100 years ago) with the climate of today shows that the territory of the Ukraine has become arid due to human activities. Consequently, wind erosion has become wide-spread even in areas formerly unaffected by wind erosion**
- **Meteorological statistics over the past 40 years indicated the frequency of dust storms was found to be 3–5 per year in the steppe zone, with an average duration of 8–17 h**
- **Dust storms in the Ukraine are typically associated with wind speeds of 20 m s^{-1} and more with Chernozemic soils being the most susceptible to wind erosion**
- **During dust storms, these soils can lose 70 t of soil per ha and hour**
- **Dust transport from the Ukraine into Central Europe is an unusual feature, and has not been documented in the literature**

Uncovered, active fields of eolian sand dunes with grass and limited shrub vegetation; surroundings of Velyki Kopani village, Kherson region

Macroscopic appearance of the sediment (24 April, 2007)

A -Nízké Tatry Mts (Slovak R.), B - Krkonoše Mts. (Czech R.), C - Krušné hory Mts. (Czech R.), D - Town of Púchov (Slovak R.), E -Town of Brno, F - Town of Blansko

Dust source activation on 23 March 11:00 UTC over the Southern Ukraine (SEVERI on board the MSG satellite)

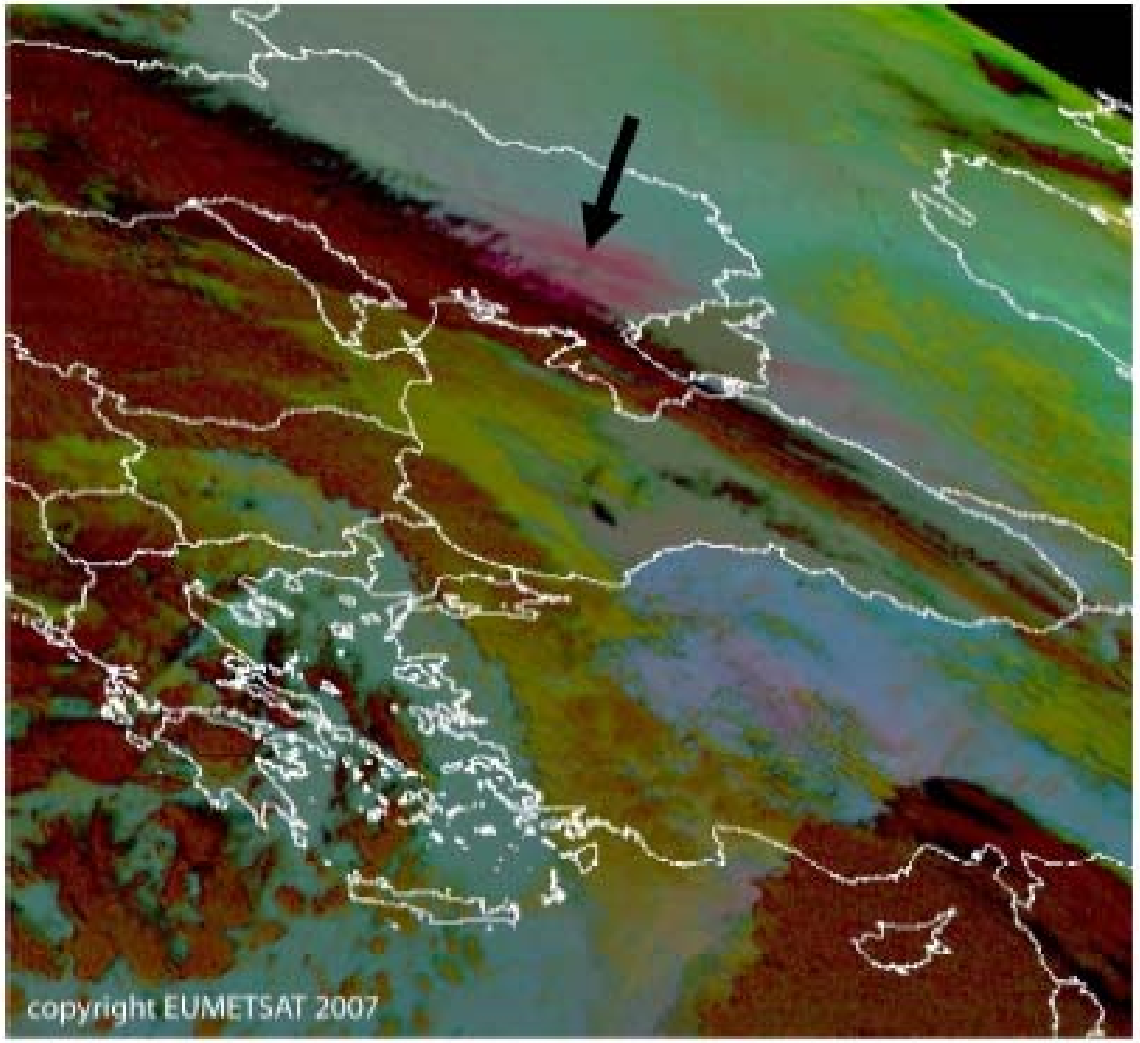

The MODIS-Aqua composite image of Southern Ukraine

on 23 March 2007, 10:50 UTC

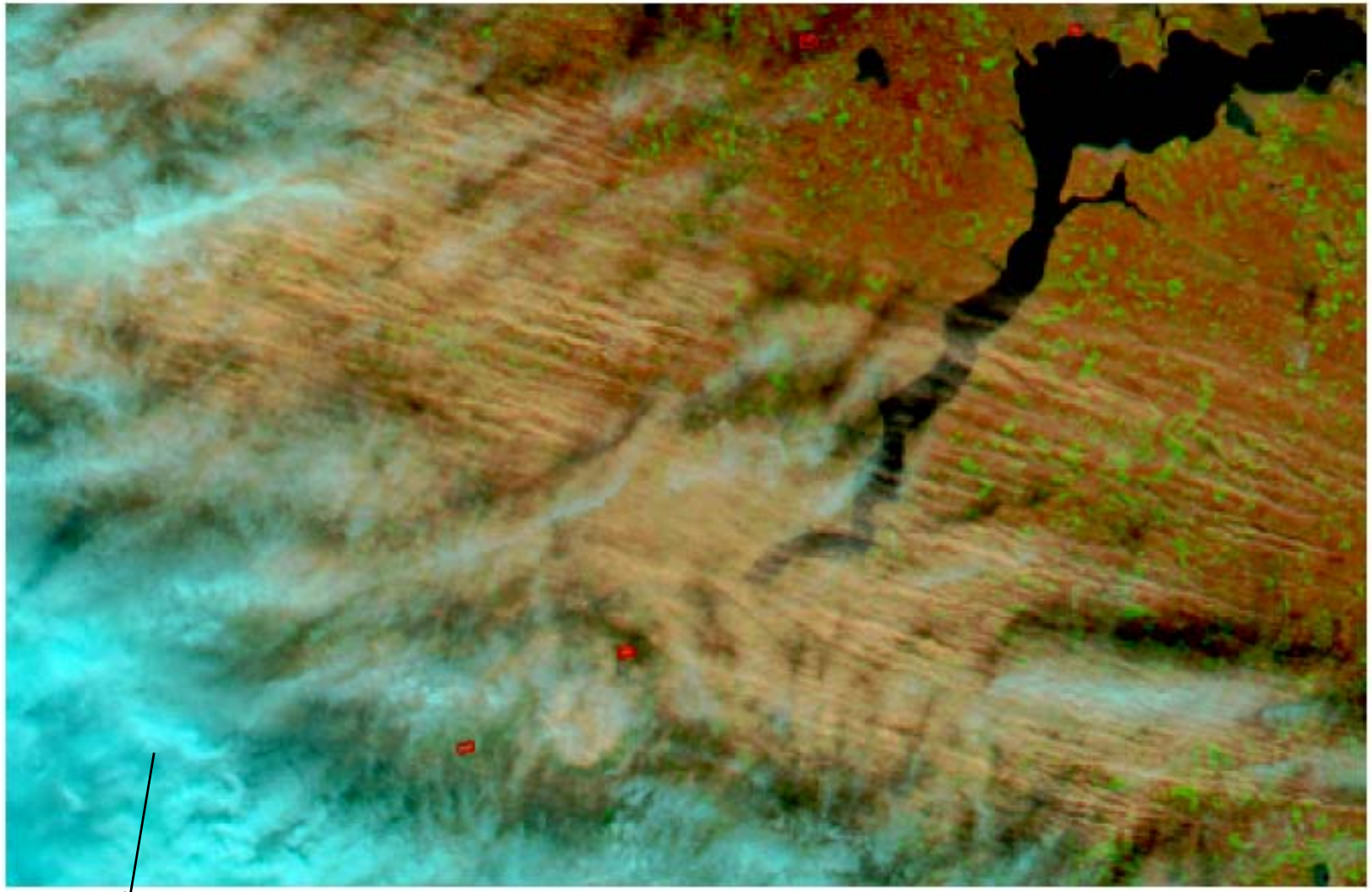

- **On 23 March, meteorological observations in the southern and eastern area around the Kahkova Reservoir report average wind speeds up to 15 m s^{-1} and wind gusts up to 25 m s^{-1} and confirm "observations of atmospheric dust"**
- **It is likely that these unusually high surface wind speeds in combination with a preceding drought period of two weeks as well as the lack of vegetation in March led to the high dust emission rates**
- **On 23 and 24 March 2007 the synoptic situation over Europe was governed by a high-low dipole pattern due to a low pressure area over the Mediterranean Sea and a high pressure region built up by a permanent anticyclone located over Fennoscandinavia and an anticyclone located over South Russia**
- **The eastward moving Mediterranean depression on the one side and the persistent high pressure area on the other side forced an increasing pressure gradient over the Black Sea and Southern Ukraine, generating a low-level jet into Central Europe**
- **The low-level jet effected the transport of a dry and subsiding air from the Black Sea area to Central Europe along a narrow corridor and reaches Germany on 24 March**

Geographic map with three particle trajectories originating at the same site (48°N, 33°E) from different heights

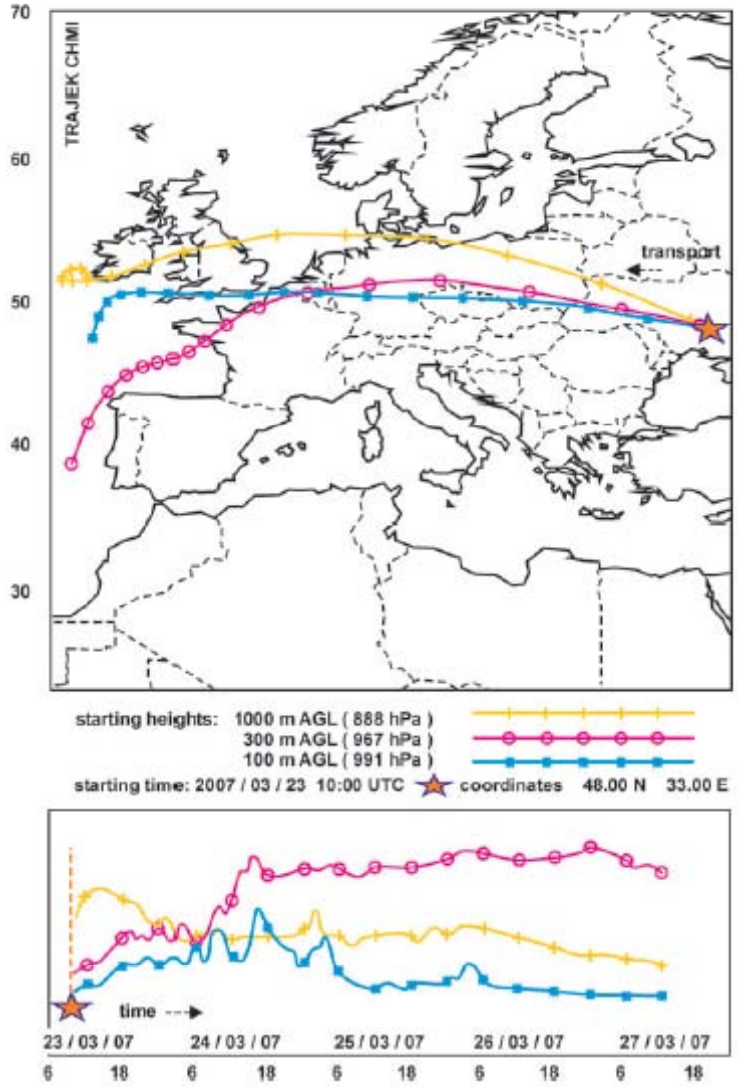

Charts of sealevel pressure (hPa) and horizontal surface wind speeds in Beaufort (colour code) on 23 and 24 March 2007, 12:00 UTC respectively

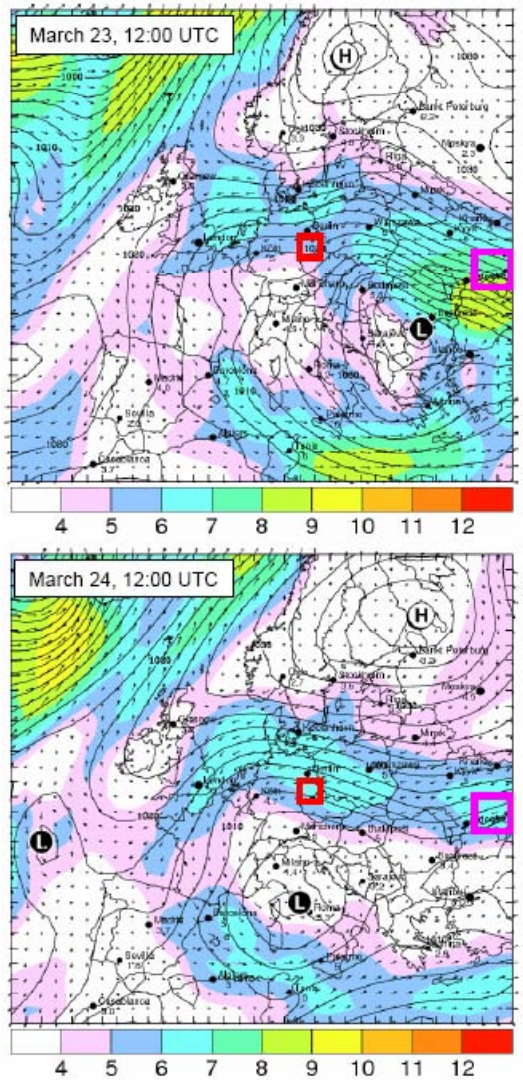

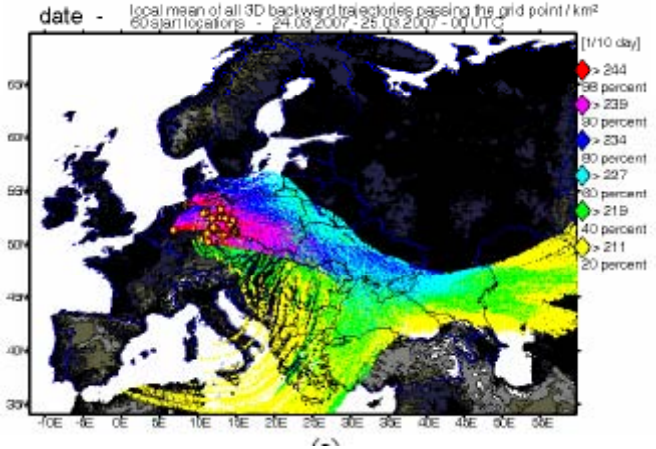

Superposition of back trajectories originating on 24 March 2007 at 20 receptor sites in Germany

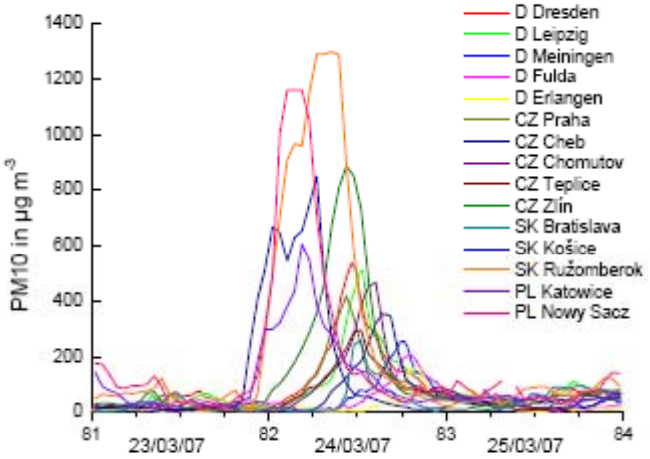

Time series of PM_{10} mass concentrations at a number of selected air quality monitoring stations in Slovakia, the Czech Republic, Poland, and Germany

Dust concentration and its altitude variation

- **Hourly PM_{10} mass concentrations reached 1400 µg m^{-3} in Slovakia and 1200 µg m^{-3} in Poland. The maximum hourly value in Germany was 640 µgm−3, where rural PM_{10} levels are typically around 20 µg m^{-3}. As a result of the dust event the legal daily limit value of PM_{10} (EU First Air Quality Daughter Directive (1999/30/EC)) was exceeded over an area spanning several EU member states**

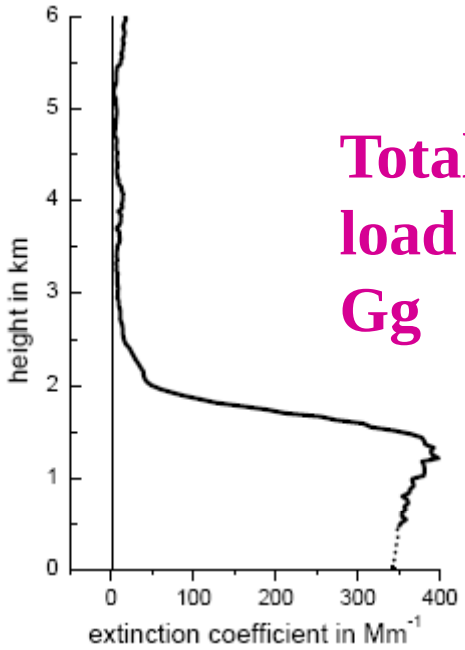

Total dust load is about 3 Tg and the load based on PM_{10} – related mass is 60 Gg

Vertical profile of the volume extinction coefficient of the aerosol as retrieved from Lidar observations at 0.532 µm wavelength at Leipzig, on 24 March 2007, 12:33–13:44 UTC

Mineralogical and Chemical Composition of the dust

- **Besides the preferentially entrained and delivered quartz, the sediment contains also perthitic feldspar, chlorite and chloritoids, and notably low amounts of mica, clay minerals and carbonate**

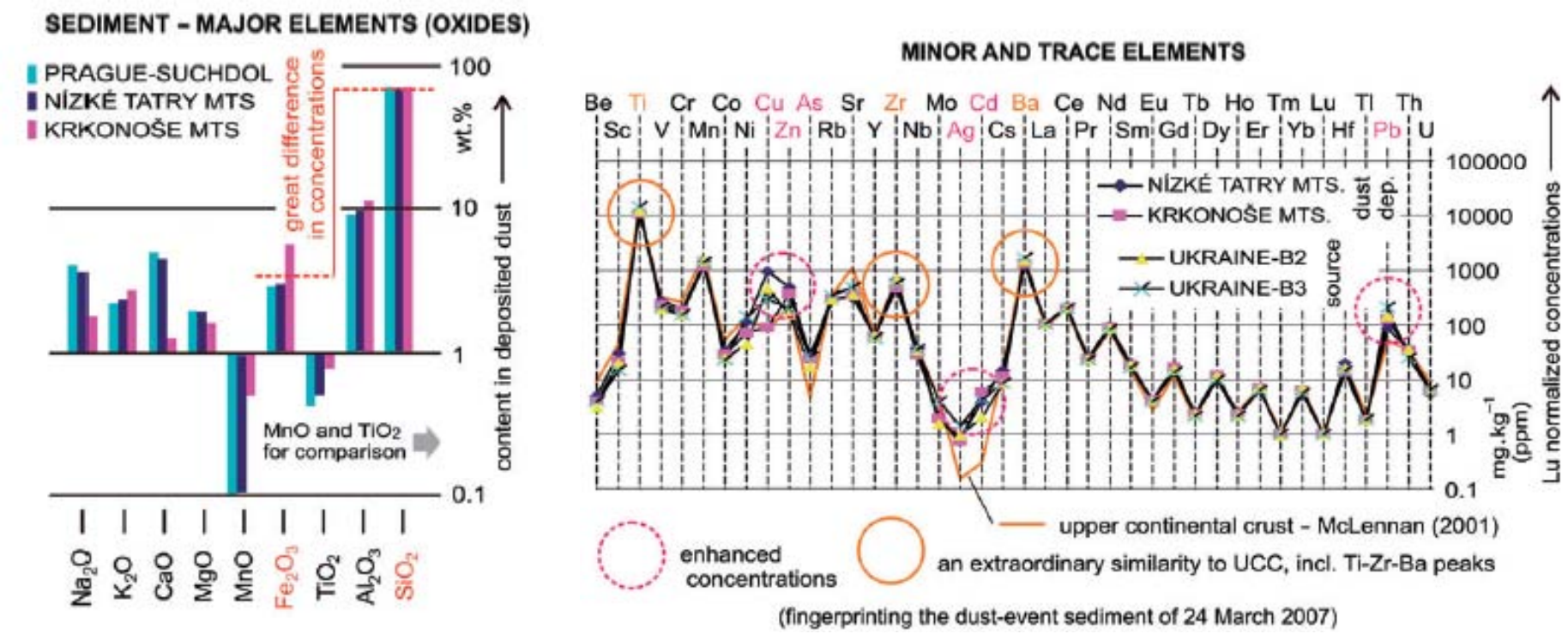

A plot of lead isotope ratios. Based on published data, an attempt was made to separate the North African–Middle East trendline from the Central–East European signatures

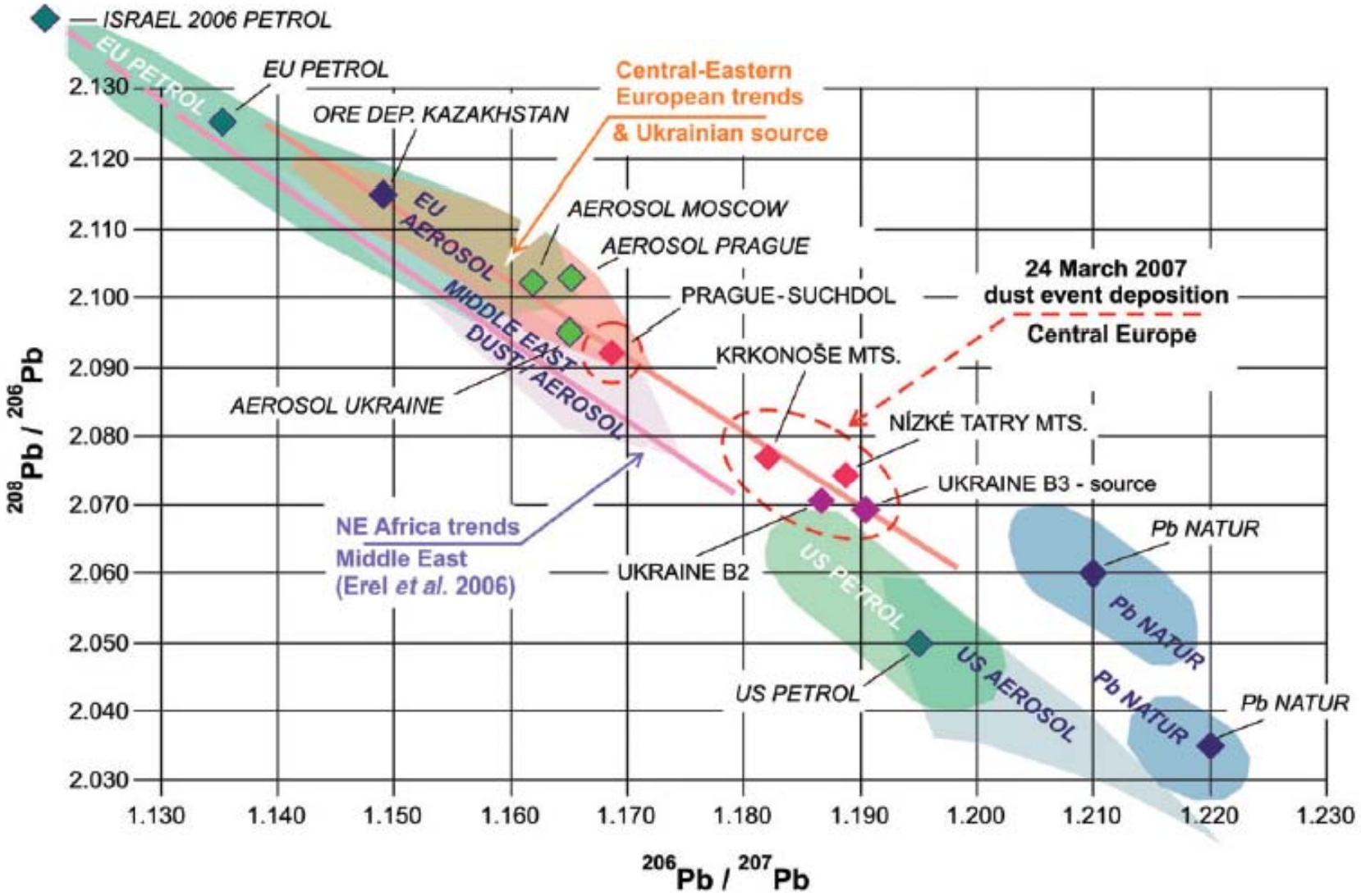

- **The study revealed that the deposited sediment is characterized by polydisperse and multimodal particle-size distributions and consists predominantly of angular to subrounded quartz particles of silt size. Only a few percent of coarser and finer material are contained**
- **Among the major element characteristics, the Na_2O/K_2O, CaO/MgO and MgO/Fe_2O_3 ratios are very close to those obtained for the upper continental crust**
- **In minor and trace elements, the Hf/Sc, Zr/Hf, Th/U ratios are only slightly higher than those of the most common UCC or sedimentary materials**
- **The Pb isotope signatures correspond to a considerably lithogenic characteristic; only the Prague sample shows a certain overprint probably influenced by EU-type petrol combustion**
- **The element content does not contradict the supposed source based on meteorological observations, *i.e.*, from surface argillaceous and sandy soils east of Kherson, Ukraine**

Transport of fine particles to Southern Finland

- The composition and mass concentrations of fine aerosol particles ($PM_{2.5}$) in clean background areas are strongly affected by long-range transport
- During transport and aging, particles of different origin may change their properties due to coagulation and cloud processes as well as due to reactions with gases via various heterogeneous pathways
- Differences in sources and in meteorological conditions may strongly affect composition, mixing state, concentration and size of different particle types observed
- The clean background areas in Finland are especially favorable for investigation of the properties of aged, long-range transported aerosols with clearly different origin
- The aerosol samples were collected at a rural background site in Southern Finland in May 2004 during pollution episode (PM_1 ~ 16 µg m^{-3}, backward air mass trajectories from south-east), intermediate period (PM_1 ~ 5 µg m^{-3}, backtrajectories from north-east) and clean period (PM_1 ~ 2 µg m^{-3}, backtrajectories from northwest/north)

Backward air mass trajectories arriving at 250 m level to Hyytiala during the six sampling periods in May 2004

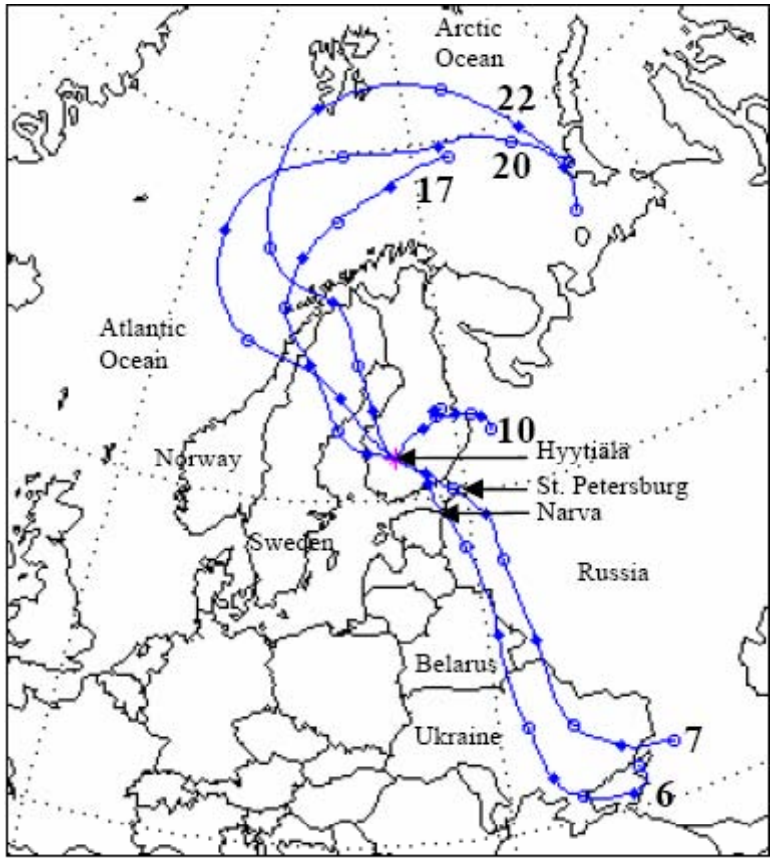

TEM images of different particle types from PM0.2−1 sample 7 collected during the pollution episode; (a) tar ball, (b) soot and (c) Si-rich fly ash mixed with (ammonium)sulphates containing material. The rest of the particles were classified as "(ammonium) sulphates and their mixtures with C, K, soot

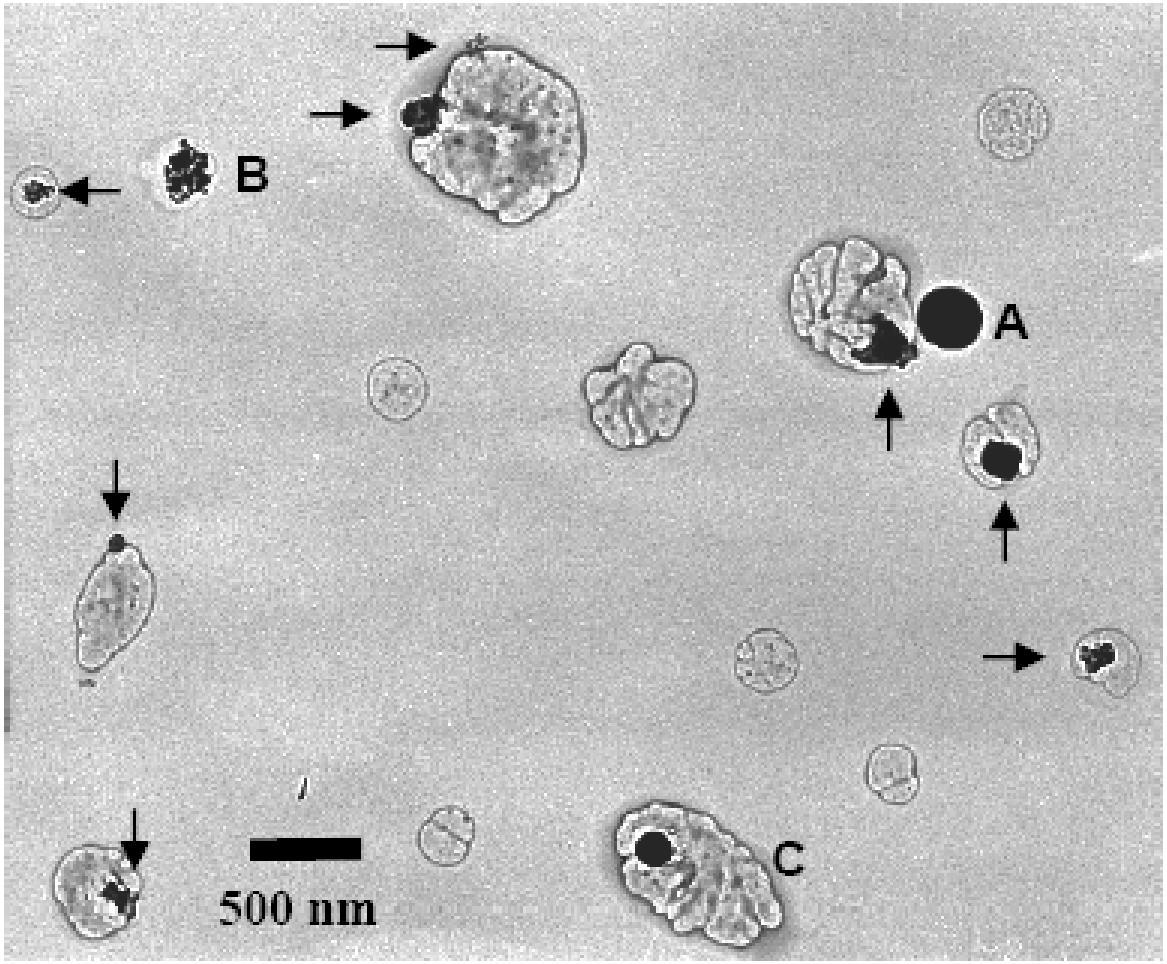

Particle group	Elemental characteristics
Tar balls	Abundant C with minor S, often minor K
Soot	Abundant C, often minor S, K and/or Si
(Ammonium)sulphates and their mixtures with C, K and/or different inclusions	S with variable amounts of C and/or (usually minor) K
Silicates	Abundant Si, usually with Al, variable minor Fe, Ca, K, Mg, Na, Ti,and/or S
Metal oxides/hydroxides	Abundant Mn, Fe, Zn and/or Pb
Ca/Mg carbonates, sulphates and/or nitrates	Abundant Ca with C and/or S, sometimes with abundant Mg and/or minor Si
Sea salts	Abundant Na, variable Cl and S, minor Mg, K and Ca
Porous Na-rich particles	Abundant Na with S and K, noMg and Ca
Biological particles	Abundant C, usually minor K and/or P
C-rich fragments	Abundant C

- **The major particle types in $PM_{0.2–1}$ samples were soot and (ammonium)sulphates and their mixtures with variable amounts of C, K, soot and/or other inclusions. Number proportions of those two particle groups in $PM_{0.2–1}$ samples were 0 – 12% and 83 – 97%, respectively**
- **During the pollution episode, the proportion of Ca-rich particles was very high (26 – 48%) in the $PM_{1–3.3}$ and $PM_{3.3–11}$ samples, while the $PM_{0.2–1}$ and $PM_{1–3.3}$ samples contained elevated proportions of silicates (22 – 33%), metal oxides/hydroxides (1 – 9%) and tar balls (1 – 4%). These aerosols originated mainly from polluted areas of Eastern Europe, and some open biomass burning smoke was also brought by long-range transport**
- **During the clean period, when air masses arrived from the Arctic Ocean, $PM_{1–3.3}$ samples contained mainly sea salt particles (67 – 89%) with a variable rate of Cl^- substitution (mainly by NO_3^-)**
- **During the intermediate period, the $PM_{1–3.3}$ sample contained porous (sponge-like) Na-rich particles (35%) with abundant S, K and O. They might originate from the burning of wood pulp wastes of paper industry. The proportion of biological particles and C-rich fragments (probably also biological origin) were highest in the $PM_{3.3–11}$ samples (0 – 81% and 0 – 22%, respectively)**

Transport of combustion aerosols to Crete Island

- **Long-term (5-yr) measurements of carbonaceous (BC, OC) aerosols were reported in the Mediterranean Basin (Crete Island)**
- **Their seasonal trends demonstrate two peaks (early spring and summer) corresponding to long-range transported biomass burning aerosols originating from apart to agriculture (post-harvest wheat residual) waste burning in the countries surrounding the Black Sea (i.e. at 1000–2000km upwind of Crete)**
- **The contribution of biomass burning to the concentrations of BC and OC have been shown to be rather small on a yearly basis (20 and 14%, respectively) but could be significant for some months (34 and 32% of BC and OC, respectively, for the month of August) and are expected to present a strong seasonal/interannual variability**
- **Noteworthy, these biomass burning aerosols are expected to have an even more important impact at the emission sources (mainly in Ukraine and surroundings countries) as observed from Aerosol Optical Depth measurements performed in Moldova**
- **As this country has the largest agriculture land area in Europe and the highest European values for energy-crop potential, agriculture (wheat crop residual) waste burning in this region is likely to represent a non-negligible source of combustion aerosols in the near future over Europe**

Hotspot fire maps (FIRMS data) for the year 2004

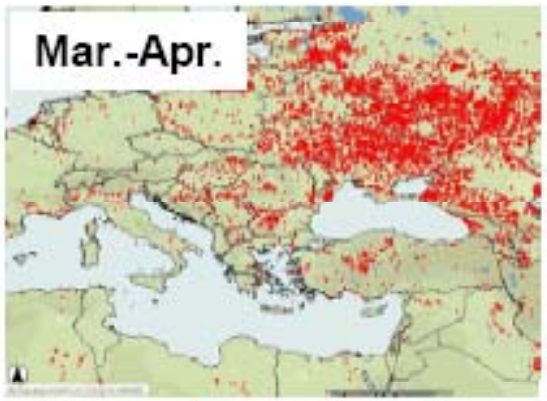

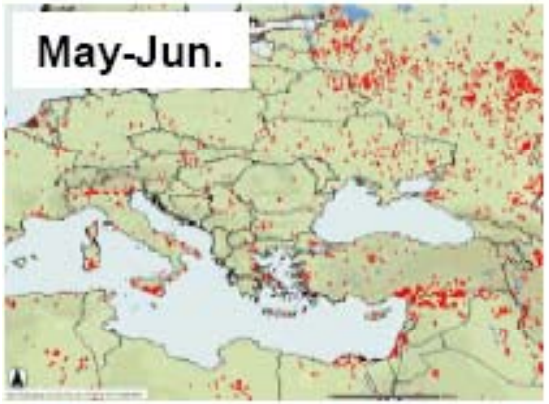

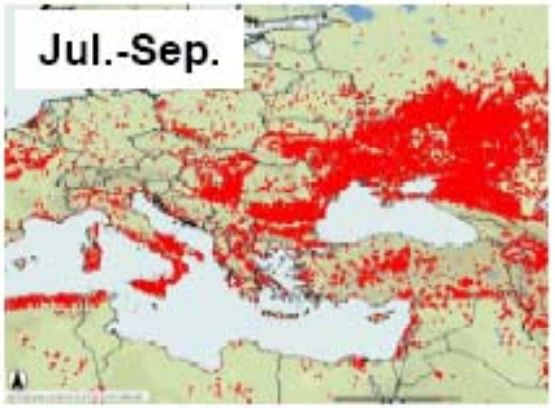

Yearly-based wind direction occurrences for the 4 sectors (North, West, East, and South) at Finokalia station in Crete Isl. M.O.Y stands for Month Of the Year

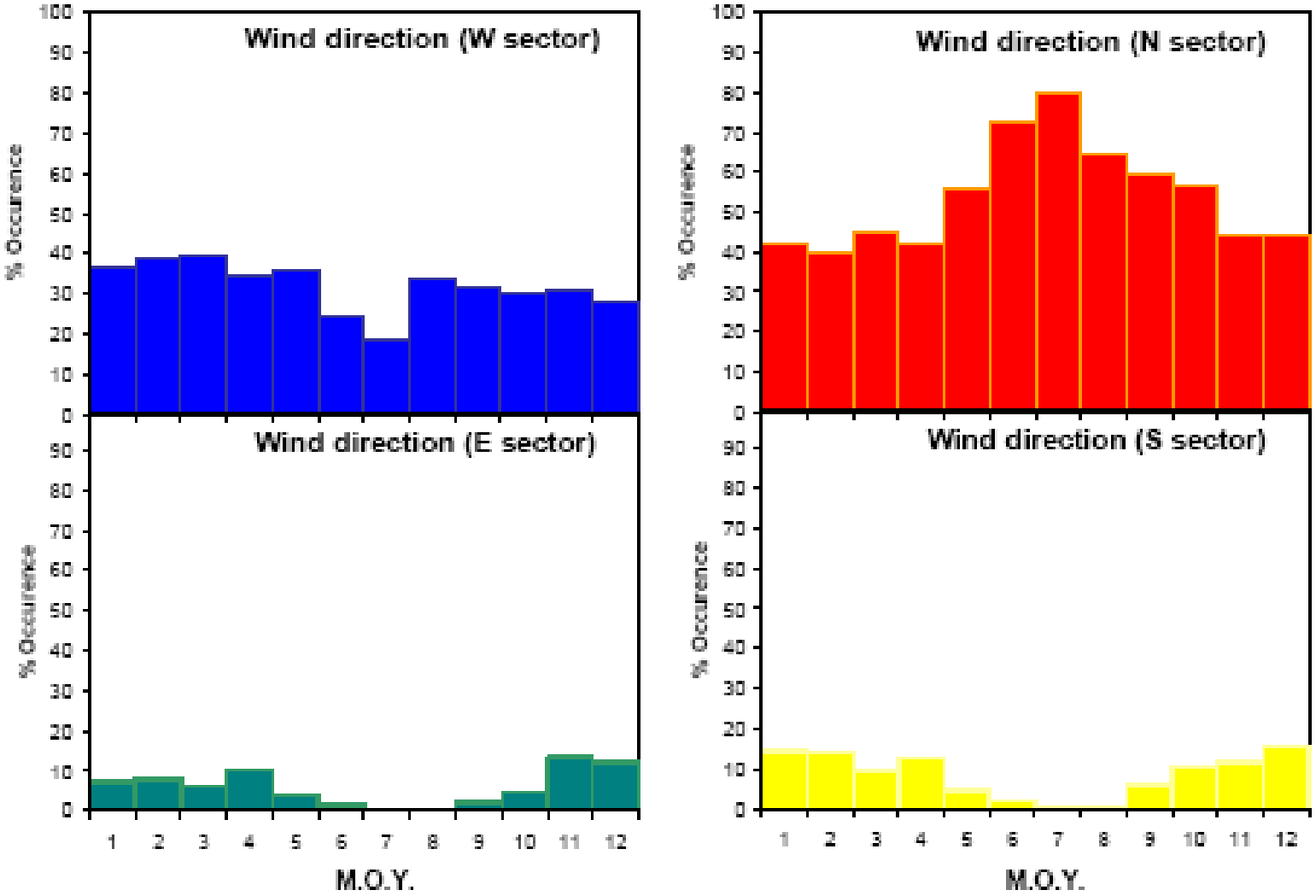

Seasonal variations of iron concentration in dust aerosols and light absorption measurements obtained from aethalometer (*b*abs (AETHALO)) corrected and uncorrected from the light absorption due to dust aerosols (*b*abs (Fe_2O_3))

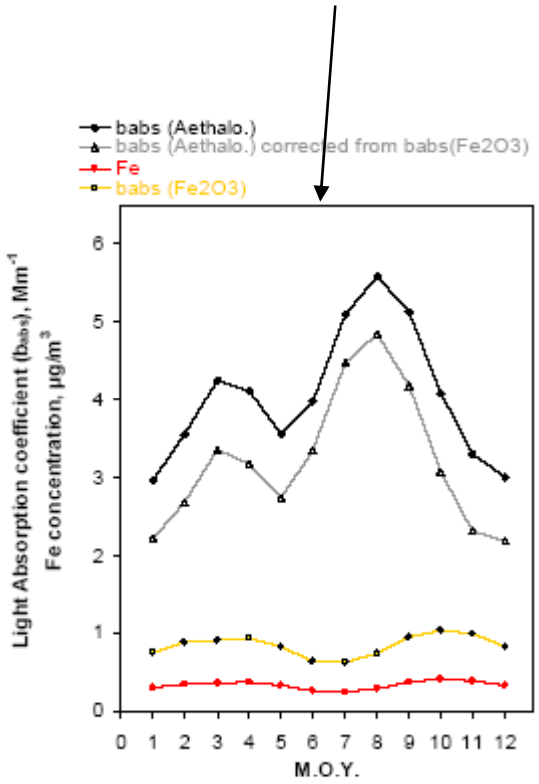

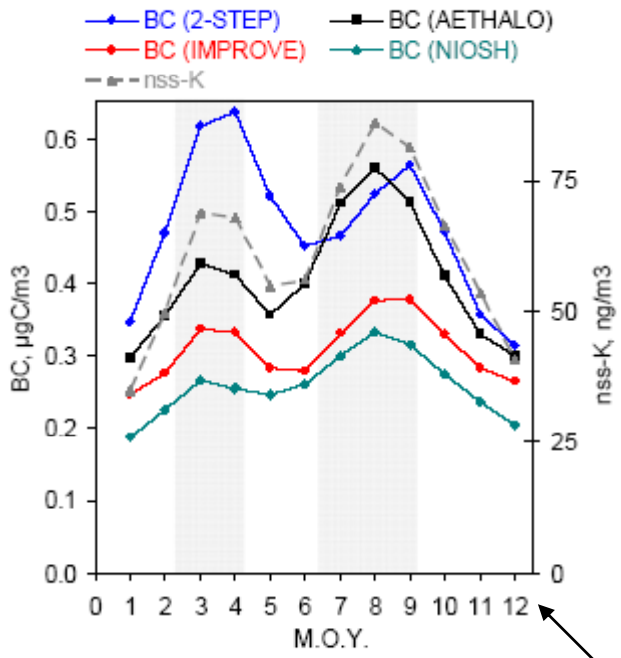

Weighed seasonal variations of BC concentrations derived from two thermo-optical (IMPROVE and NIOSH) one optical (AETHALO) and one thermal (2-STEP) protocol. Non-sea salt potassium (nss-K) concentrations are those from the fine mode (<1.5 μm)

Temporal variations of monthly mean BC, OC and nss-K concentrations in Crete Island

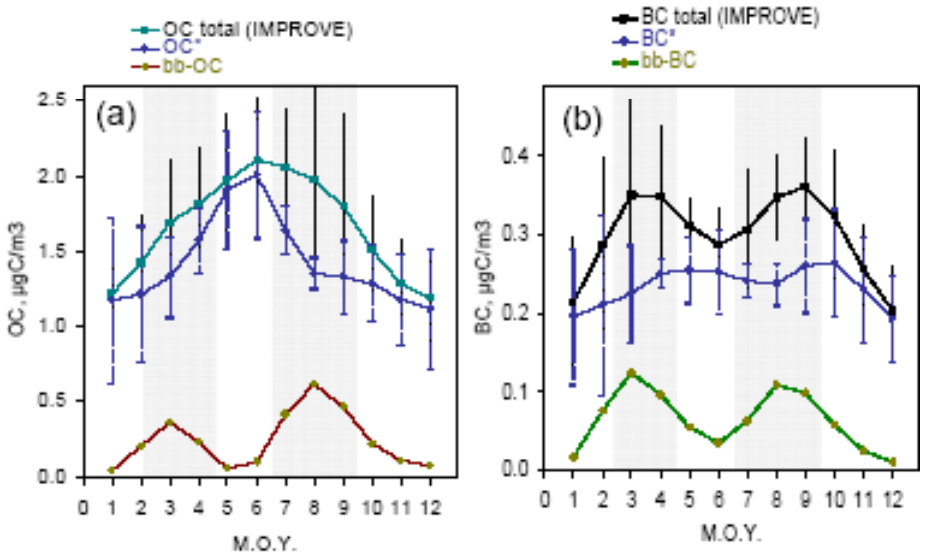

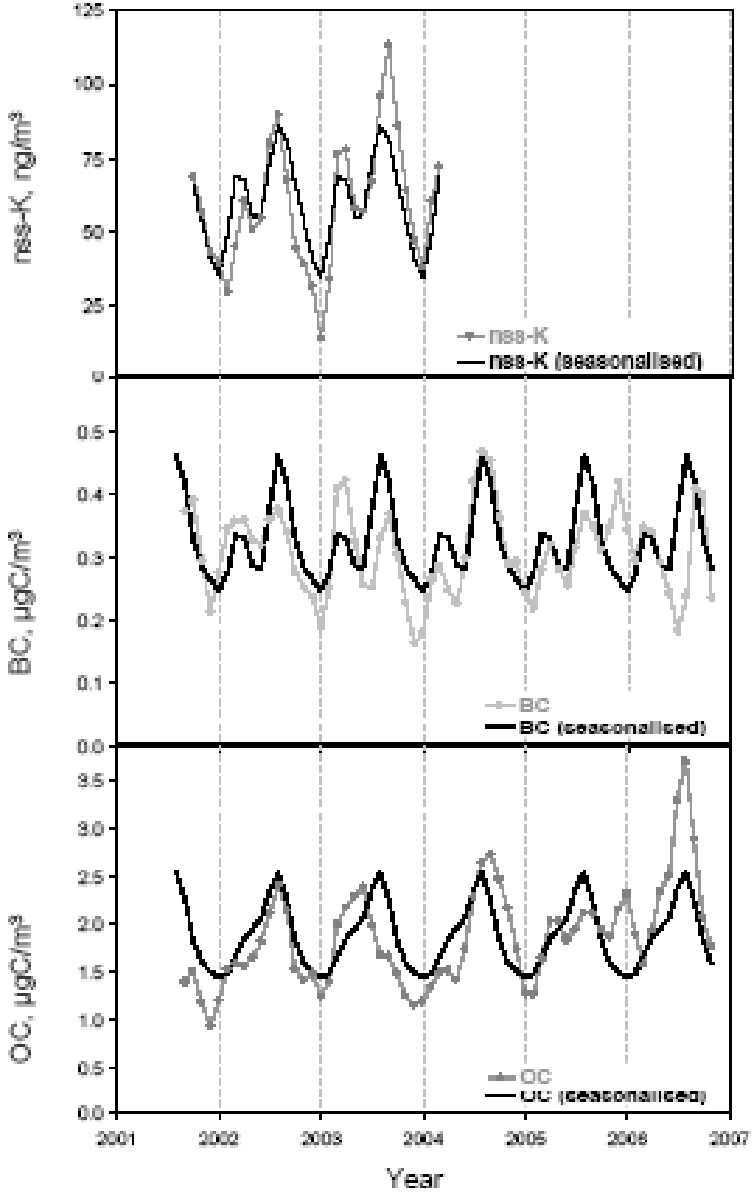

Transport of mineral particles to Israel

- During the summer months aerosols collected in Israel are highly polluted by metals (EF_{Ni} = 120, EF_{Cu} = 320, EF_{Zn} = 30, EF_{Pb} = 540)
- The fraction of European Pb of mostly industrial sources is 61% (21% in Jerusalem), and the fraction of European Cu, Zn, Ni, and aerosols should be on the same order
- Whenever a steep pressure gradient is built between the barometric trough originating from the Persian Gulf and the subtropical ridge along the African coast, stronger westerly winds and cooler temperatures (deep Persian Trough) prevail over the Middle East, and higher amounts of European pollution are observed in the atmosphere

$^{208}Pb/^{206}Pb$ and $^{206}Pb/^{207}Pb$ values of the sampled aerosols
The values of alkyl-Pb emitted in Israel are from soil samples collected near major roads

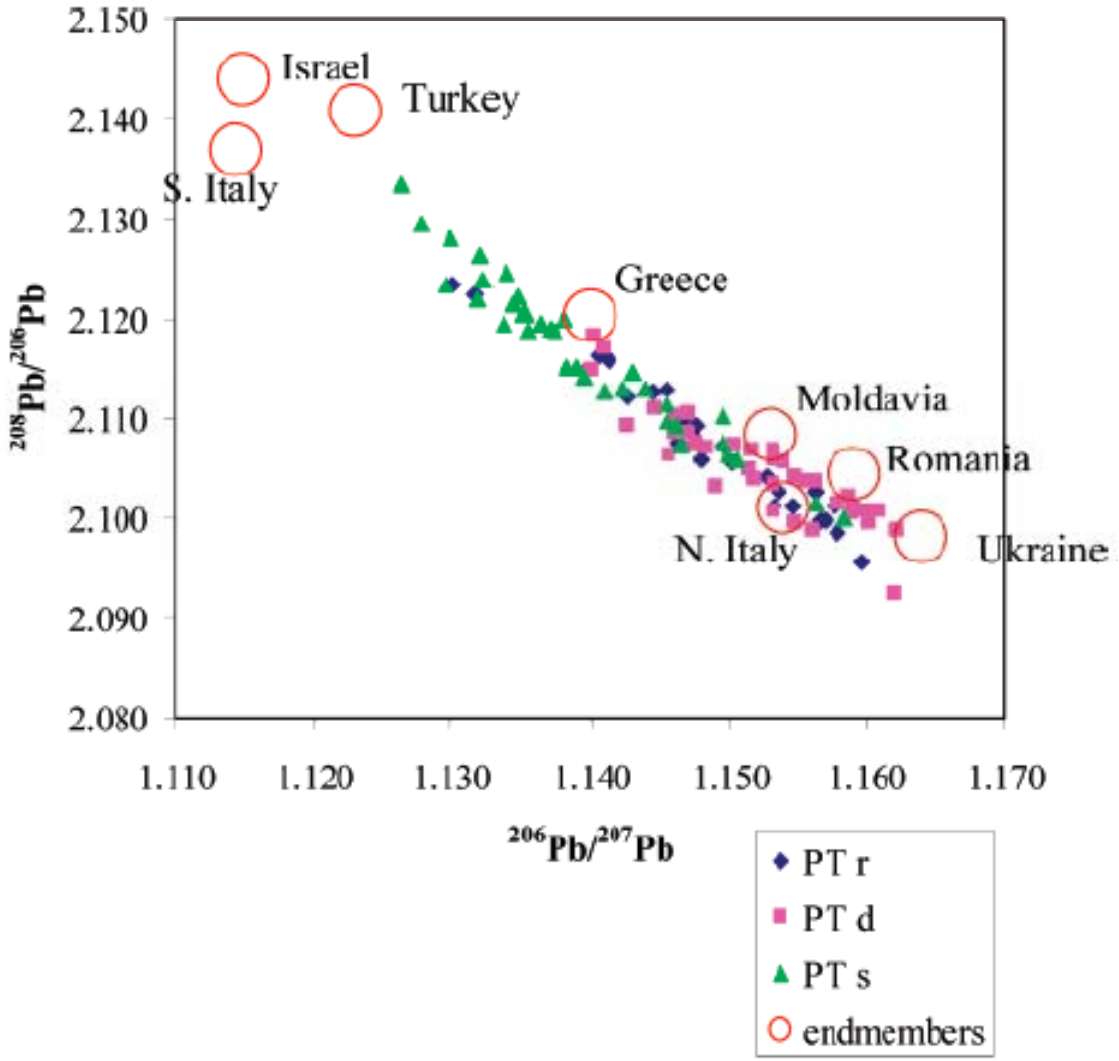

All samples collected in the current study contain high concentrations of Pb, Cu, Zn, and Ni, and the enrichment factors (EF) (metal/Al)smp/(metal/Al)UC); UC) upper continental crust) vary between 64 and 945, 44 and 555, 0.9 and 66, and 1.8 and 275, respectively

The current study demonstrates how changes in synoptic conditions are responsible for changes in sources of pollution and how the impact of emissions in one part of the World affects air quality in another part.

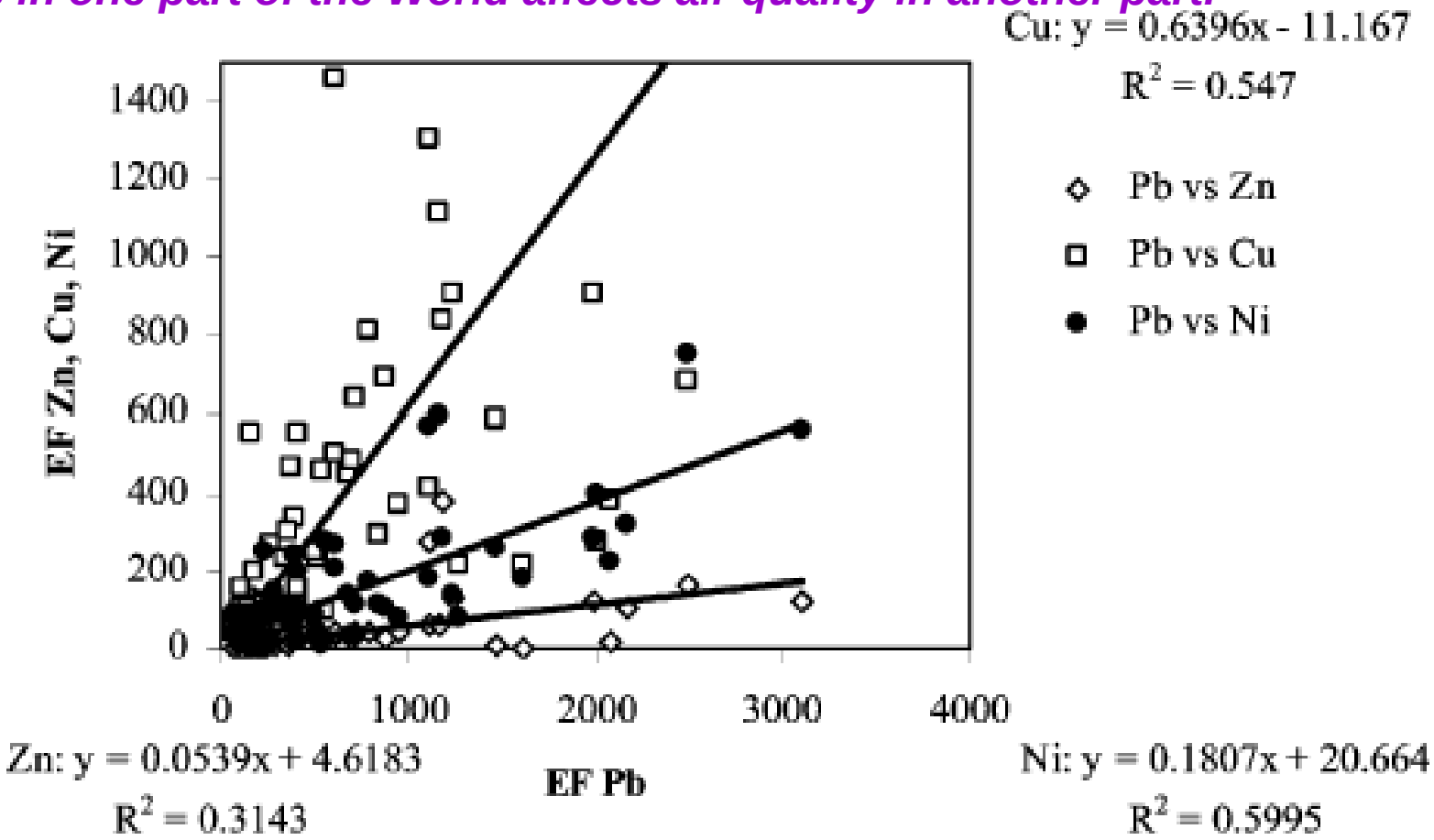

Transport of PM_{10} to Turkey

- **Ground-based aerosol optical measurements were conducted within the framework of the Aerosol Robotic Network (AERONET) program at the IMS-METU site at Erdemli (36°33′N, 34°15′E) along the Turkish coast of the northeastern Mediterranean from January 2000 to June 2001**
- **Dust storms affecting the region primarily originate from the central Sahara in spring, the eastern Sahara in summer, and the Middle East/Arabian peninsula in autumn. Summer and autumn dust intrusions usually occurred at higher altitudes (above 700 hPa), whereas urban-industrial aerosols from the north over the Balkan region, Ukraine, and Anatolia were transported to the region at lower altitudes**
- **Simulated Istanbul PM10 response to 50% change in anthropogenic emissions during 5–12 January 2002**

Country	Total emission[a] (2001)	Istanbul PM10 response to 50% increase	
	(Gg)	Ave (%)	Max (%)
Bulgaria	2016	2	7
Romania	4566	4	13
Poland	7104	1.5	7
Ukraine	5703	1.5	8
Russia	20,066	0.5	8

Spatial distribution of calculated mean annual dust suspension flux of different particle size in 2005: (a) – $PM_{2.5}$; (b) – PM_{10}; (c) – PM_{20}, $\mu g/m^2/s$

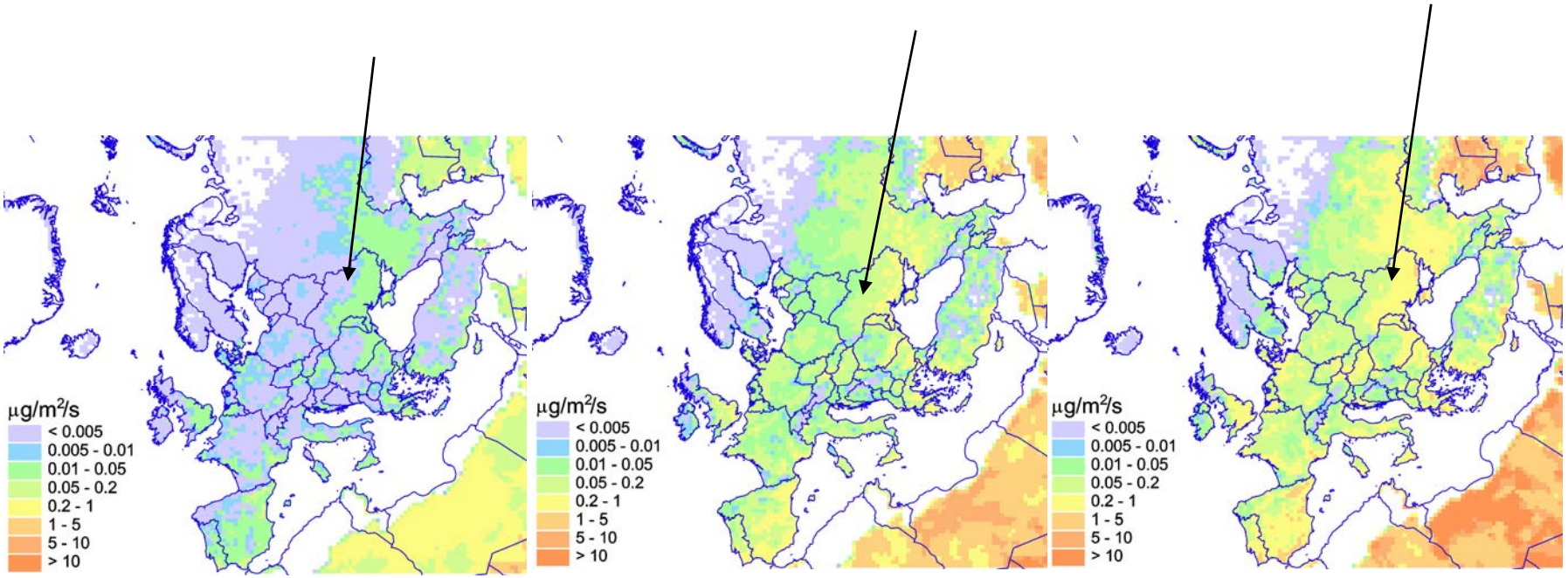

a **b** **c**

EMEP, 2005

Spatial distribution of annual averages of specific aerosol surface over Europe

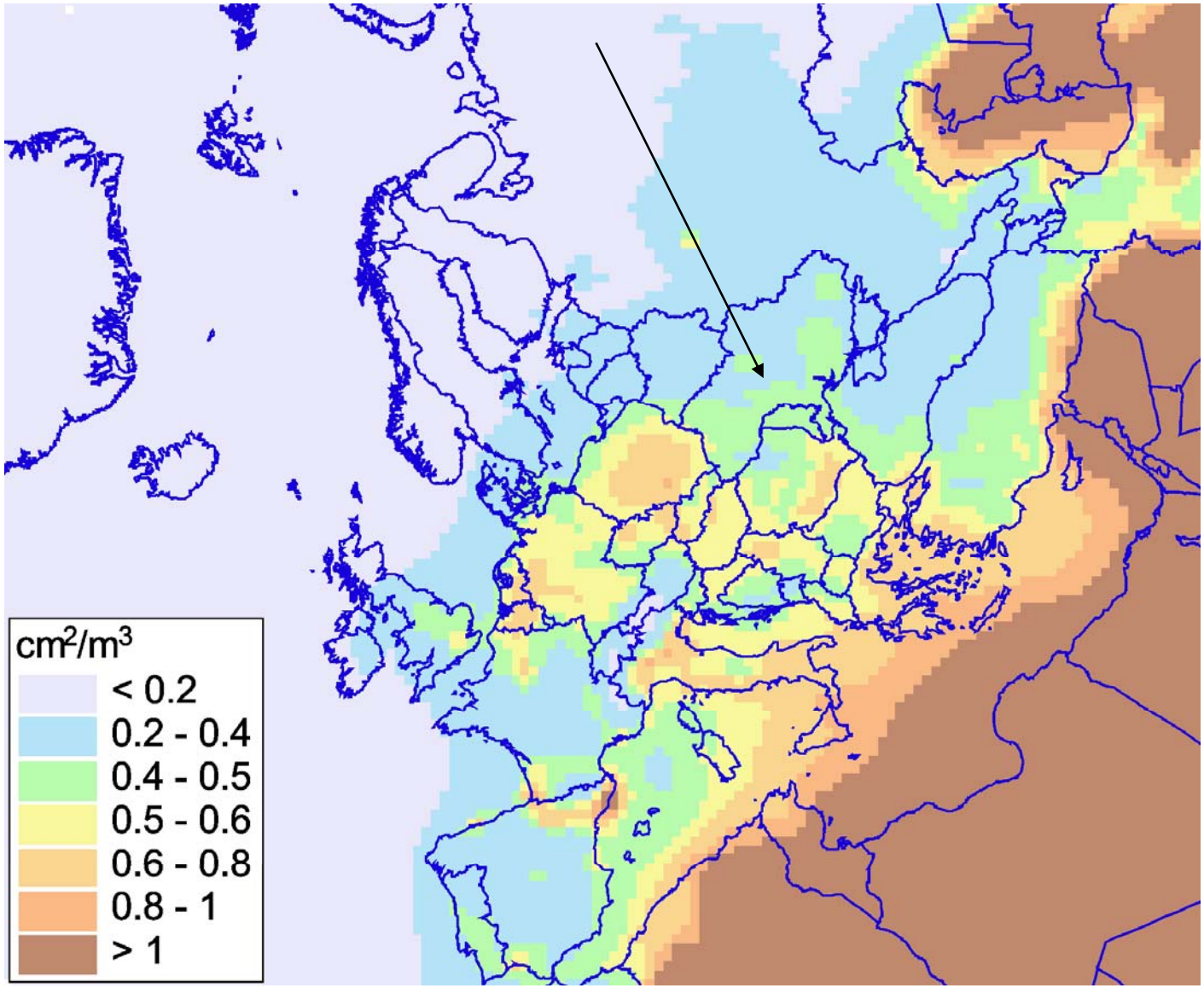

Absolute contribution of European countries to lead transboundary transport in Europe in 2005 and relative fraction of national emissions in this contribution, t/y

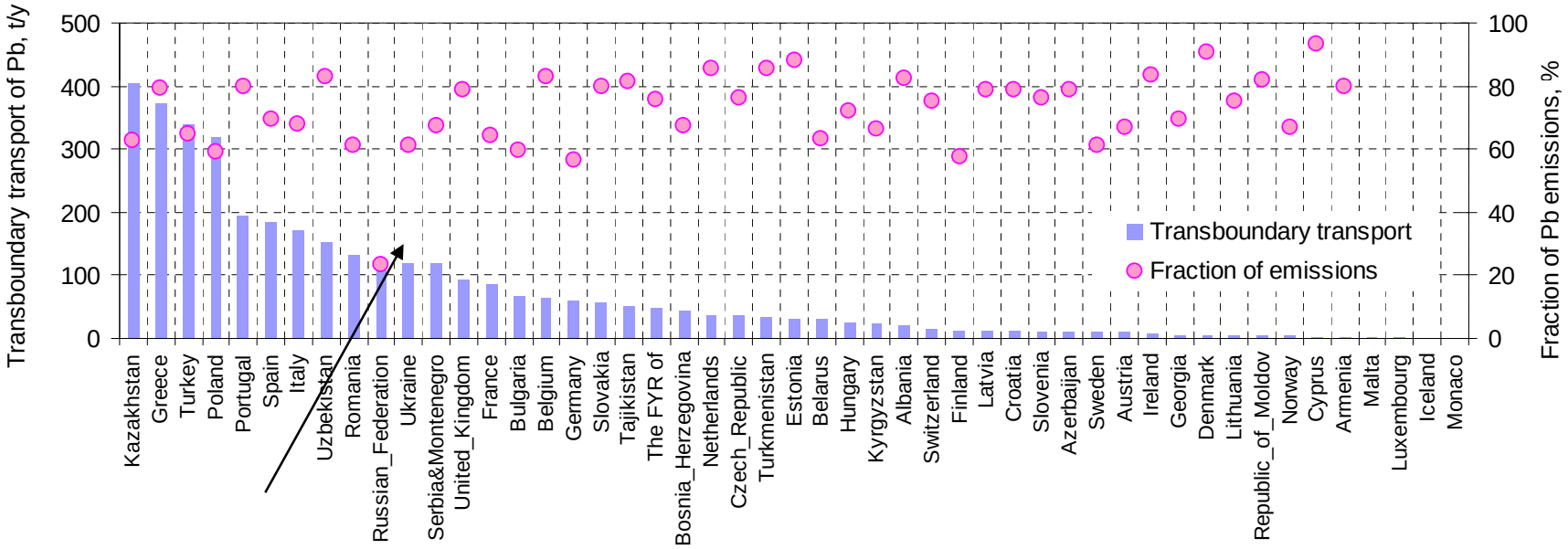

Absolute contribution of European countries to mercury transboundary transport in Europe in 2005 and relative fraction of national emissions in this contribution, t/y

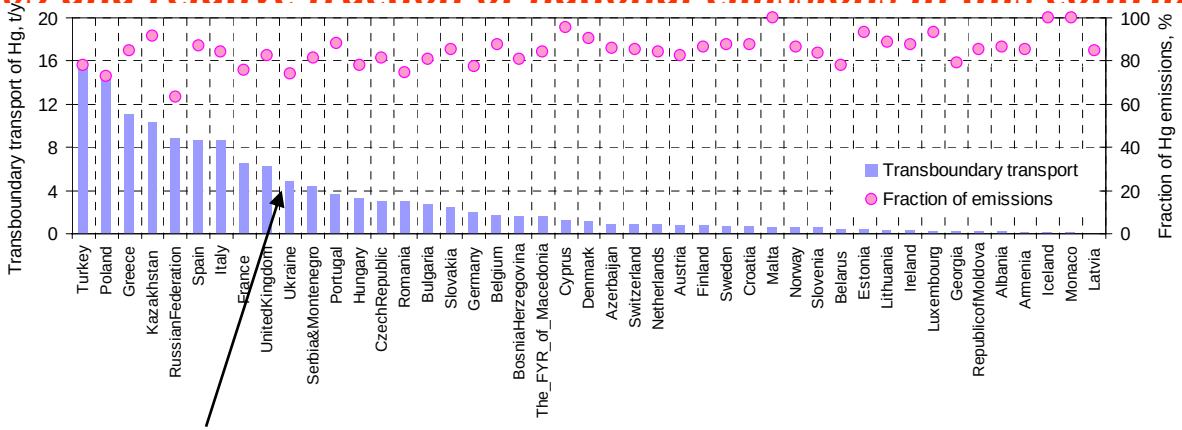

Figure 1 Emissions of particulates in Europe in 1995

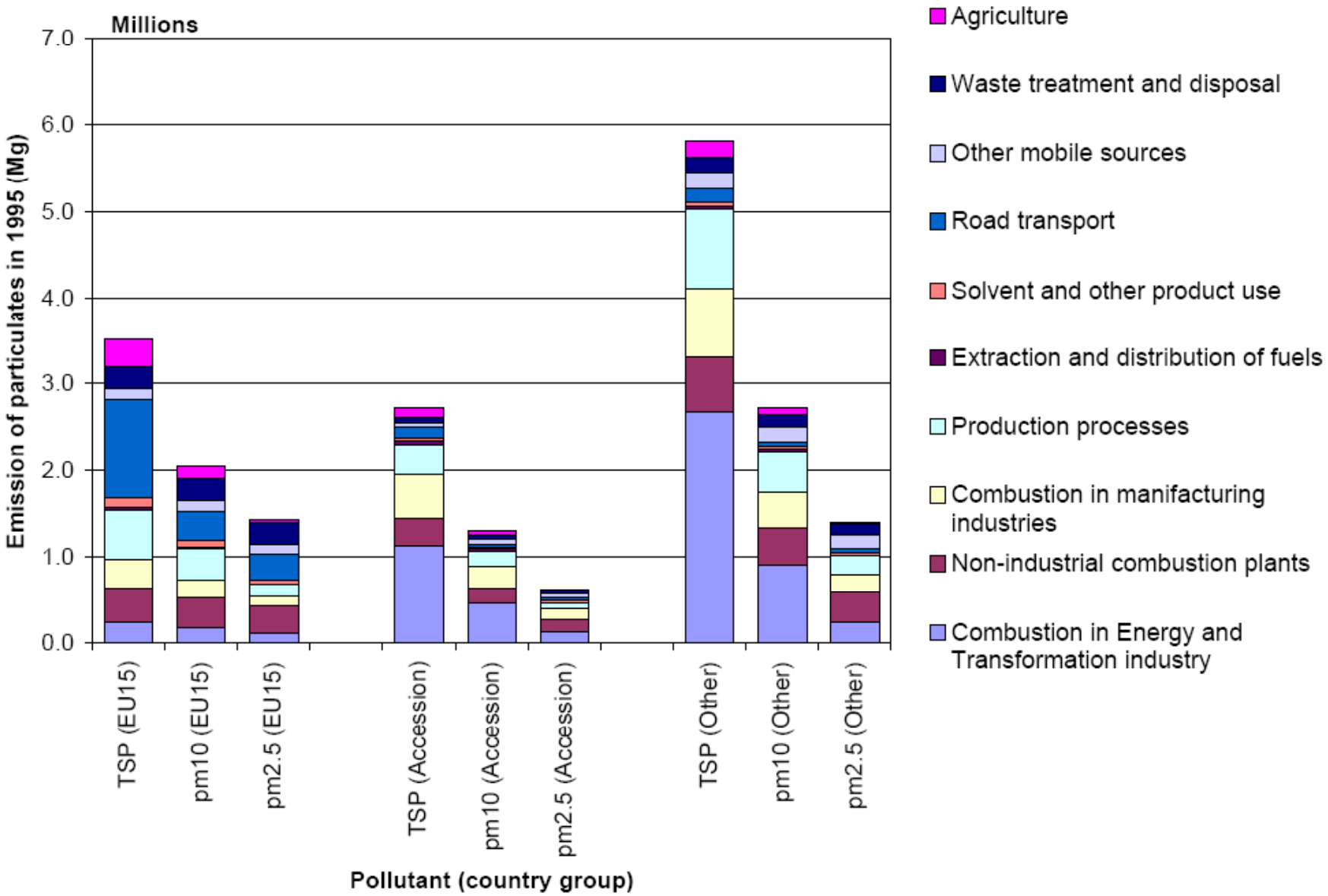

Spatial distribution of emissions from Ukraine in 2005

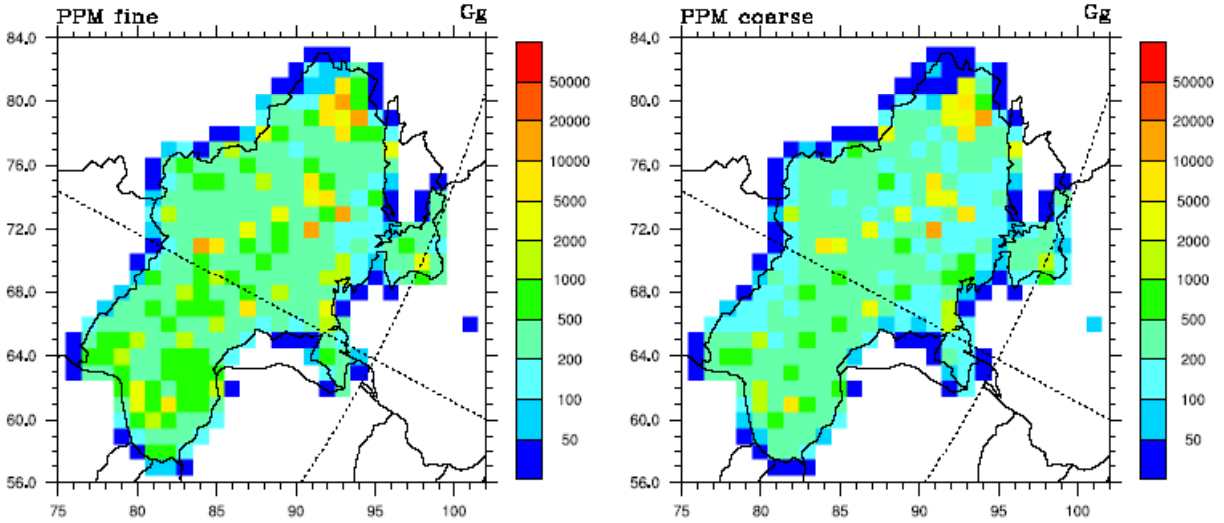

Trends in mean concentrations of particles since 2000. Units: µg/m^3

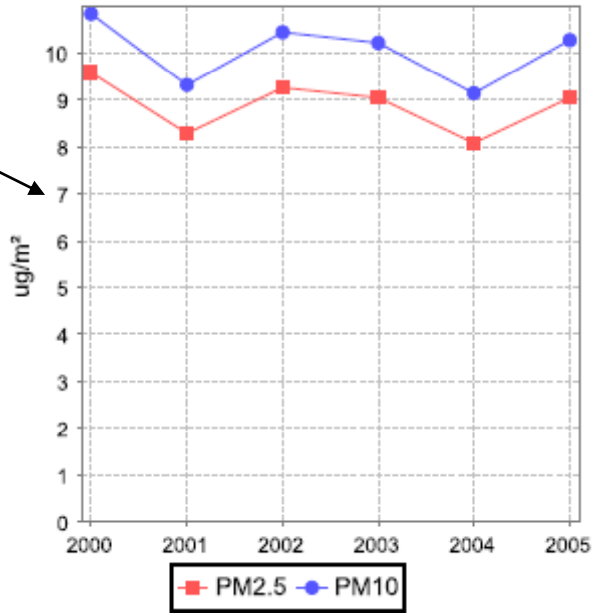

Transboundary Fluxes in 2005

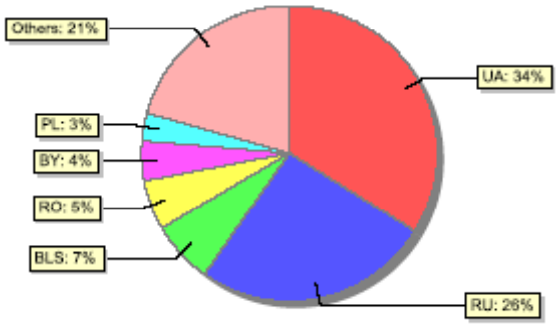

oxidized sulphur deposition

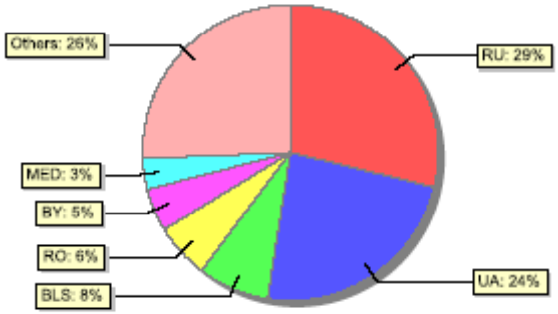

oxidized nitrogen deposition

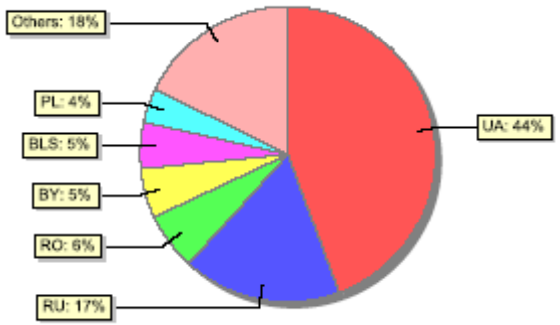

reduced nitrogen deposition

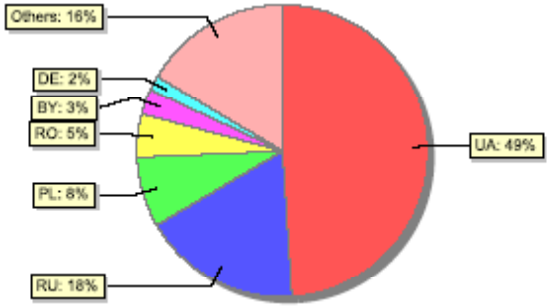

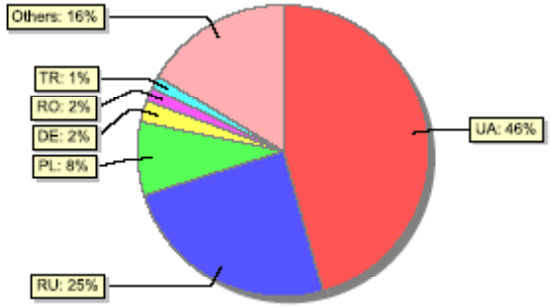

Main contributors to PM2.5 (left) and PMcoarse (right) concentrations in Ukraine

Importance of atmospheric aerosols

- Solid and liquid aerosols affect on:
- biogeochemical cycles of C, O, N, Cl, Br, I, S, P, As, Cd, Pb, Fe, Cu, Co, Ca, etc.
- human and ecosystem health
- chemical composition of atmosphere
- visibility of atmosphere
- radiative atmospheric budget
- Earth's climate

They are also carriers for transport of moderate and low-volatile persistent toxic organic atmospheric pollutants (POPs) over a long distances from their industrial and agricultural sources

Main persistent organic pollutants

Chlorinated pesticides:

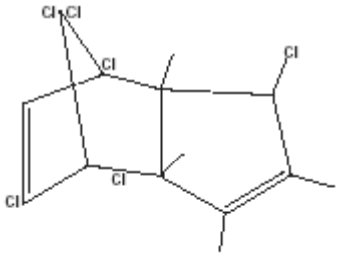

Heptachlor

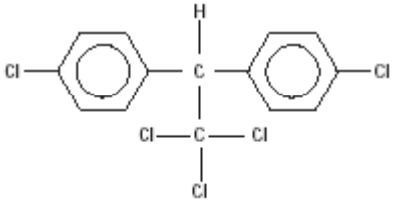

p,p'-DDT

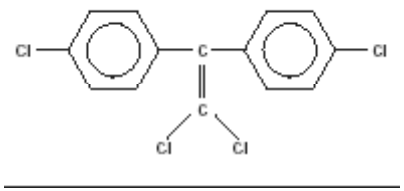

p,p'-DDE

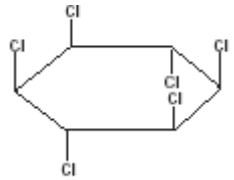

γ-HCH

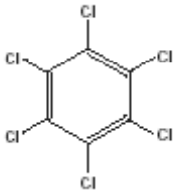

HCB

Polychlorinated dibenzo-p-dioxins:

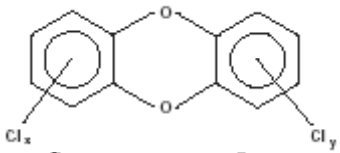

Polychlorinated dibenzofurans:

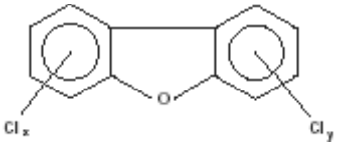

Polychlorinated biphenyls:

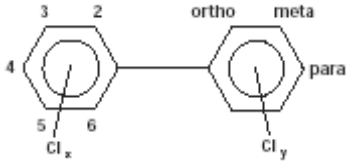

Polycyclic aromatic hydrocarbons:

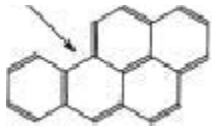

Benzo[a]pyrene

Polybrominated diphenyl ethers:

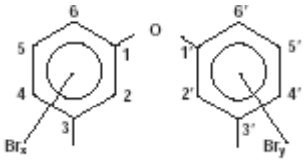

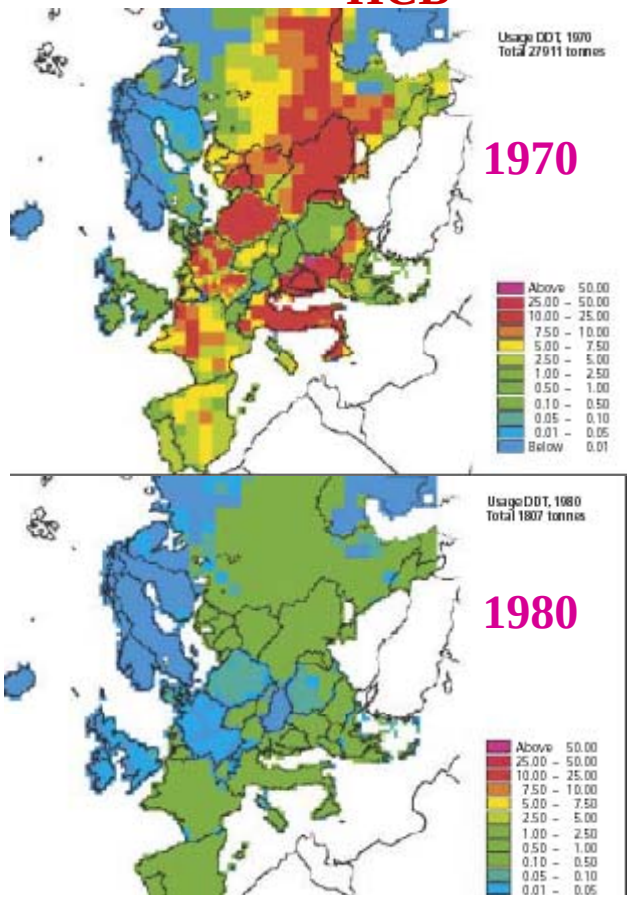

1970

1980

Long-range transport potential, L_A, and persistence, τ_A, for selected POPs in air as estimated by TaPL3 model

POPs	L_A, km	τ_A, h
Carbon tetrachloride	498960	1443
Hexachlorobenzene	200910	3516
3,4-Benzopyrene	493	1507
Pentachlorophenol	2554	132
Chlordane	1357	428
γ-hexachlorocyclohexane	3021	755
Heptachlor	1636	5.7
α- hexachlorocyclohexane	4473	270

Distribution of a pollutant between gaseous and an aerosol form

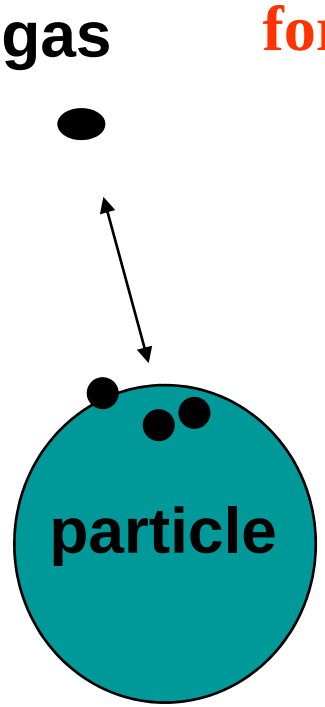

$$C_{gas} + particle \overset{K_p}{\leftrightarrow} C_{part}$$

- **What happens when a semivolatile organic (POP) encounters a particle?**

Partitioning Modes

- Mode of POP-particle interaction depends on the particle
  - **Adsorption** Solid particle, no organic liquid layer (dust, inorganic salts)
  - **Absorption** Particle either liquid, or has substantial liquid layer (combustion particles, secondary organic aerosol)
- POPs such as PAHs, and alkanes primarily partition to organic or carbonaceous aerosols rather than to mineral-based aerosols

$$\log K_p = -\log p_L^0 + \log \frac{N_s a_{tsp} T e^{(Q_1 - Q_v)/RT}}{1600}$$

$$\log K_p = -\log p_L^0 + \log \frac{f_{om} 760 RT}{MW_{om} \zeta 10^6}$$

p_L^o (torr): vapor pressure of the pure compound
N_s (sites/cm^2): surface conc. of sorption sites
a_{tsp} (m^2/g): particle surface area
Q_1, Q_v (kJ/mol): enthalpy of vaporization
R: gas constant T (K): temperature

f_{om}: weight fraction of TSP in organic matter (om) phase
MW_{om}: mean molecular weight of the om phase
z: activity coefficient

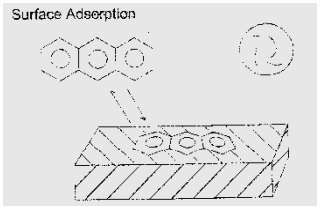

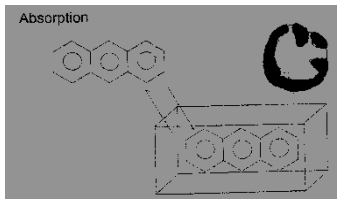

Partition Coefficient K_p: Adsorption & Absorption

Langmuir adsorption:

$$K_p = \frac{N_s a_{tsp} T e^{(Q_1 - Q_v)/RT}}{1600 p_L^o} \propto \frac{\#\,\text{sites, area}}{\text{vapor pressure}}$$

Absorption into a liquid film:

$$K_p = \frac{f_{om} 760 RT}{MW_{om} p_L^o \gamma 10^6} \propto \frac{\text{organic fraction}}{MW_{\text{org phase}}, \text{vapor press}, \text{activity}}$$

$$\log K_p = m_r \log P^o_L + b_r$$

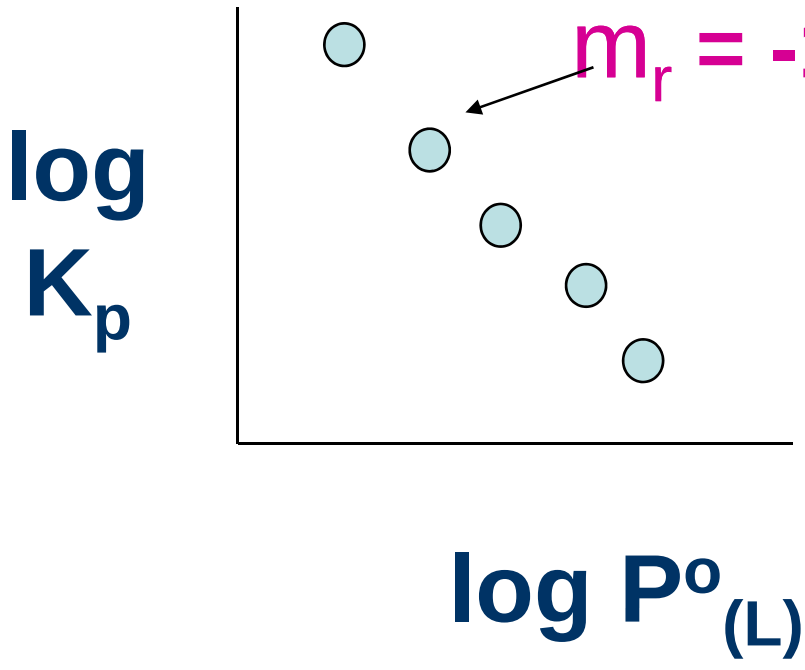

- PAHs,
- alkanes
- chlorinated organics

If b_r is constant….

If absorption is important, K_{oa} may be a better predictor of K_p

those previous equations used p as the descriptor variable.

we could also use K_{oa} :

$$K_P = f_{om} \frac{MW_{oct} \cdot \zeta_{oct}}{MW_{om} \cdot \zeta_{om} \cdot \rho_{oct} \cdot 10^{12}} K_{oa}$$

K_{oa} = n-octanol-air partition coefficient
f_{om} = fraction of organic matter
MW_{om}, MW_{oct} = molecular wt of NOM or n-octanol
ξ_{om} , ξ_{oct} = activity coeff. of SOC in NOM or n-octanol
r_{oct} = density of n-octanol

Distribution of PCDD/F content in the environment between main environmental media in 2004 (EMEP, 2007)

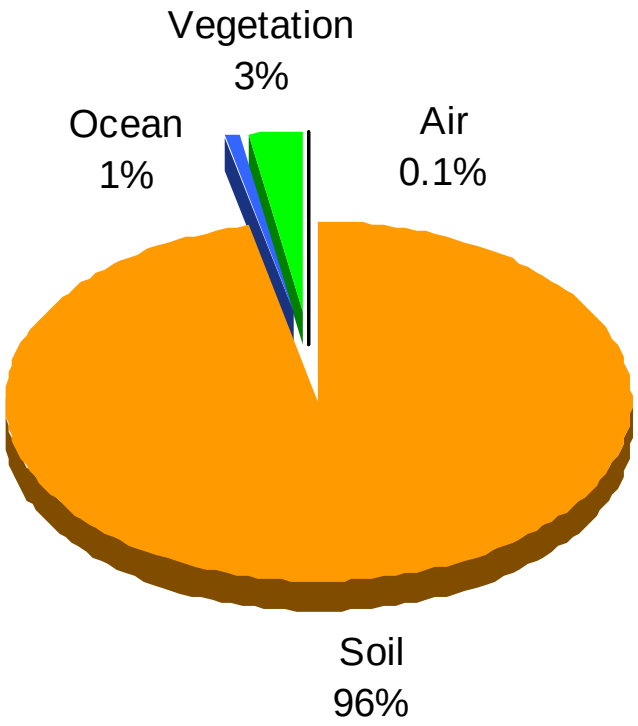

Transport of POPs in Europe (EMEP estimates, 2005)

- **Calculations of pollution levels of polychlorinated dibenzo(p)dioxins and dibenzofurans (PCDD/Fs) in the EMEP region were performed for total PCDD/F toxicity with use of physical-chemical properties of "indicator congener" 2,3,4,7,8-PeCDF**

- **Air concentrations of PCDD/Fs** **Deposition fluxes**

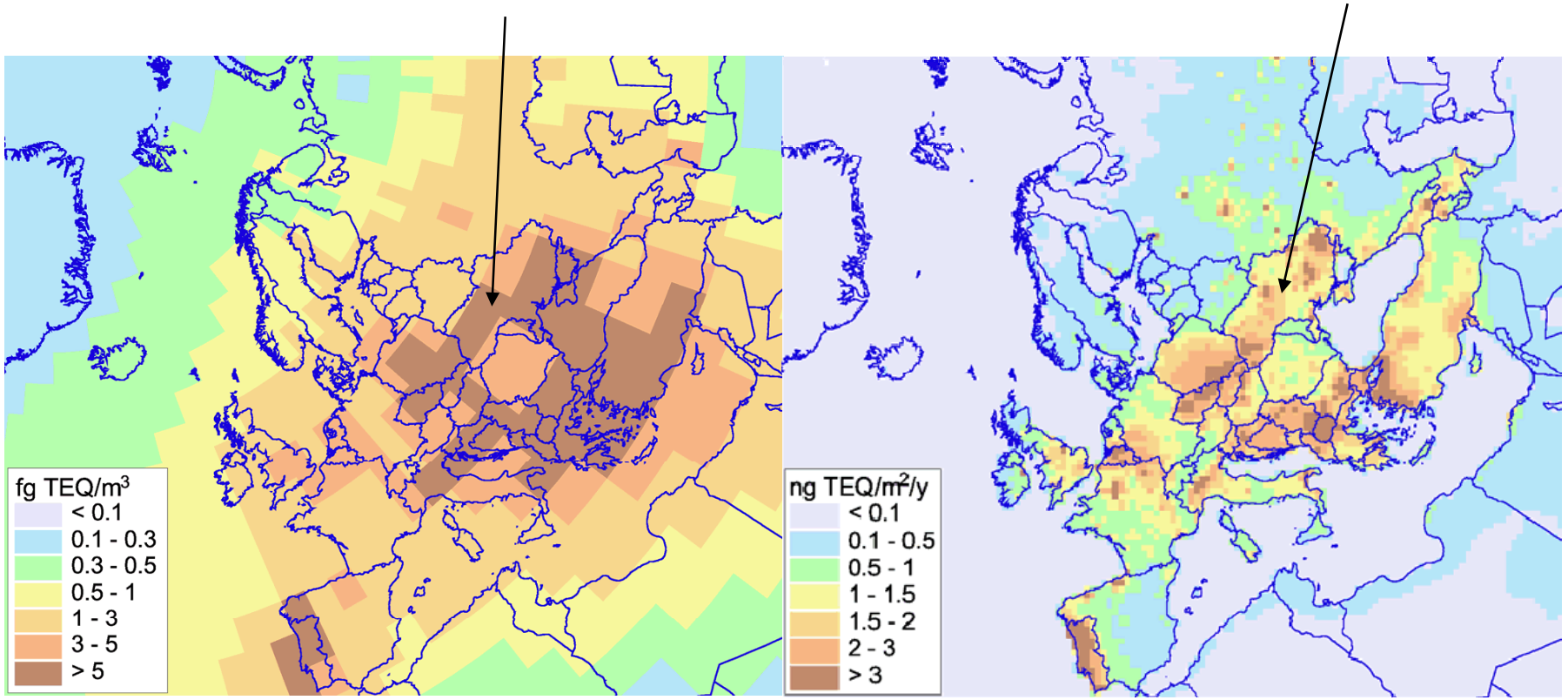

Depositions of PCDD/Fs to the own territory and to the rest EMEP territory due to national emissions of European countries

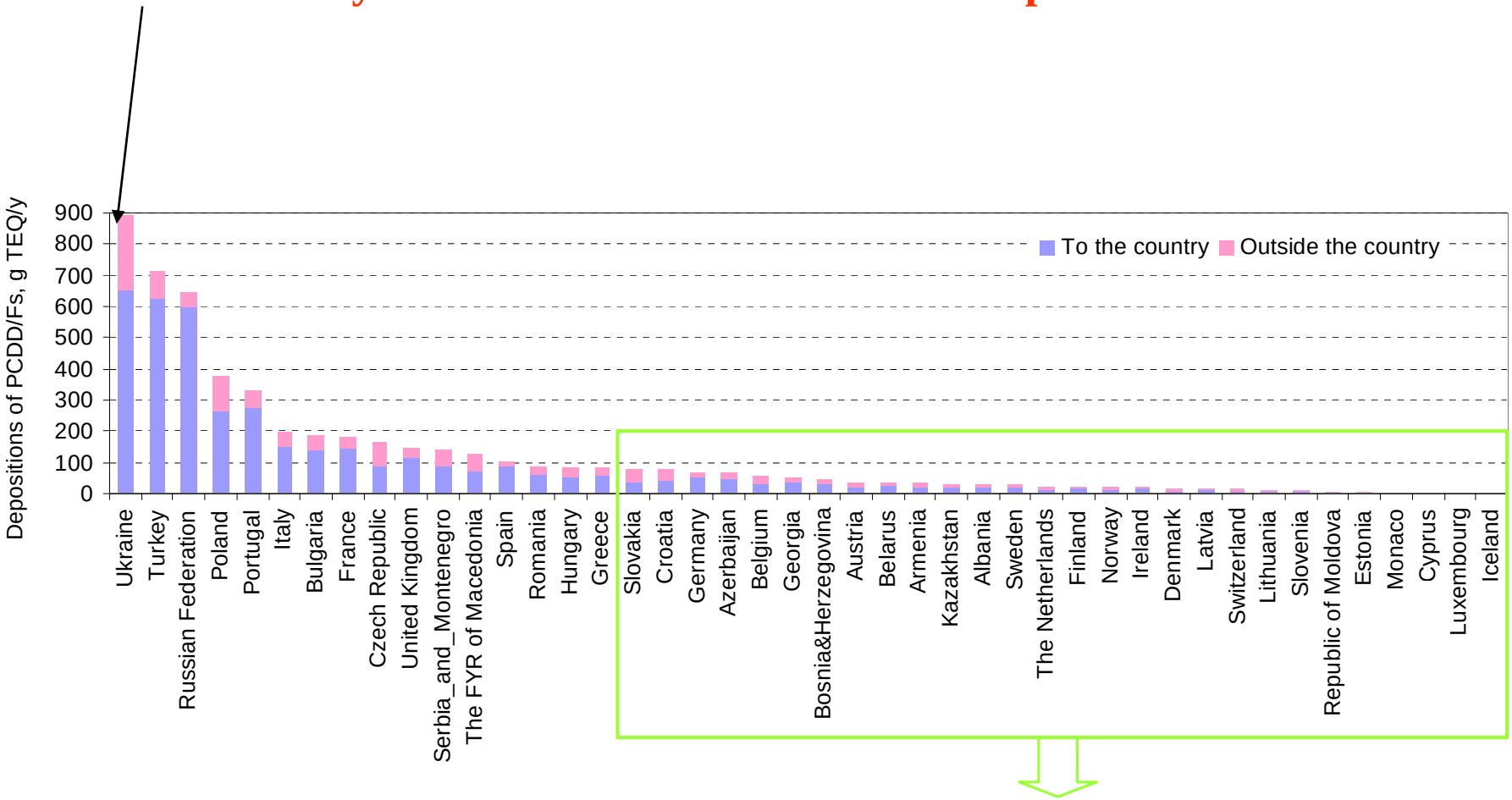

Calculated air concentrations, soil concentrations and total depositions of PCDD/Fs in European countries in 2004 in comparison with emission densities

Country	C_A, fg/m^3	C_S, TEQ/g	TD, pg/m^2/day	ED, pg/m^2/day
Belarus	2.5	241.8	2.6	0.5
France	4.4	522.9	5.3	1.5
Germany	6.5	806.4	6.1	2.0
Hungary	6.6	380.4	5.5	2.2
Italy	5.0	331.2	4.9	2.9
Poland	6.2	495.9	5.7	4.2
Moldova	4.0	226.2	2.8	0.4
Romania	4.2	248.6	3.7	1.2
Russia	1.4	106.1	1.4	0.5
Slovakia	6.7	566.0	6.0	3.7
Turkey	5.1	115.6	3.8	3.5
Ukraine	6.0	277.2	4.9	4.7
United Kingdom	3.4	299.4	2.1	3.2

Average PCDD/F air concentrations in European countries in 2004

(red line indicates the average air concentrations over all European countries)

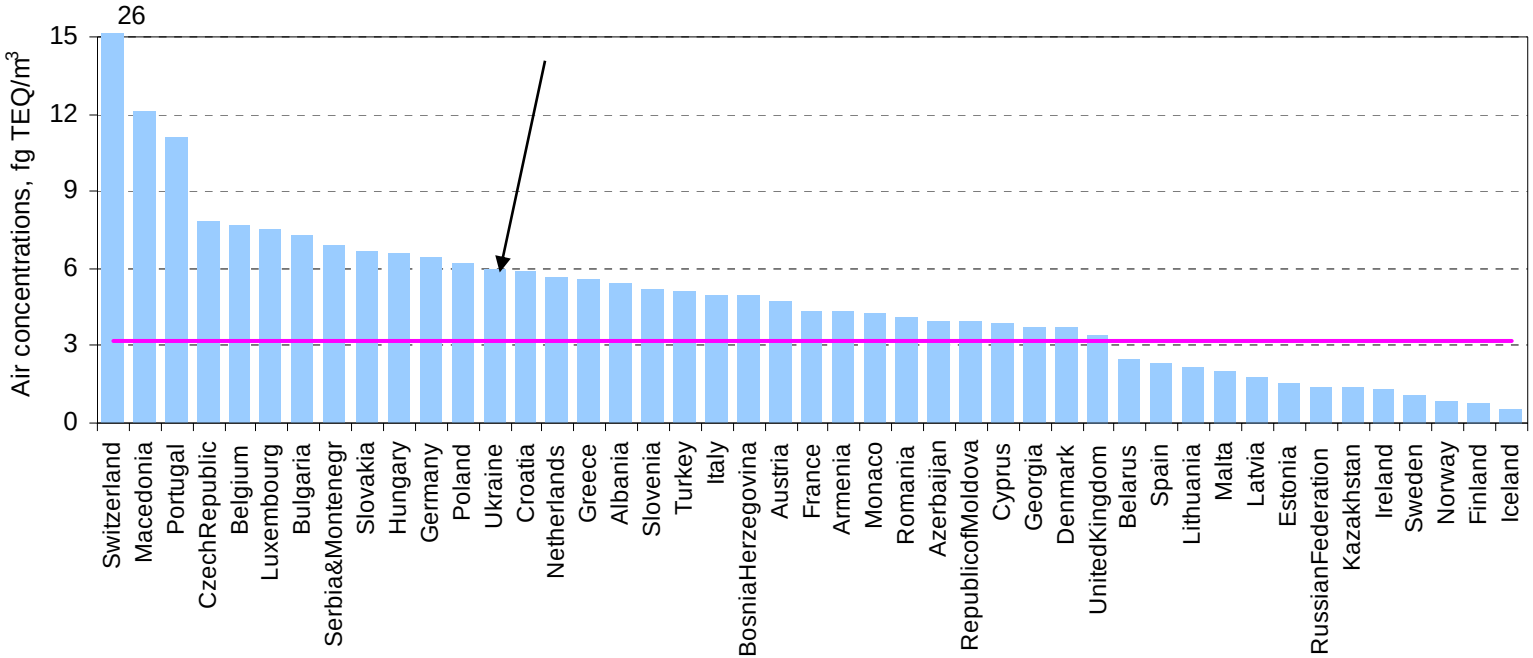

Trends of PCDD/F air, soil concentrations and emissions in Ukraine from 2005 to 2020

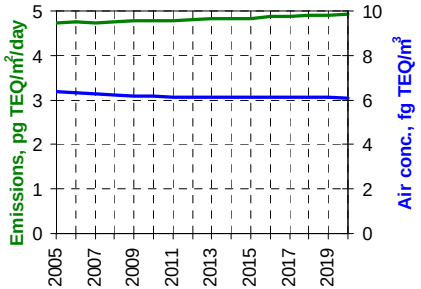

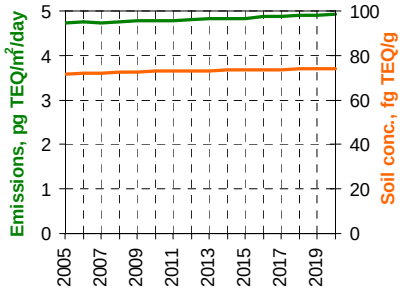

Emission of PCDD/Fs in Ukraine will be increased by about 4% and only minor reduction of air concentrations (about 4%) takes place from 2005 to 2020

Calculated air concentrations, ng/m^3 (a) and deposition fluxes, g/km^2/y (b) of B[a]P in 2005 in comparison with emissions, g/km^2/y (c)

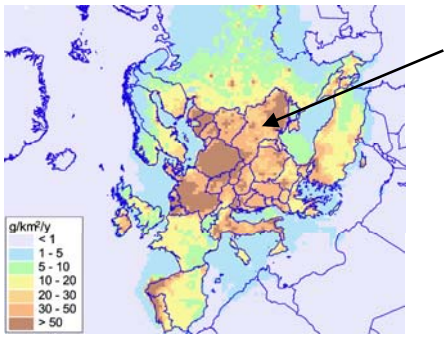

a.

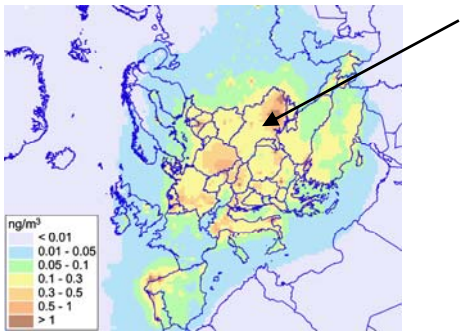

b.

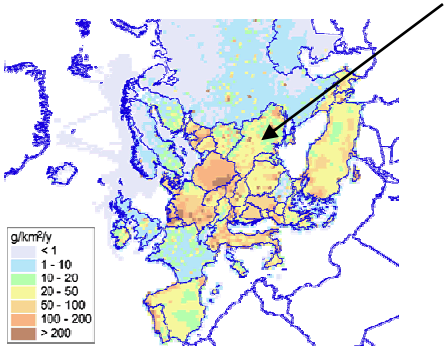

c.

Depositions of B[a]P to the own territory due to national emissions of European countries, t/y

Spatial distribution of POPs annual emissions, g/km^2/y (a), annual mean air concentrations, pg/m^3 (b), and total depositions, g/km^2/y (c) for 2005

PCB-28

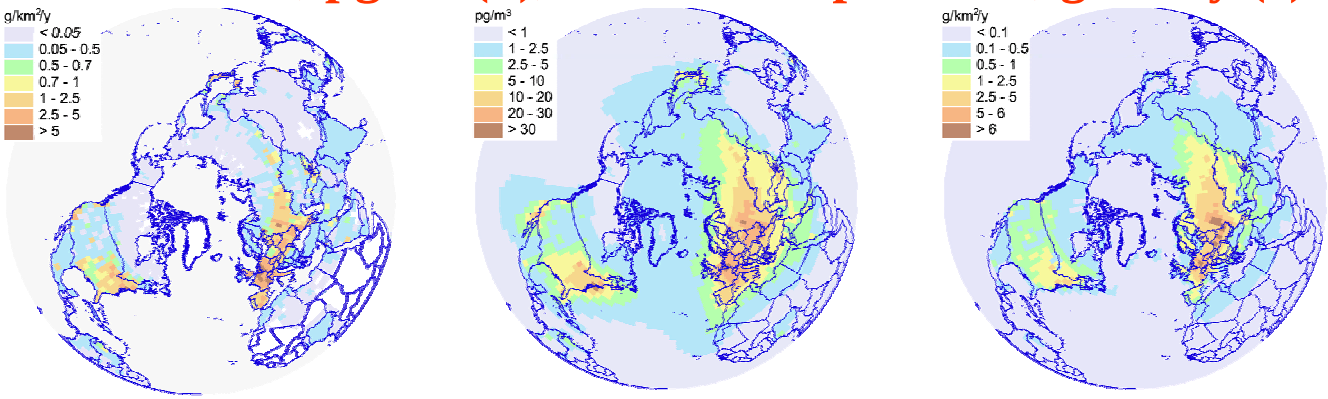

a. **b.** **c.**

γ-HCH

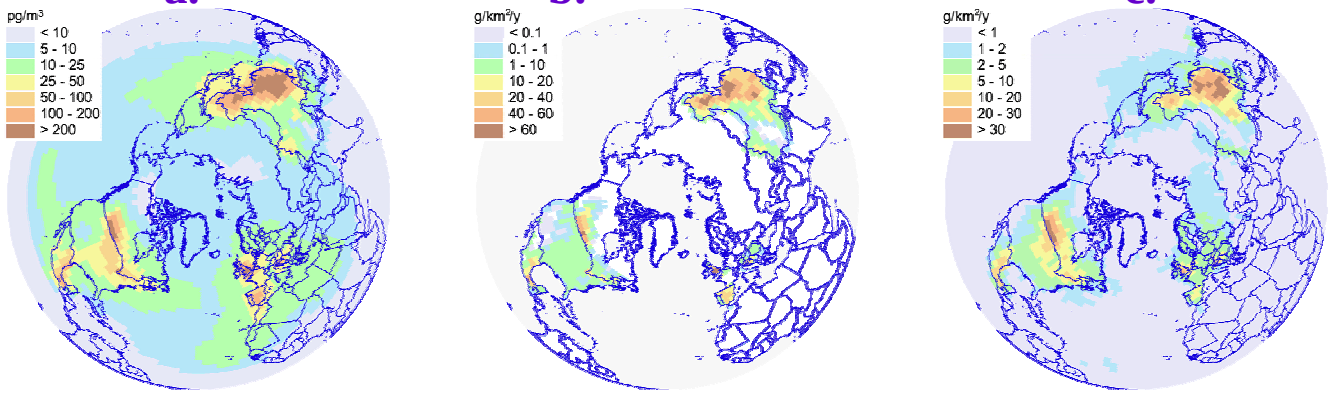

HCB

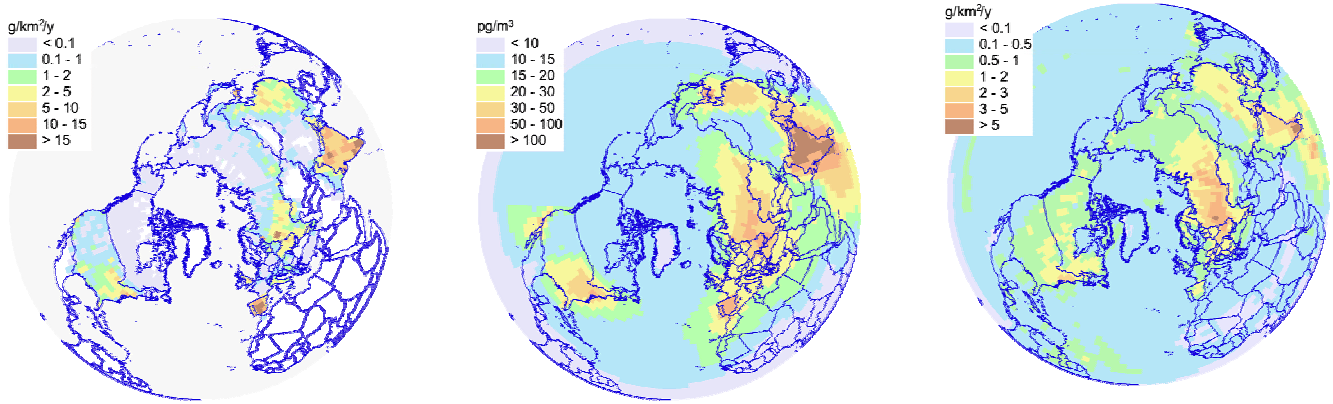

Effect of bounding with aerosols and temperature on transboundary transport of POPs

- Calculation of K_P values at different temperatures
- Use of "iso-equilibrium" dependence:

$\Delta H_{ij} = \Delta G_{ij}(T_{is}) + T_{is}\Delta S_{ij}$; $-2.3RT\log K_{ij} = a\Delta H_{ij} + b$

$\Delta H_{OA} = -38.9 \pm 8.4 - (4.89 \pm 0.96)\log K_{OA}$ (N = 6, r = - 0.931)

$\Delta H_{OW} = -36.9 \pm 15.7 + (3.4 \pm 2.6)\log K_{OW}$ (N = 6, r = 0.540)

$\log K_{IA}(15\ ^{o}C) = 0.635 \times \log L^{16} + 5.11 \times \Sigma\beta_2^{H} + 3.60 \times \Sigma\alpha_2^{H} - 8.4$

$$\ln K_{ij}(T) = \ln K_{ij}(T_{ref}) - \frac{\Delta H_{ij}}{R}\left(\frac{1}{T} - \frac{1}{T_{ref}}\right)$$

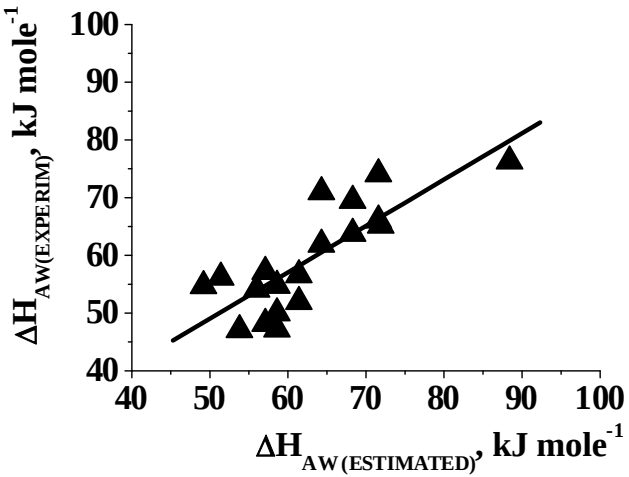

Main modes for transport of POPs in range from 25° to 0 °C can be distinguished from dependences of their log K_{AW} versus log K_{OA} quantities:

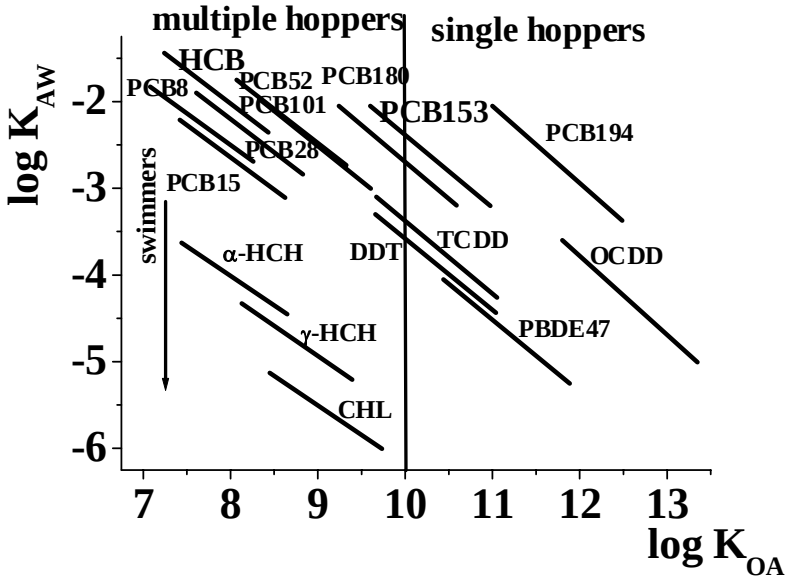

The DDTs, heavy PCBs, PCDDs and PBDE congeners are "single hoppers" and they have potential to easily irreversible deposition to environmental surfaces, whereas HCB, HCHs and light PCBs congeners are "multiple hoppers" and they would be readily exchanged between air and underlying surfaces in response to the temperature changes

SORPTION TO ATMOSPHERIC PARTICULATES

- **The atmospheric particle-bound fractions of the POPs, Φ_P:**

$$\Phi_P = \frac{K'_P}{1 + K'_P} \qquad K'_P = f_{OM} v_Q (\rho_{part} / \rho_{oct}) K_{OA}$$

v_Q is the volume fraction of particles in the atmosphere,
f_{OM} is the volume fraction of organic matter in the particle,
ρ_{part} and ρ_{oct} are the densities of the particles and n-octanol

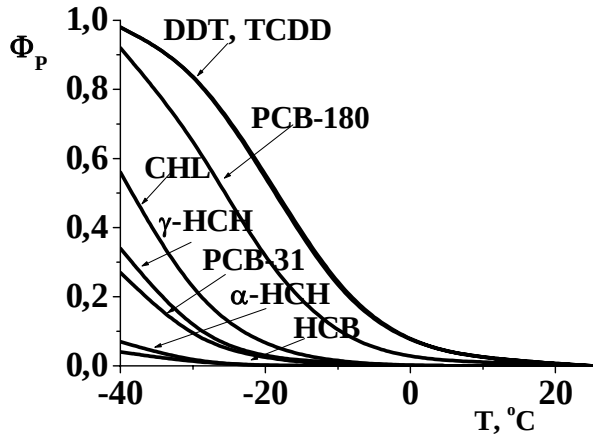

The heavy PCBs congeners (starting with penta-CB), TCDDs, TCDFs and their more heavy congeners, and DDT would be entirely particle-bounded at typical winter temperatures. These POPs, called "single hoppers", are usually deposited irreversibly to the Earth' surface. The rest of the POPs are referred to "multiple hoppers" and they readily undergo air – underlying surface exchange

SCAVENGING BY SNOW FROM AIR

- The snow - gas-phase scavenging ratio ($W_{gas,snow}$) being given by:

$$W_{gas\text{-}snow} = K_{IA} SA_s \rho_w$$

K_{IA}: the water/air interface – air partition coefficient

SA_s: the snow specific surface area

ρ_w: the density of water

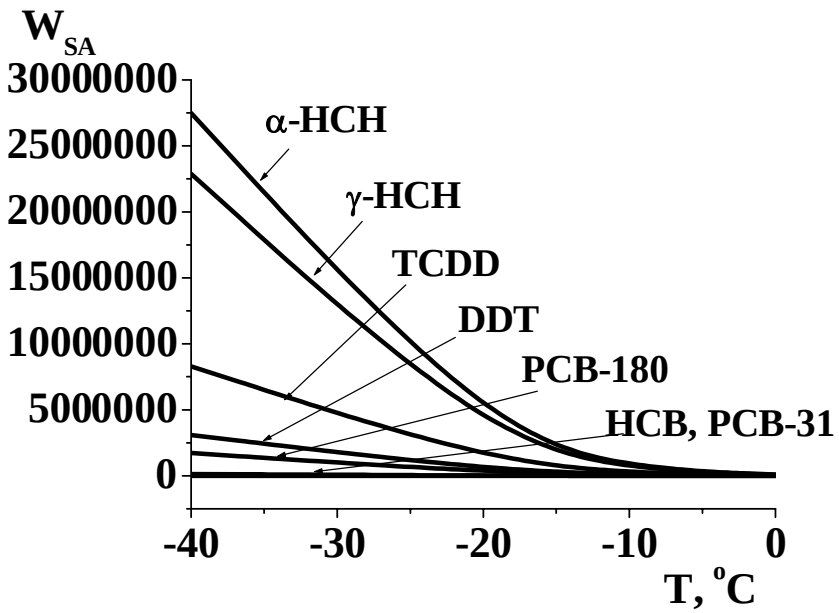

The snow scavenging at low air temperatures would be very effective way for removal of the POPs from atmosphere, with the exception of HCB and light PCBs congeners

ATMOSPHERIC PERSISTENCE

- **The drop of temperature strongly influences on atmospheric half-live of the POPs ($\tau_{1/2}$)**
- **Reaction of gaseous POPs with OH radical in atmosphere is the major loss process**
- **Lowering the temperature leads to deceleration of the reaction due to reduction both of the rate coefficient and the atmospheric concentration of OH radical**
- **Second effect of the temperature lowering is the increase of non-reactive particle-bound fraction for the OCs. Sorption of the OCs on atmospheric particulates can lead to growth of their gas phase half-lives**

$$\tau_{1/2(A,P)} = \frac{\ln 2\{1 + f_{OM}(\rho_{part} / \rho_{oct})K_{OA}\nu_Q\}}{k_{OH}[OH]}$$

k_{OH} is the bimolecular rate coefficient for reaction of a chemical with OH radical and [OH] is the concentration of OH radical in air

ATMOSPHERIC PERSISTENCE

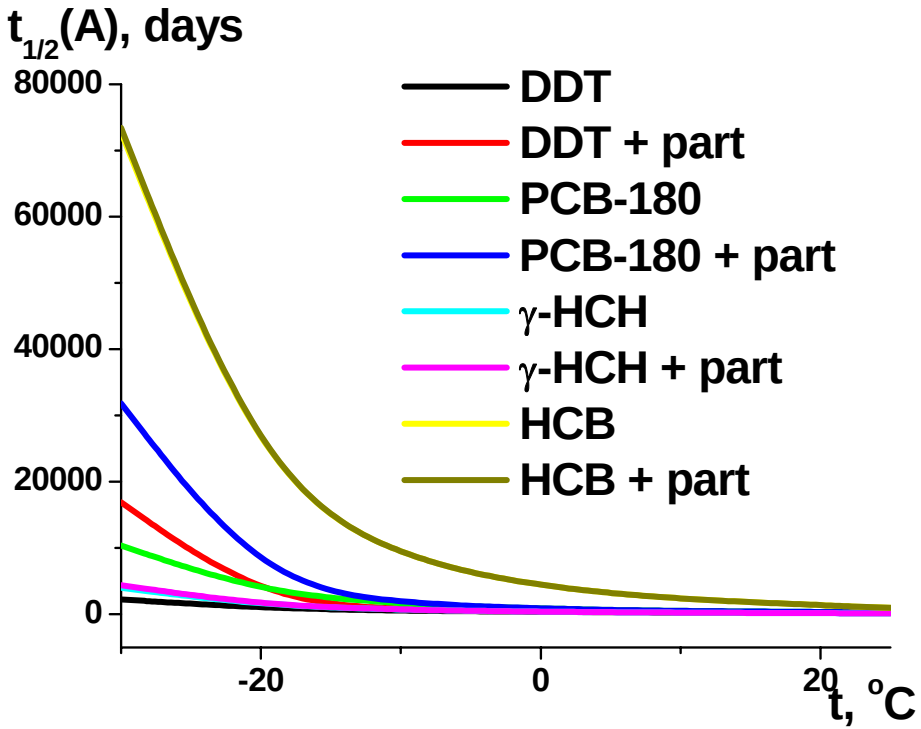

The gas-particle partitioning at low temperature greatly increases the gas phase half-lives for the POPs. This effect is more pronounced for heavy PCBs, PCDDs and PCDFs congeners and for DDTs family. The loss of the POPs by degradation in cold tropospheric atmosphere is insignificant way of their removal and such sinks for the POPs on the underlying surfaces as their microbial decomposition in the soils, lake and river sediments would be more considerable

Intermediate conclusions

- **Now, the dust particles, combustion and industrial aerosols from Ukraine are observed in several parts of Central, Northern and Southern Europe**
- **These particulates can affect on radiative atmospheric budget, visibility of atmosphere, its chemical composition, climate and on the human and ecosystem health in Europe**
- **They are also carriers for transport of POPs over a long distances to Europe from their industrial and agricultural sources in Ukraine**
- **It was found that heavy PCB congeners (starting from penta-CB), TCDDs, TCDFs and their more heavy congeners, and DDTs would be entirely particle-bounded at low tropospheric temperatures**
- **The snow scavenging at low temperatures would be very effective way for removal of the POPs from atmosphere, with the exception of HCB and light PCB congeners**
- **The gas-particle partitioning at low temperature greatly increases the gas phase half-lives of the POPs. This effect is more pronounced for heavy PCBs, PCDDs and PCDFs congeners, and for DDTs family**
- **International cooperation with Europian countries and national funding are need to develop the modern aerosol observational network, the detailed study of the aerosol' composition and the modeling the aerosol' dynamics in Ukraine. This is an exceptional national problem together with such main problems as monitoring of greenhouse gases and ozone level in Ukraine**

Most of heterogeneous transformations on the aerosols surface can be an important way of sink for inorganic (HCl, HBr, HI, HNO_3, NO_2, N_2O_5, SO_2, COS, CS_2, O_3) organic impurities (VOCs, CFCs, HCFCs, PAHs, POPs) and radicals (HO, HO_2, NO_3, RO, RO_2) in air

They are comparable on the rate with such homogeneous ways of their sink, as their photolysis or their interaction with HOx and NO3 radicals

The considerable sink of these impurities from troposphere via the heterogeneous mechanism is bound to be substantially in their photochemical cycles, and in the content of O_3, HO_x, NO_x, SO_2 and halogen oxides in troposphere, especially at night time

- **Volatile organic compounds (VOCs) used as solvents and refrigerants are important priority toxic pollutants because exposure to the dangerous VOCs can be injurious to human health and ecosystems**
- **VOCs participate in much heterogeneous industrial and natural processes, such as developing of stratospheric ozone hole over Antarctica and decreasing the tropospheric oxidation potential**
- **Knowledge of VOCs adsorption from gas phase to such interfaces as water, snow, plants, rocks, soils and sediments, organic, carbonaceous and mineral aerosols is important for assessing the partitioning and transport of the organics in our environment**

The following problems in description of VOCs interaction with surface of atmospheric aerosols:

- **Current air/particle partition models ignored the effect of different surface chemistry of the particles and non-additivity of the VOCs/surface interaction on the partitioning**
- **Quantitative "structure-activity" relationships are not developed for uptake kinetics of VOCs by aerosol surfaces**
- **Also, these models ignored the effect of significant surface heterogeneity of the solid aerosols on the partition thermodynamics and on the reaction surface kinetics of VOCs**
- **Development of QSARs for VOCs interaction (adsorption equlibrium, chemisorption kinetics)**
- **Description of adsorption thermodynamics of VOCs, their chemisorption, desorption and bimolecular reaction kinetics on the heterogeneous surface of the solid aerosol components**

Building Blocks of the Partitioning Model

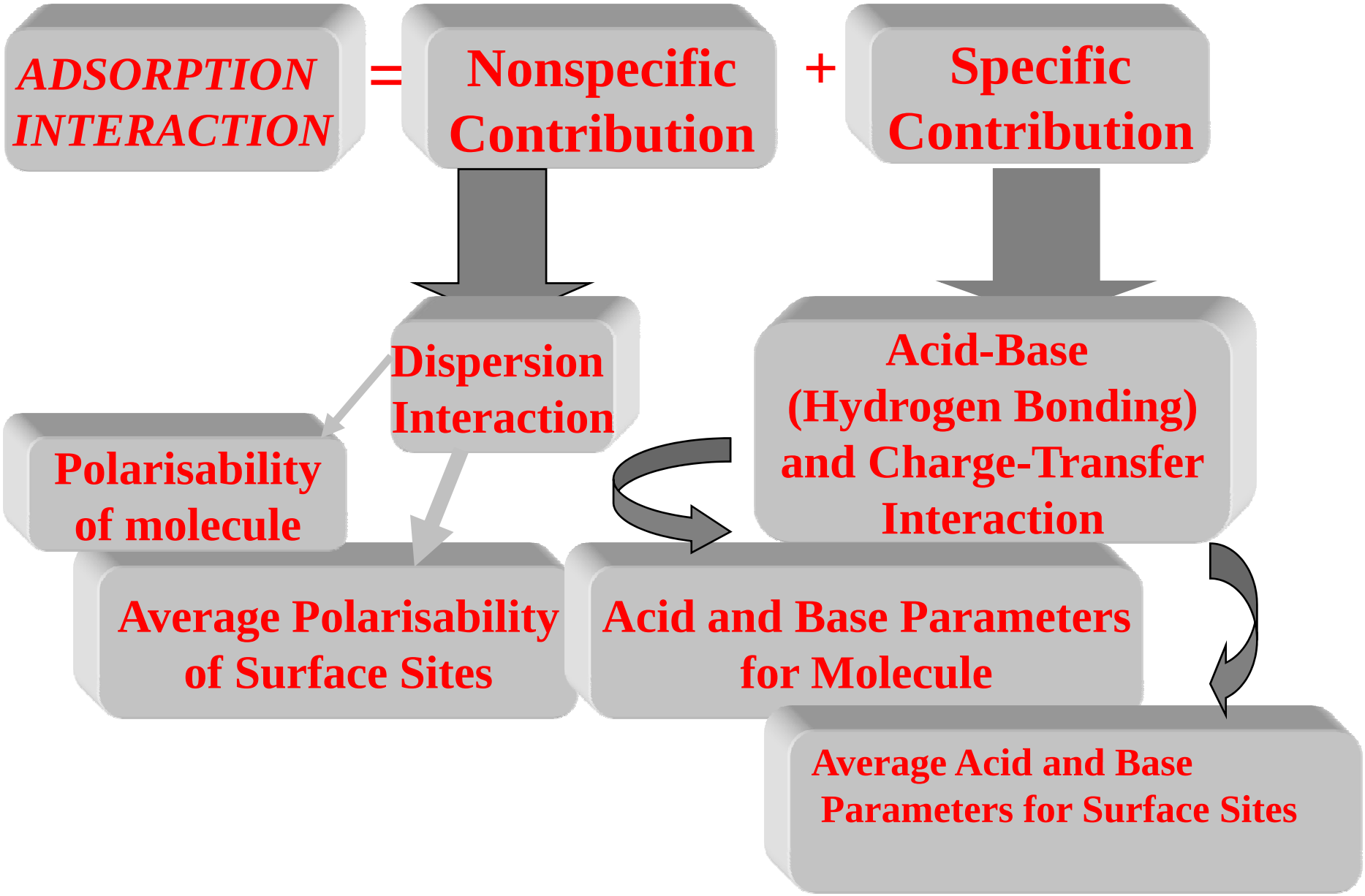

Non-specific interaction

$$\Delta H_A = \Delta H_A^{nsp} + \Delta H_A^{sp}$$

$$\Delta G_A = \Delta G_A^{nsp} + \Delta G_A^{sp}$$

$$w_d = -\frac{3}{2} h \left(\frac{\nu_1 \nu_2}{\nu_1 + \nu_2}\right) \alpha_{e1} \alpha_{e2} \frac{N_A}{(4\pi\varepsilon_0)^2} \left(\frac{1}{r_{1,2}}\right)^6$$

$$-\Delta G_A^{nsp} = K_G \times \alpha_e + \zeta_G \qquad K_G = 0.0397(52.6 - 0.058T)^{1/2} (\gamma_S^D)^{1/2}$$

$$-\Delta H_A^{nsp} = K_H \times \alpha_e + \zeta_H \qquad K_H = K_G \frac{T_{is}}{T_{is} - T}$$

Specific interaction

$$-\Delta G_A = K_G \times \alpha_e + \alpha_{S(G)} \times \Sigma\beta_2^H + \beta_{S(G)} \times \Sigma\alpha_2^H + \varsigma_G$$

$$-\Delta H_A = K_H \times \alpha_e + \alpha_{S(H)} \times \Sigma\beta_2^H + \beta_{S(H)} \times \Sigma\alpha_2^H + \varsigma_H$$

$$-\Delta H_A^{sp} = 3.2 \times K_B \times \Sigma\alpha_2^H + 2.6 \times K_A \times \Sigma\beta_2^H + 0.5 \times K_B - 0.3 \times K_A$$

$$-\Delta H_A^{sp} = 1.1 \times K_B^* \times \Sigma\alpha_2^H + 2.6 \times K_A \times \Sigma\beta_2^H + 0.04 \times K_B^* - 0.3 \times K_A$$

$$\alpha_{S(H)} = \alpha_{S(G)} \frac{T_{is}}{T_{is} - T} \qquad \beta_{S(H)} = \beta_{S(G)} \frac{T_{is}}{T_{is} - T}$$

Compensation effect at adsorption of VOCs on solid materials

$\Delta G_A = a\Delta H_A + b$; $\Delta H_A = \Delta G_A(T_{is}) + T_{is}\Delta S_A$;

$a = 1 - T/T_{is}$; $b = \Delta G_A(T_{is})\, T/T_{is}$

Carbopack

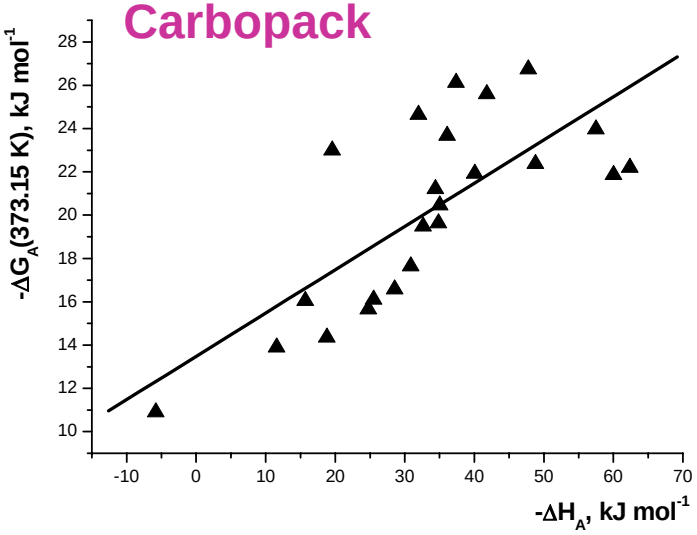

Carbosil

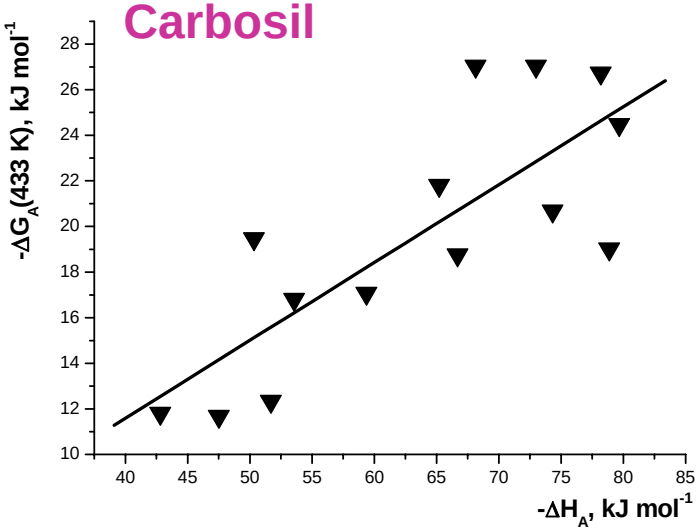

Silica Gel

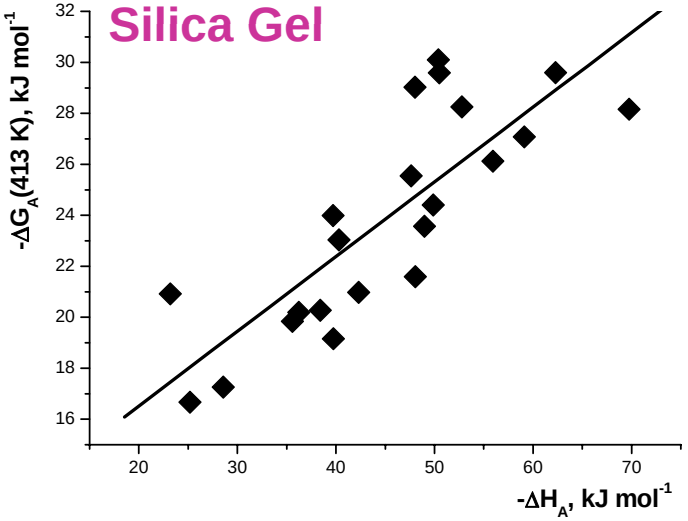

Titania and titania/alumina/silica

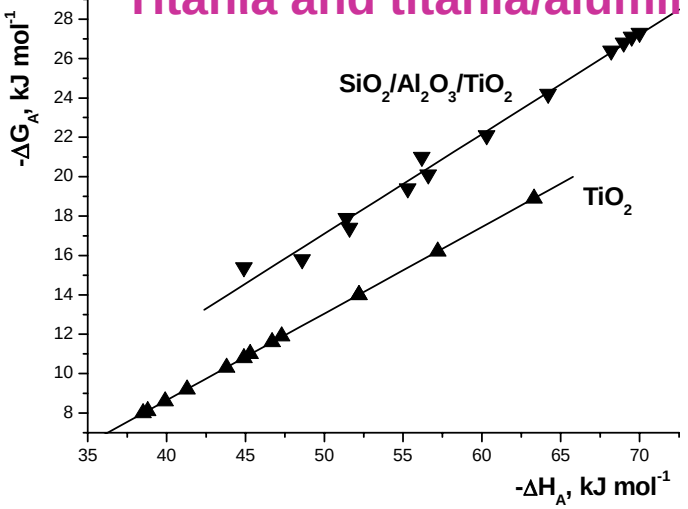

Estimation of acid-base descriptors for VOCs

[basicity] ~ [proton affinity, (*PA*)] ~
[maximum negative charge on an atom in molecule, (q^-_{max})] ~
[basicity in an standard equilibrium]

[acidity] ~ [XR-H dissociation energy, (*ER-H*)] ~
[maximum positive charge on an H atom in molecule, (q^+_{max})] ~
[acidity in an standard equilibrium, (pK_{HB})]

$\Sigma\alpha_2^H = -0.11\pm0.03 + (2.7\pm0.3)\times q^+_{max}$; N = 52; r = 0.820

$\Sigma\beta_2^H = -0.04\pm0.04 + (1.5\pm0.2)\times q^-_{max}$; N = 52; r = 0.827

$\Sigma\alpha_2^H = 0.135\cdot H^+_{max} - 0.01$; N = 32; r = 0.780

$\Sigma\beta_2^H = 0.00334\cdot PA - 0.444$; N = 15; r = 0.834

$\Sigma\beta_2^H = 0.0071\cdot \nu_{OH} + 0.08$; N = 5; r = 0.994

QSARs for air/particle partitioning of POPs with their quantum chemical descriptors

$$\log(K_P) = a + b \times \alpha_e + c \times q^-_{\max}$$

$\log(K_P) = -3.6\pm1.6 + (0.05\pm0.02)\alpha_e + (6.1\pm8.6)q^-_{max}$, $R^2 = 0.899$
5 PAHs on urban aerosols (Athens, Greece)

$\log(K_P) = -4.7\pm1.4 + (0.20\pm0.04)\,\alpha_e + (23.1\pm4.3)\,q^-_{max}$, $R^2 = 0.776$
8 PCBs and PCDD/Fs on urban aerosols (Auxburg, Germany)

$\log(K_P) = -16.5\pm1.7 + (0.52\pm0.05)\alpha_e + (7.6\pm3.2)q^-_{max}$, $R^2 = 0.941$
16 PCDD/Fs on urban aerosols (Tokyo, Japan)

$\log(K_P) = -14.4\pm0.9 + (0.54\pm0.02)\alpha_e + (0.3\pm1.6)q^-_{max}$, $R^2 = 0.983$
16 PCDD/Fs on background aerosols (Alert, Canadian Artic)

$\log(K_P) = -9.2\pm6.0 + (0.30\pm0.03)\alpha_e + (13\pm32)q^-_{max}$, $R^2 = 0.937$
8 PAHs on model secondary organic aerosols at RH = 10%

$\log(K_P) = 0.9\pm0.5 + (0.27\pm0.02)\alpha_e + (9.7\pm1.8)q^-_{max}$, $R^2 = 0.908$
24 PCBs on sandy soils near Beirut, Libyan

Comparison of coefficients in the QSARs for different solid and liquid surfaces

i. Parent and modified carbonaceous solids

for microporous solids: $K_G(0) = K_G\left(1-\frac{d}{2a}\right)^3 \quad K_H(0) = K_H\left(1-\frac{d}{2a}\right)^3$

ii. Parent and modified inorganic solids

$$K_G = 0.540 A_H^{1/2}$$

$$K_{G(app)} = \sum_{i=1}^{n} \theta_i K_{G(i)}$$

A_H = -6.2±2.8 + (9.1±1.5)n_0; N = 23, r = 0.789

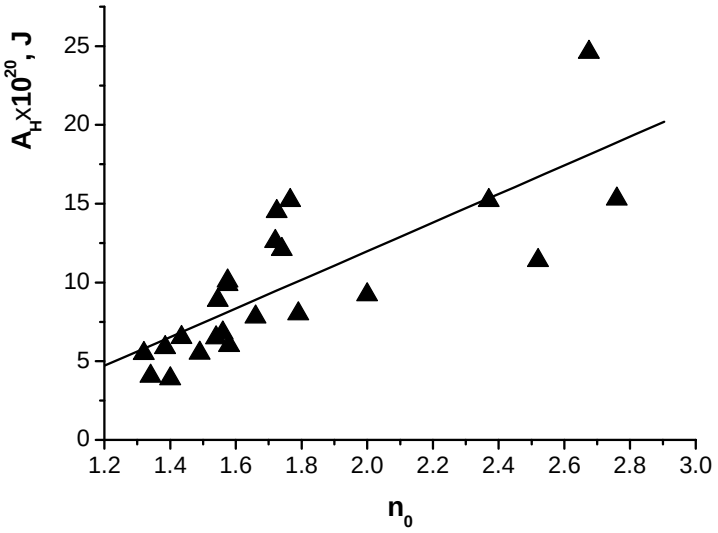

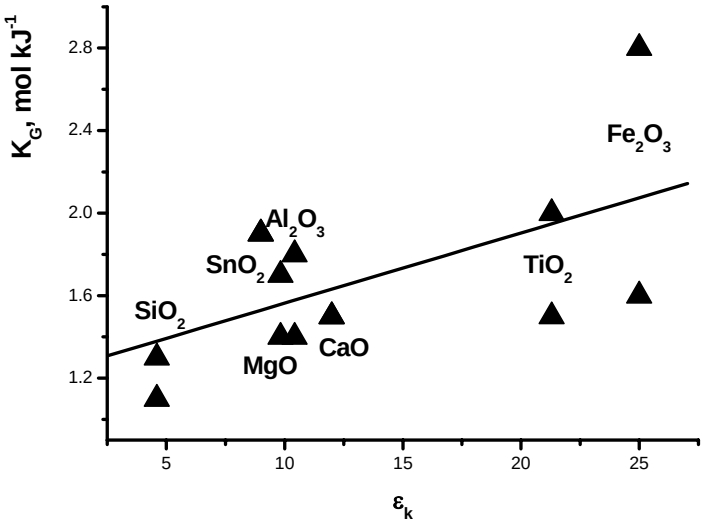

Diagrams for normalized parameters of surface sites of carbonized (1), inorganic (2), organic (3) materials and water, snow and soils (4)

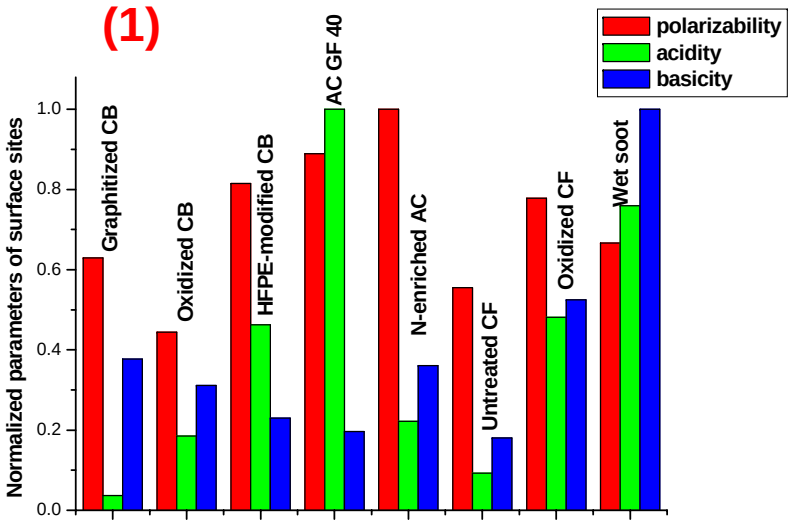

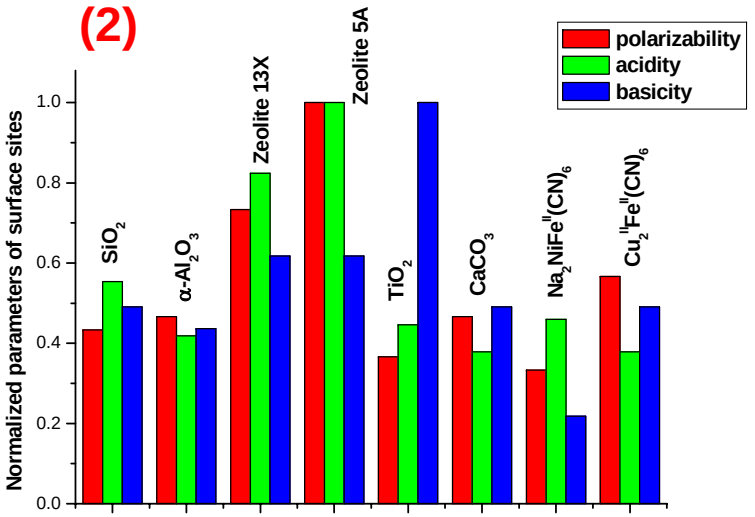

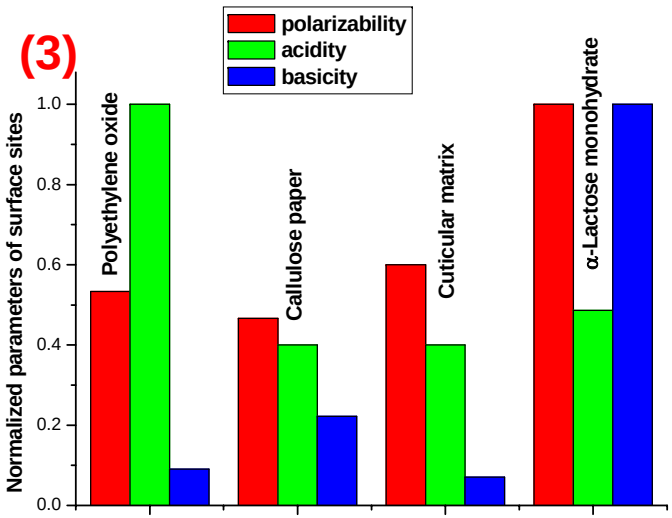

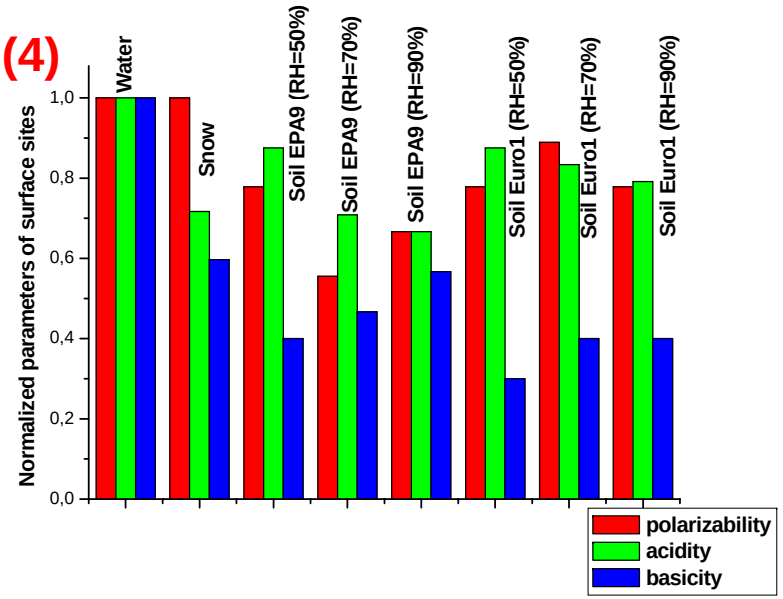

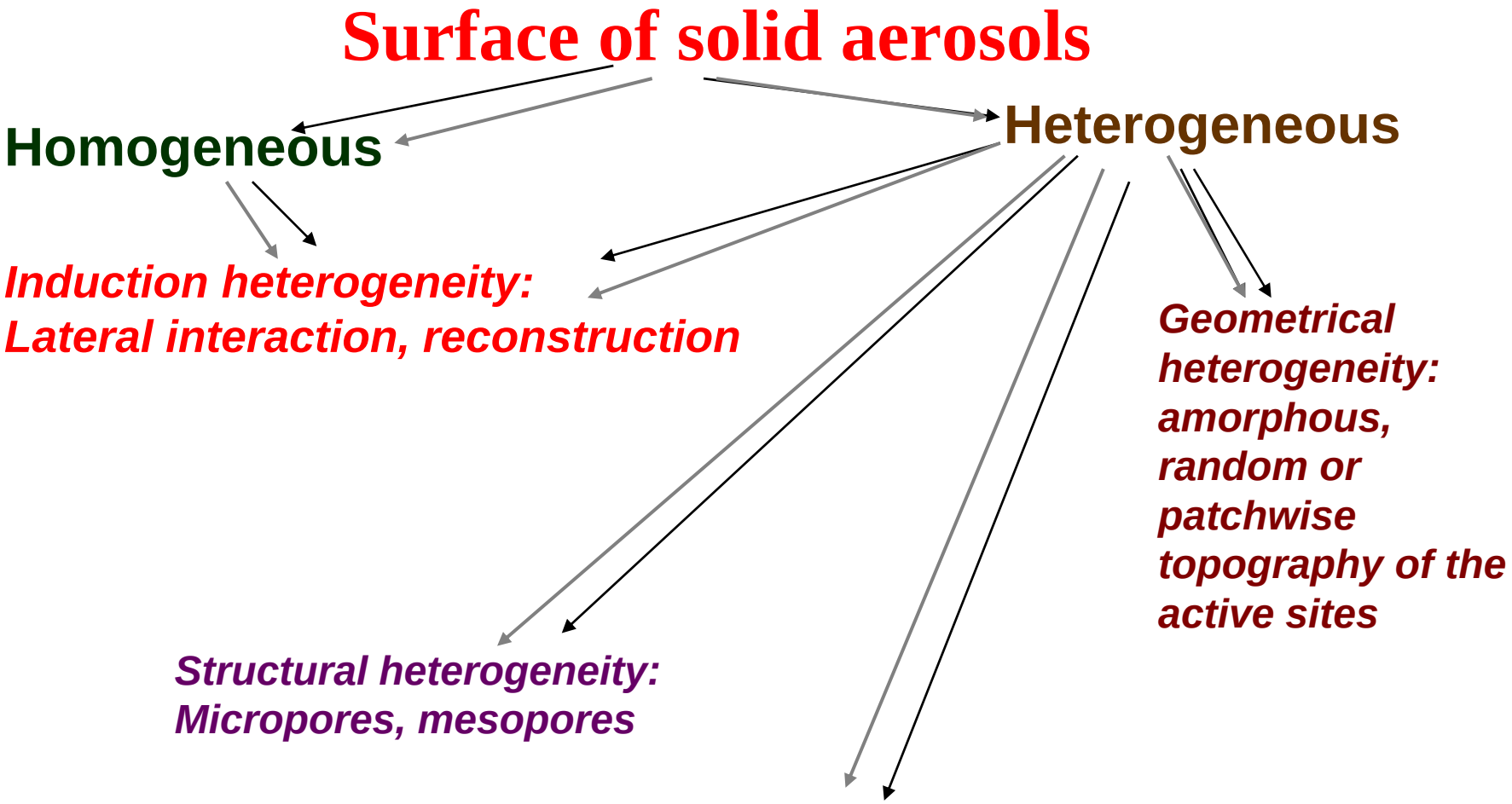
Surface of solid aerosols
Homogeneous
Heterogeneous
Induction heterogeneity:
Lateral interaction, reconstruction
Geometrical heterogeneity:
amorphous, random or patchwise topography of the active sites
Structural heterogeneity:
Micropores, mesopores
Chemical heterogeneity:
lattice defects, different types of the active sites (Lewis, Bronsted acid-base sites, etc.)

Description of adsorption energy distribution using several numerical procedures

CA: condensation approximation

RP: regularization procedure

da/dQ = f(Q): 1st derivative on isosteric adsorption heat

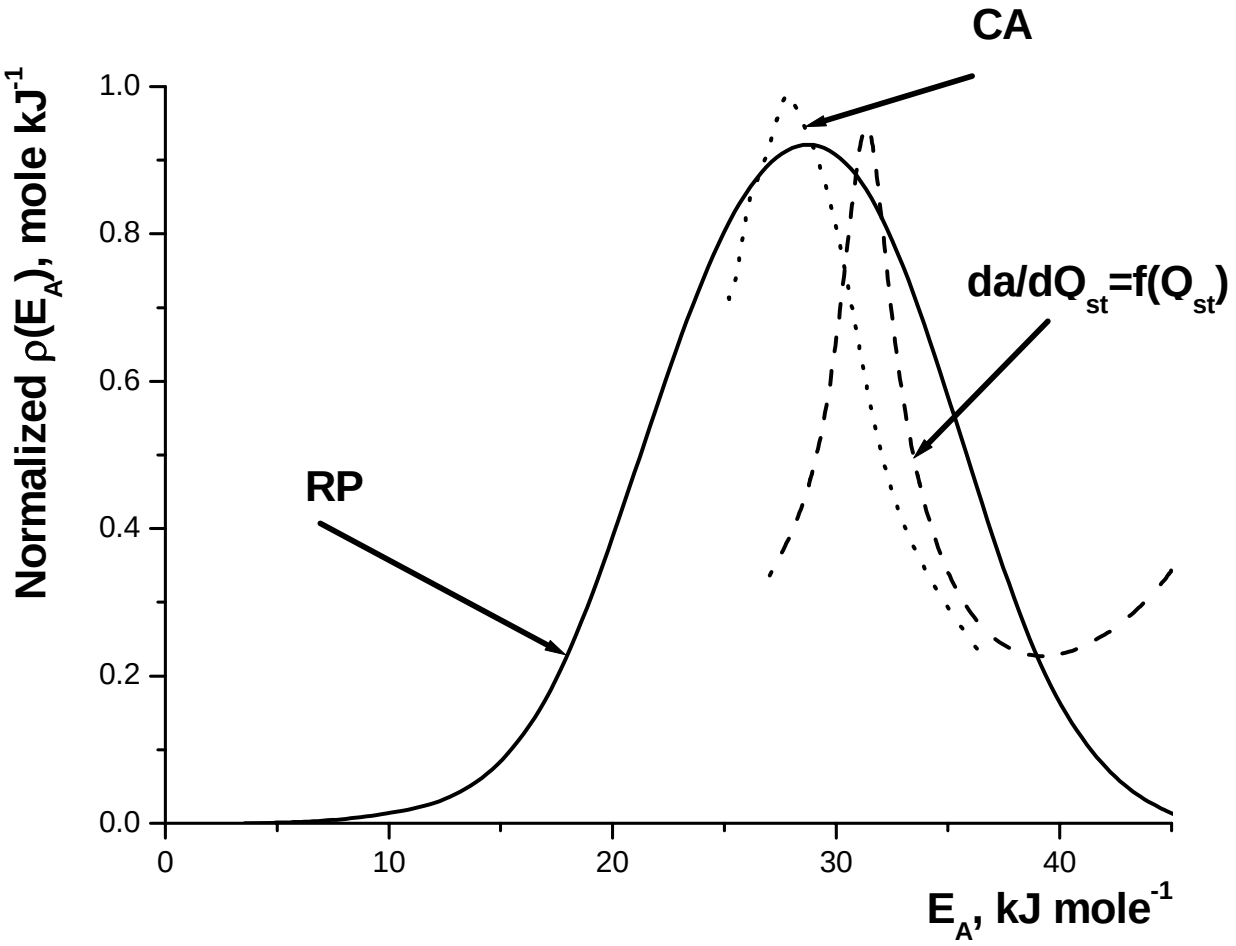

Distributions of surrogates for solid aerosols on adsorption energies of atmospheric impurities

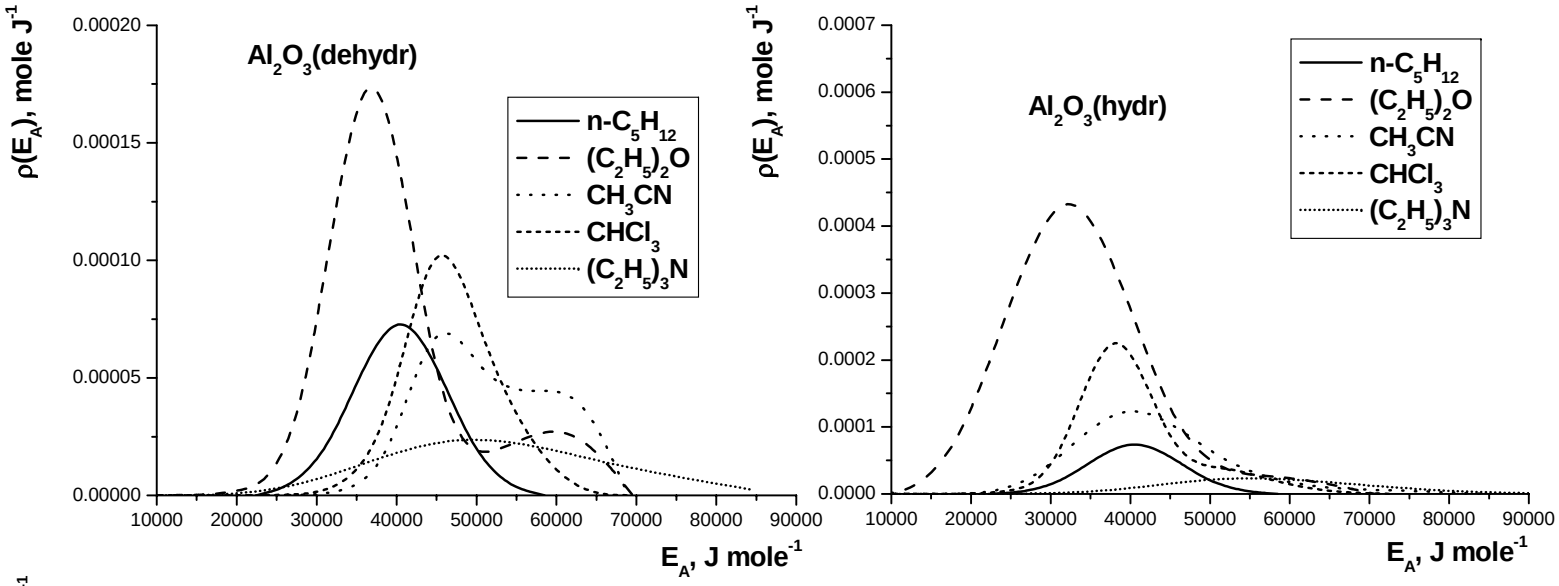

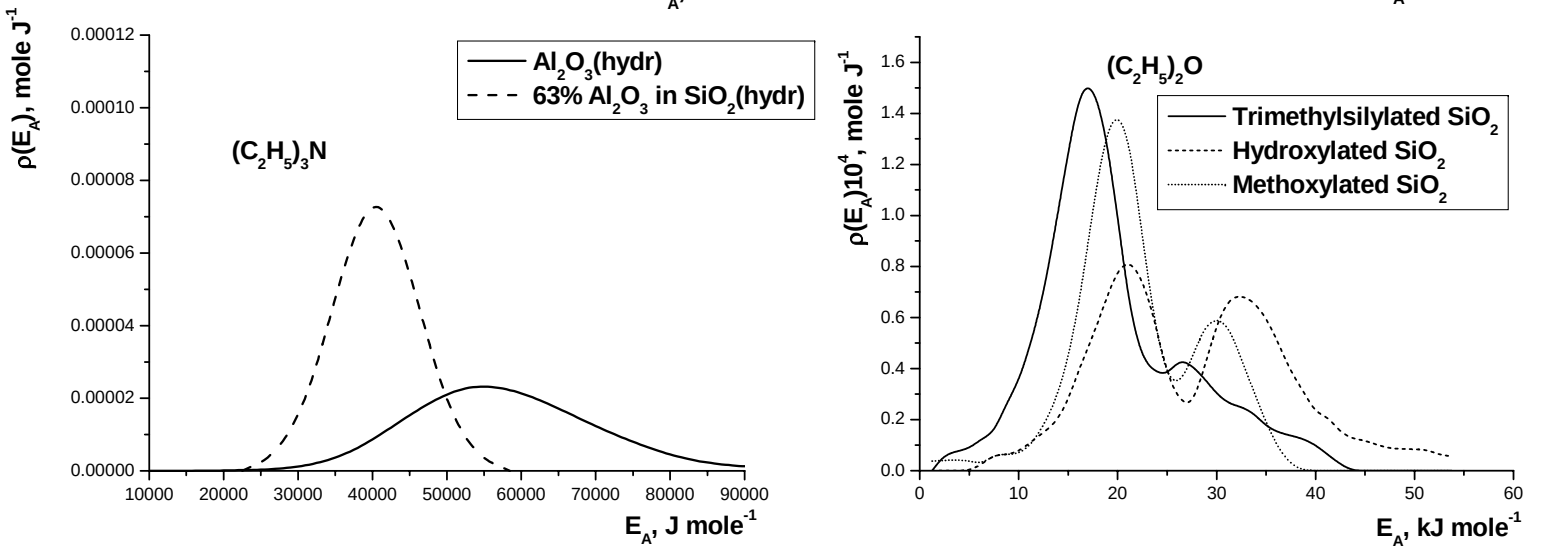

Distributions of surrogates for solid aerosols on adsorption energies of atmospheric impurities

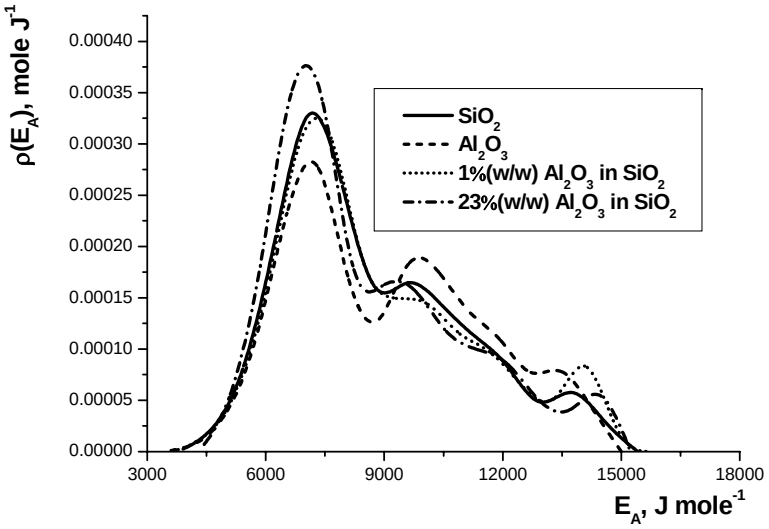

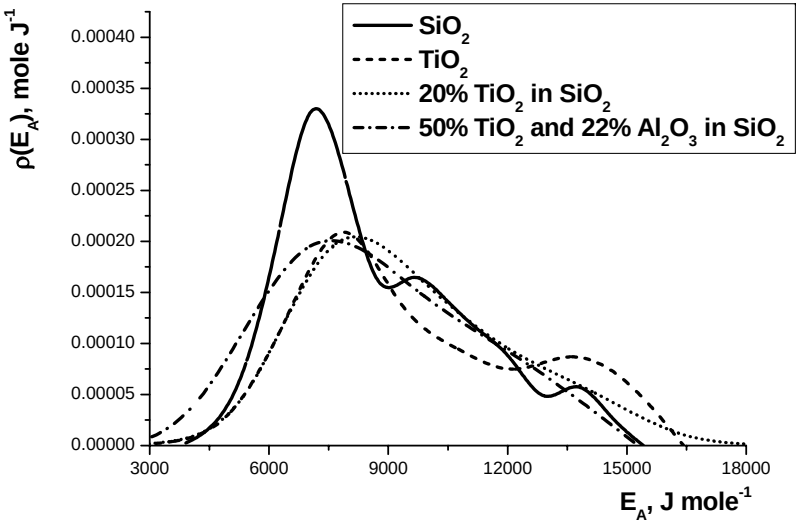

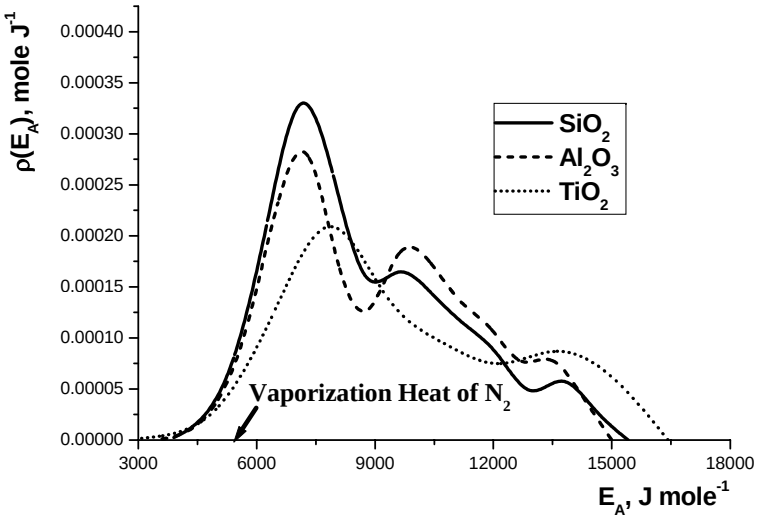

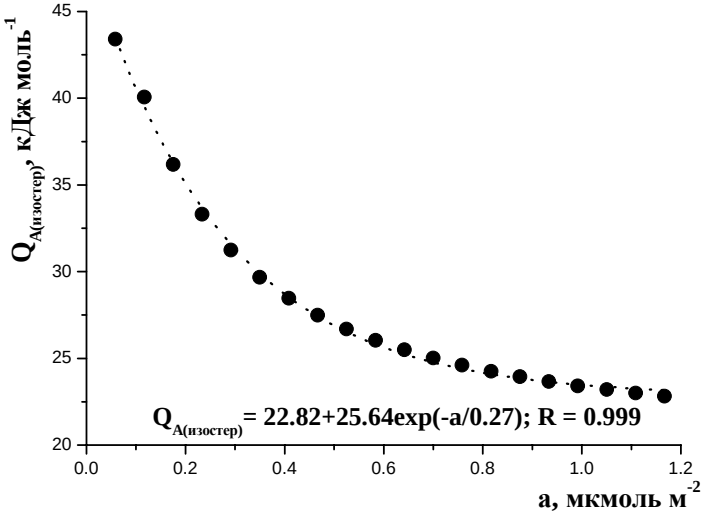

Adsorption of atmospheric impurities on surrogates of solid aerosols as revealed by IGC method at finite concentrations

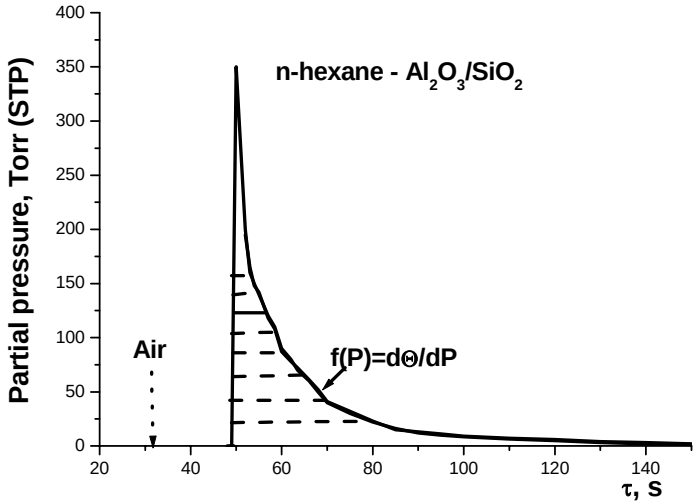

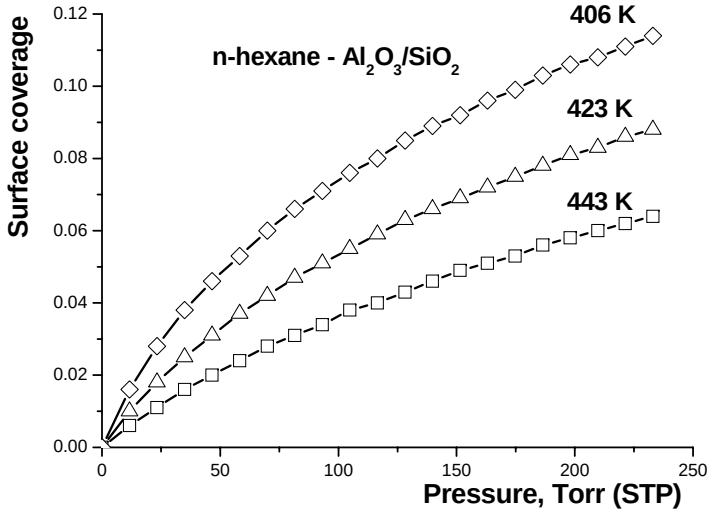

Effect of surface heterogeneity of surrogates for solid aerosols on adsorption energies of halocarbons

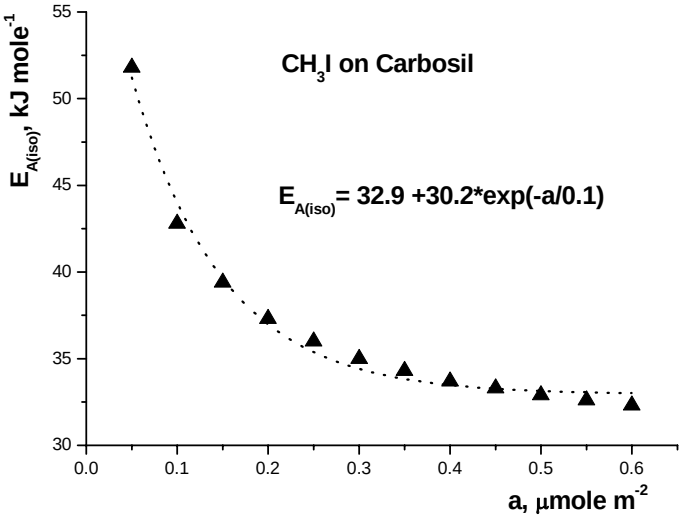

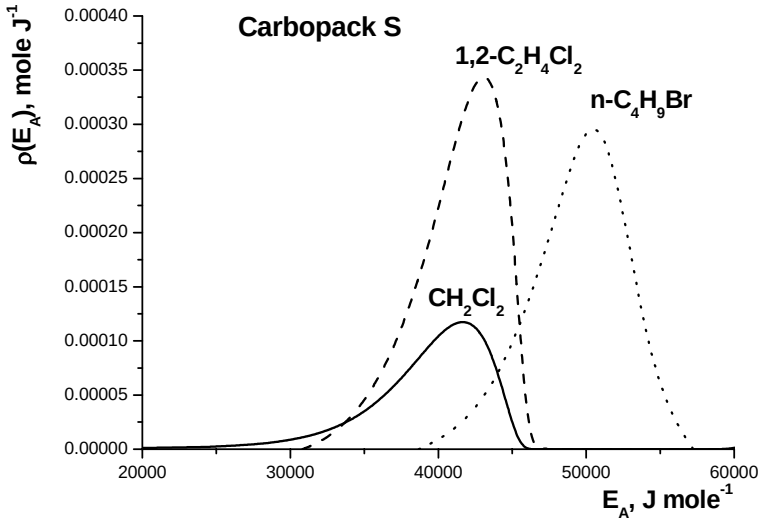

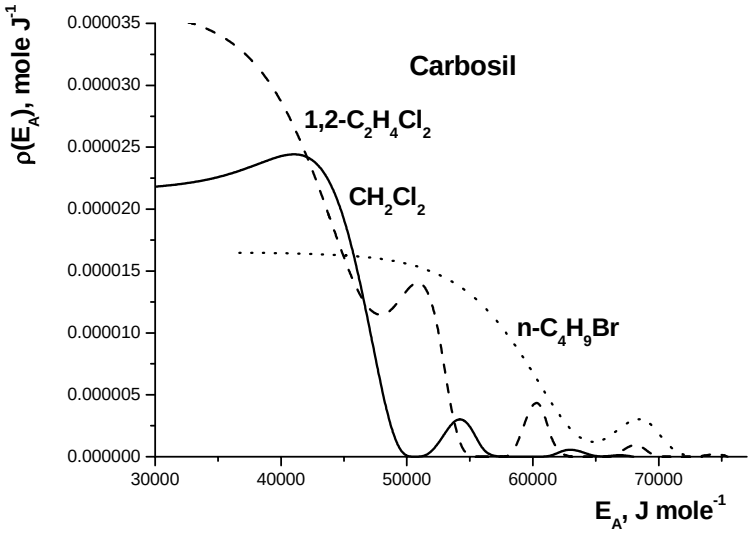

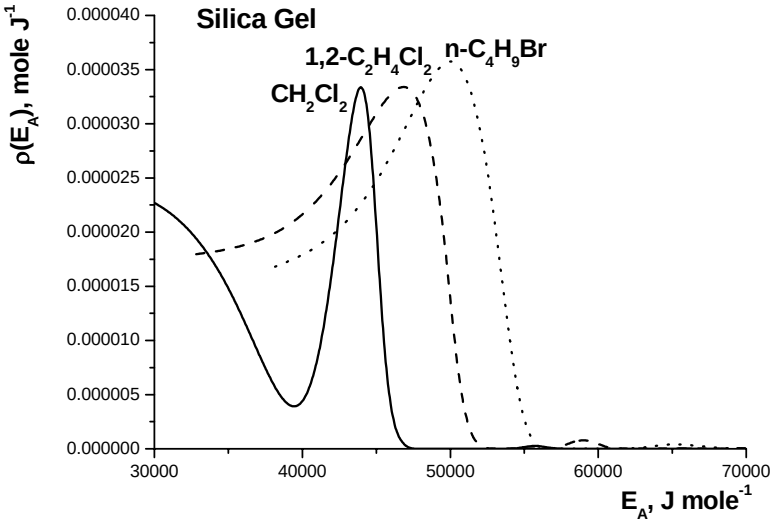

QSARs for adsorption of 23 VOCs on surface of surrogates for solid aerosols at finite concentrations

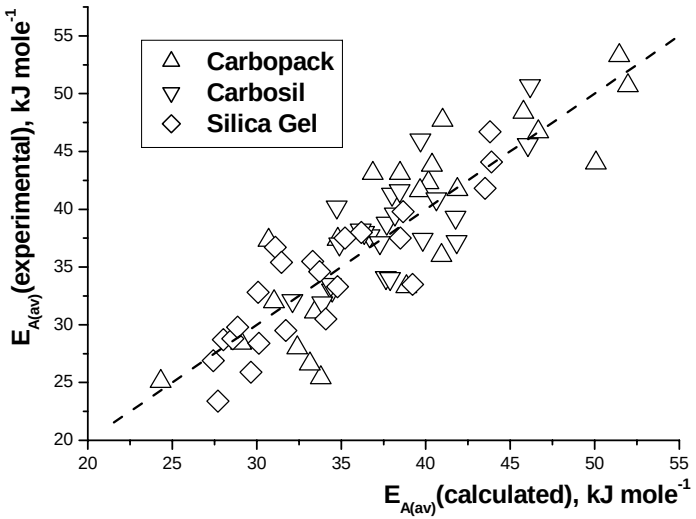

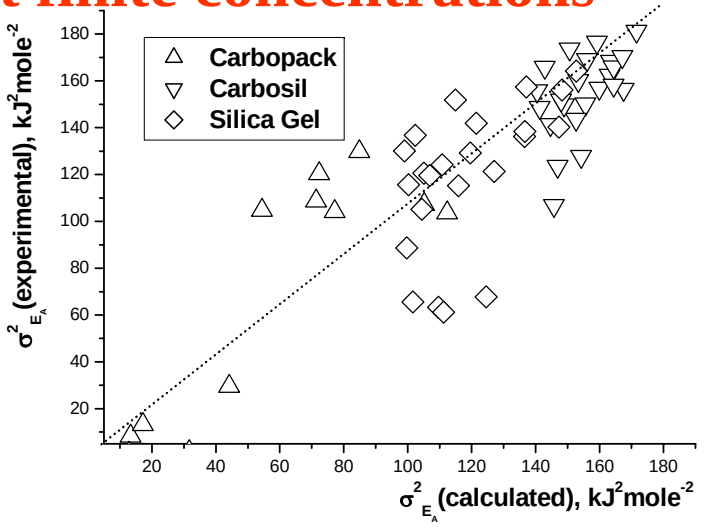

$$\Theta(P,T) = \int_{E_{A(\min)}}^{E_{A(\max)}} \theta(P,T)\rho(E_A)dE_A$$

$$\theta(P,T) = \frac{P \times K_0^{-1} \exp(E_A / RT)}{1 + P \times K_0^{-1} \exp(E_A / RT)}$$

$$\rho(E_A) = \begin{cases} \dfrac{1}{E_{A(\max)} - E_{A(\min)}} \\ 0 \end{cases}$$

$$E_{A(\min)} \le E_A \le E_{A(\max)}$$

$$E_A < E_{A(\min)}; E_A > E_{A(\max)}$$

$$K_I = E_{A(av)} = \frac{E_{A(\max)} + E_{A(\min)}}{2}$$

$$K_{II} = \sigma_{Ea}^2 = \frac{E_{A(\max)}^3 - E_{A(\min)}^3}{3(E_{A(\max)} - E_{A(\min)})} - K_I^2$$

Carbopack $E_{A(av)} = 9.8 + 3.1 \times \alpha_e + 29.2 \times \Sigma\alpha_2^H$ $\sigma_E^2 = 182 - 15.7 \times \alpha_e$

Carbosil: $E_{A(av)} = 24.4 + 1.0 \times \alpha_e + 30 \times \Sigma\alpha_2^H + 11.6 \times \Sigma\beta_2^H$ $\sigma_E^2 = 126 + 2.8 \times \alpha_e + 89 \times \Sigma\alpha_2^H$

Silica Gel: $E_{A(av)} = 21.1 + 0.66 \times \alpha_e + 19.4 \times \Sigma\alpha_2^H + 25.3 \times \Sigma\beta_2^H$ $\sigma_E^2 = 84 + 84 \times \Sigma\beta_2^H$

Compensation behavior in adsorption of halocarbons on heterogeneous surface of surrogates for solid aerosols

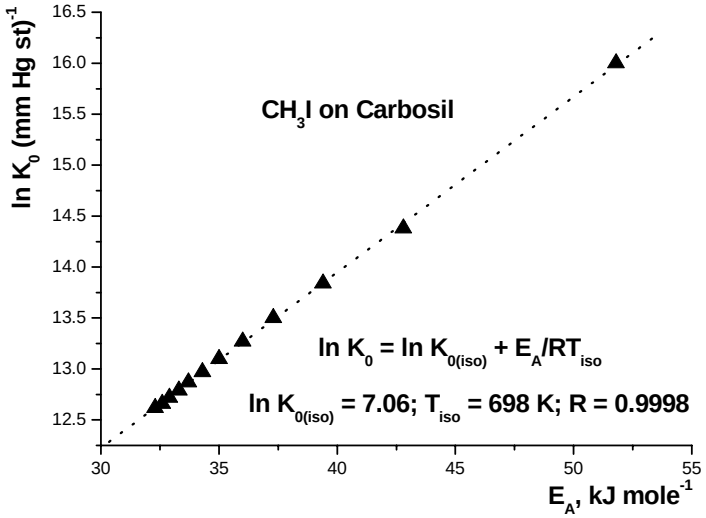

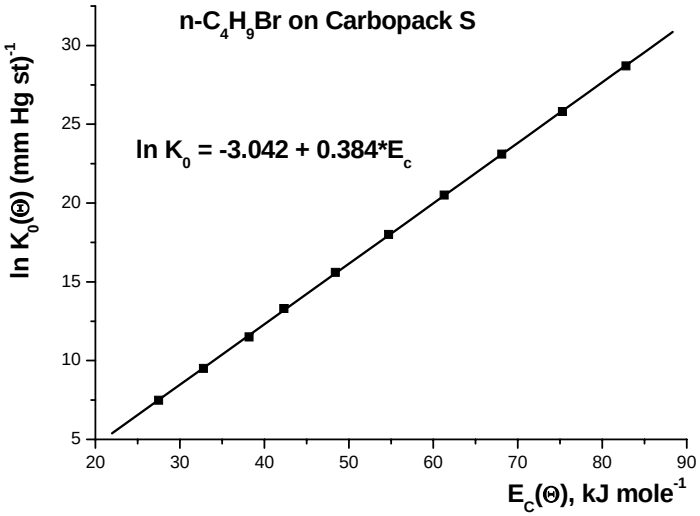

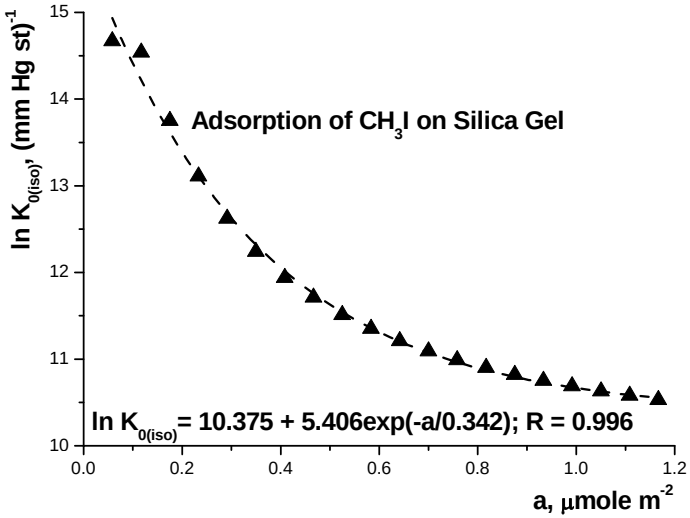

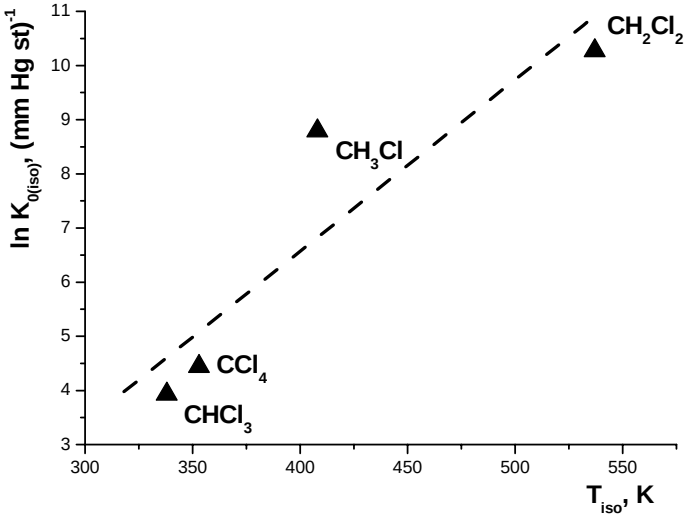

Dependencies of partition coefficients for CH_3I from air to surface of aerosol' surrogates on the relative surface coverage and temperature

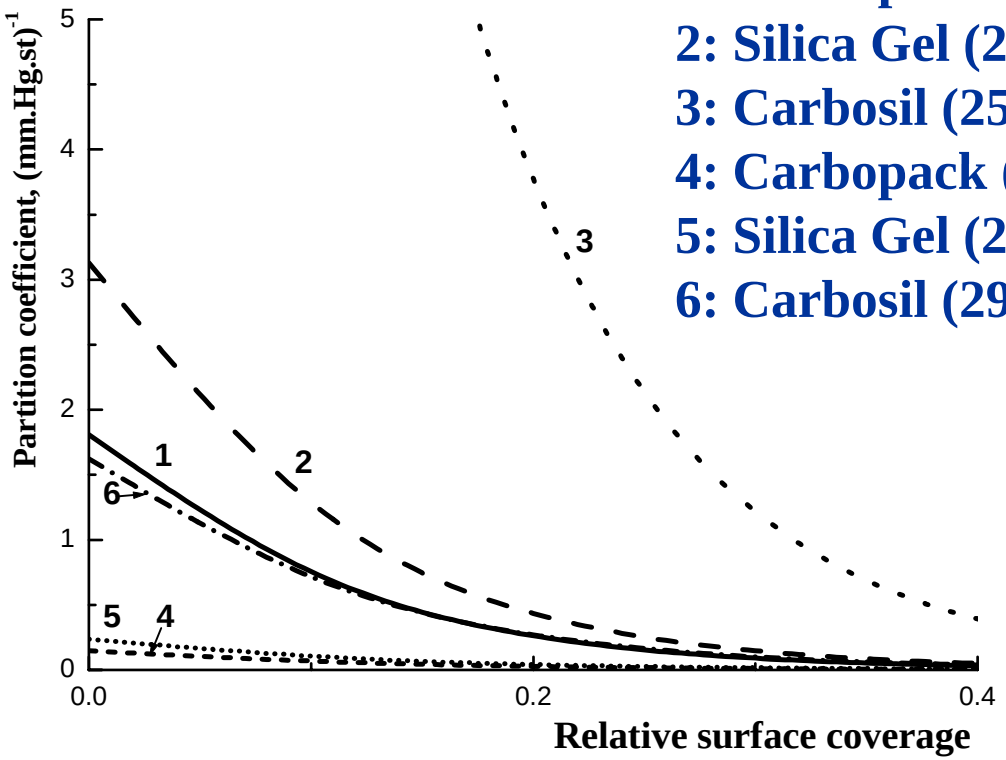

1: Carbopack (253 K)
2: Silica Gel (253 K)
3: Carbosil (253 K)
4: Carbopack (293 K)
5: Silica Gel (293 K)
6: Carbosil (293 K)

The partition coefficients vastly depend on the aerosol' surface chemistry.
They drop exponentially as the surface coverage rises even at small θ.
Reduction of the temperature results in substantial increase of the coefficients.

Influence of non-uniformity of aerosol surface on kinetics of the heterogeneous atmospheric sink for the VOCs

- **The rate of reaction of gas-phase A with the homogeneous aerosol surface sites S with formation of the chemisorbed product AS:**

A + S → AS

$$-\frac{d[A]_t}{dt} = \gamma\varpi[A]_t = \gamma\frac{\bar{c}}{4}S_A m[A]_t$$

$[A]_t$ – the gas phase concentration of A at t,
γ – the uptake coefficient,
ω – the collision rate of A with the particle surface,
$\bar{c}$ - mean gas phase velocity of A toward the particle,
S_A – specific adsorption area of the particles,
m – weight of the particles per air volume

$$[A]_t = [A]_0 \exp(-k't) \qquad k' = \gamma\varpi = \gamma\frac{\bar{c}}{4}S_A m$$

The rate equation for heterogeneous aerosol surface is:

$$[A]_t = [A]_0 \int_{k'_{min}}^{k'_{max}} \exp(-k_i' t)\rho(k')dk'$$

$[A]_0$ – the gas phase concentration of A at t = 0,
ρ(k') – the surface differential distribution function on k' coefficient
k'_{min} and k'_{max} – the minimal and maximal coefficients k'

For Γ- distribution on coefficient k': $\rho(k') = \exp(-k'_{min}\ t)\left(\frac{b}{b-t}\right)^a$

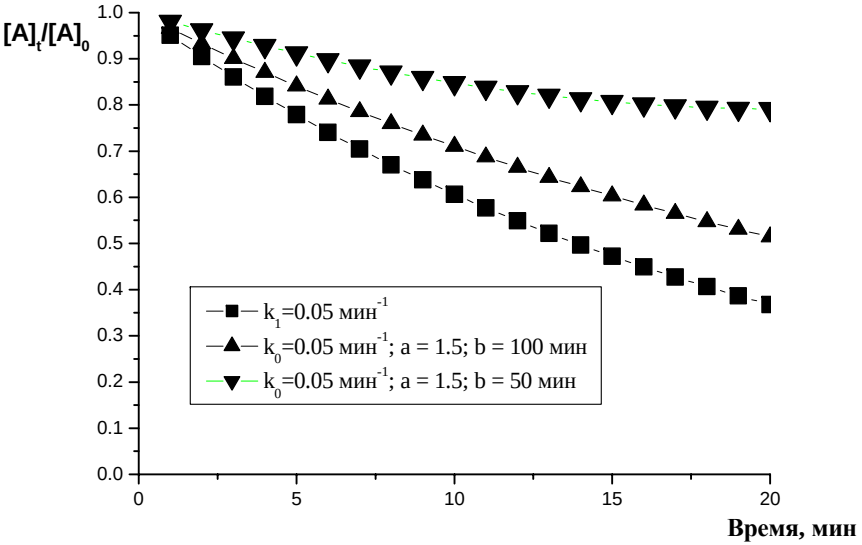

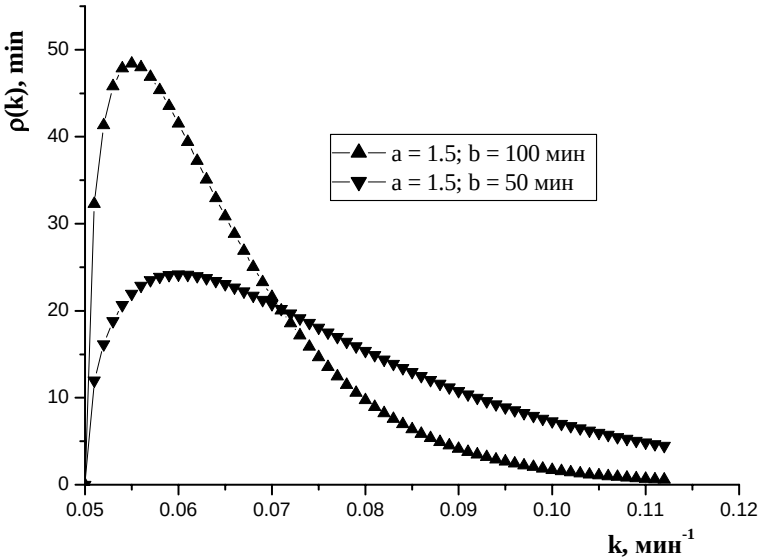

Kinetics on heterogeneous surface with its power distribution on coefficient k’

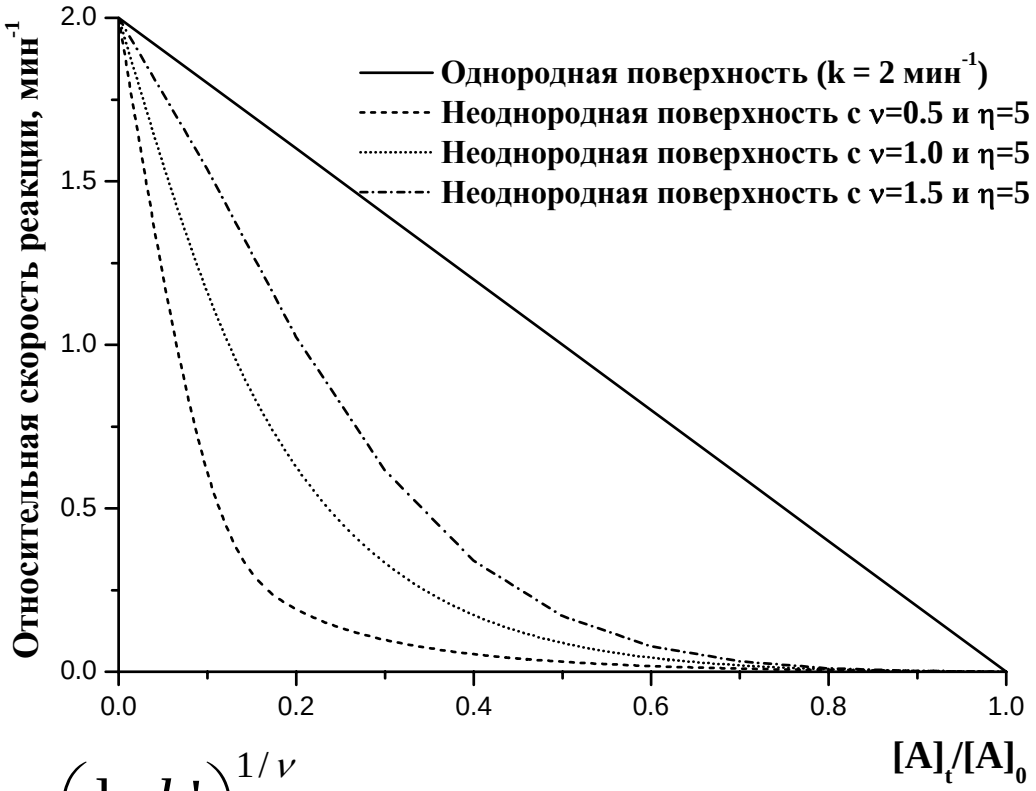

$$\rho(\ln k') = \frac{\left(\frac{\ln k'}{\eta}\right)^{1/\nu}}{\nu \ln k'}$$ **; η = ln k’$_{max}$ – ln k’$_{min}$**

Diffusion correction to rate equation on the aerosol surface

Coefficient k' depends on the dimension of the aerosol particles:

$$k' = \frac{\gamma \times \left(\frac{\bar{c}}{4}\right) m S_A}{1 + \frac{\gamma}{f(K_n)}}$$

$$f(K_n) = \frac{K_n(K_n + 1)}{0.75 + 0.283K_n}$$

$$K_n = \frac{2\lambda}{D_P} = \frac{\lambda}{R_P}$$

K_n - the Knudsen number,
λ – the gas phase mean free path
D_P – the diameter of the particle
R_P – the radius of the particle

$$\nu_A = \frac{d[A]_t}{dt} = \int_{R_{P\min}}^{R_{P\max}} 4\pi R_P^2 F(R_P) \frac{dn}{dR_P} dR_P$$

$$F(R_P) = \frac{D_A([A]_t - [A]_e)}{R_P[1 + f(K_n, \gamma)K_n]}$$

$$f(K_n, \gamma) = \frac{1{,}333 + 0{,}71K_n^{-1}}{1 + K_n^{-1}} + \frac{4(1-\gamma)}{3\gamma}$$

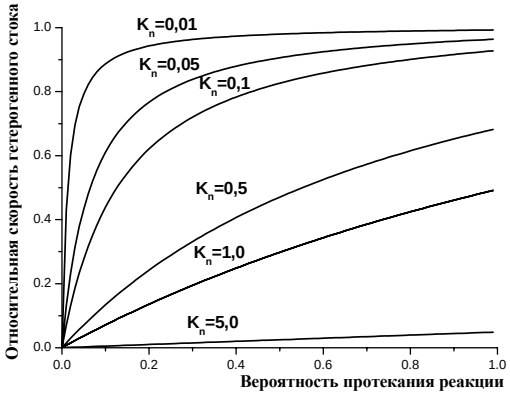

Dependence of rate of Langmuir-Hinshelwood and catalytic reactions on homogeneous and heterogeneous aerosol surfaces on the partial pressure of the gas-phase reactant

Langmuir-Hinshelwood reaction

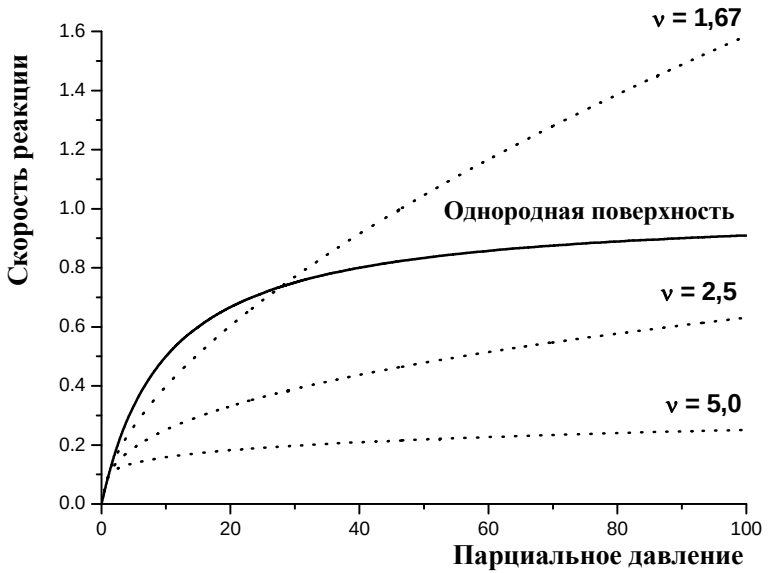

$$\nu_A = \frac{K_A P_A k_{chem}}{1 + K_A P_A}(1 - \Theta_A)$$

$$\Theta_S = K_F P_A^{1/\eta}$$

Catalytic reaction

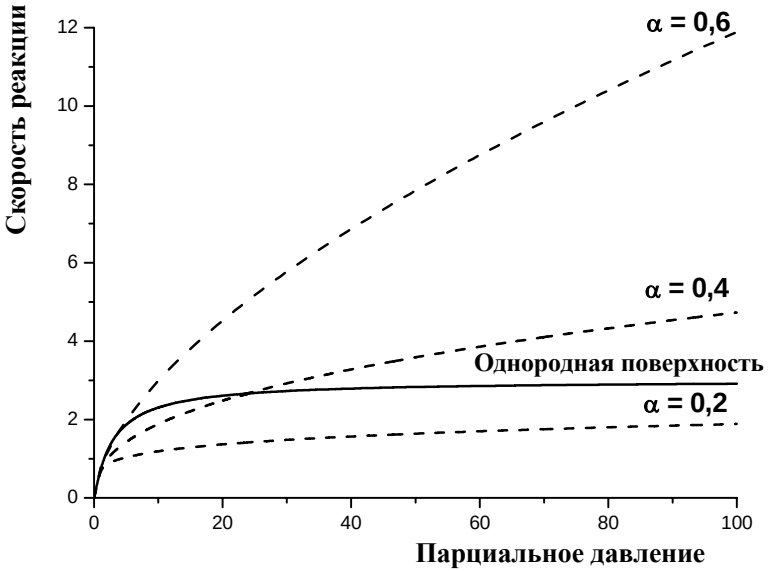

$$\nu_A = \frac{k_1 k_2 P_A}{k_1 P_A + k_2}$$

$$\nu_A = k' P_A^{\alpha}$$

Use of model for discrete heterogeneous surface to describe the uptake kinetics on atmospheric aerosols

For discrete heterogeneous surface: $\gamma_{ef} = \sum_{i=1}^{n} \alpha_{S(i)} \gamma_i$

γ_{ef} – the effective uptake coefficient for whole surface

γ_i – the uptake coefficient by surface compartment i

$\alpha_{S(i)}$ – the part of the i-th compartment in the whole surface

HNO_3 uptake

Gobi desert: $\gamma_0 = 5{,}2 \times 10^{-5}$ (48% Si, 22% Ca, 10% Fe, 10% Al, 2% Mg)

Sahara desert: $\gamma_0 = 2{,}0 \times 10^{-5}$ (80% Si, 1% Ca, 7% Fe, 8% Al,1% Mg)

SiO_2 : $\gamma_0 = 2{,}9 \times 10^{-5}$

α-Al_2O_3: $\gamma_0 = 9{,}7 \times 10^{-5}$

α-Fe_2O_3: $\gamma_0 = 5{,}3 \times 10^{-5}$ (Underwood G.M. et al, 2001)

CaO: $\gamma_0 = 6{,}1 \times 10^{-3}$

MgO: $\gamma_0 = 3{,}7 \times 10^{-4}$

O_3 decomposition: $\gamma_{0(exp(} = 6{,}0 \times 10^{-5}$, $\gamma_{0(est)} = 7{,}2 \times 10^{-5}$ (Michel A.E. et al, 2003) on dust from Sahara

The validity of the approach is confirmed by coincidence of the experimental and estimated uptake coefficients for interaction of O_3 with α-Al_2O_3 surfaces, preliminary treated by SO_2, HNO_3 and with SiO_2 surfaces, preliminary modified by 7-oct-1-enyl and 1-octyl groups, and with the parent oxide surfaces

Kinetic isotherms for chemisorption of organosilicon compounds on surface of surrogates for solid aerosols

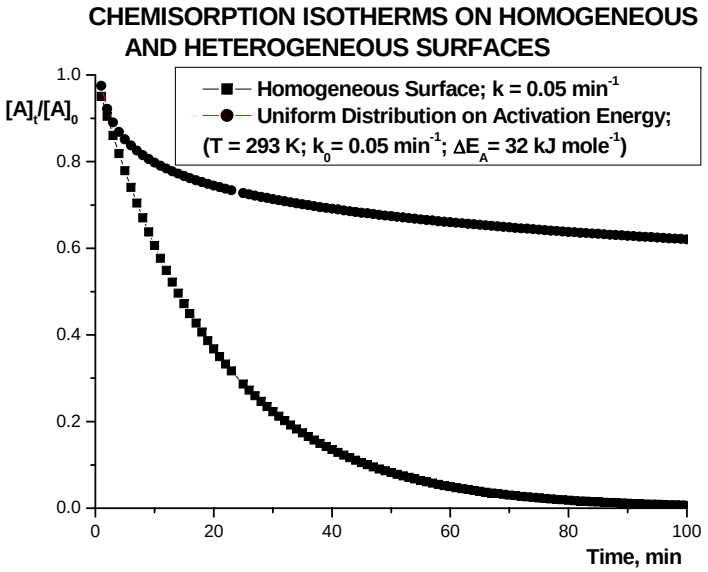

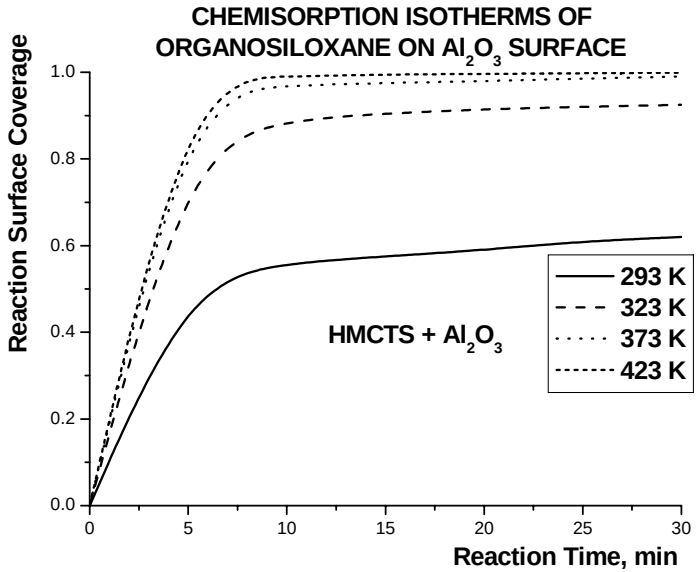

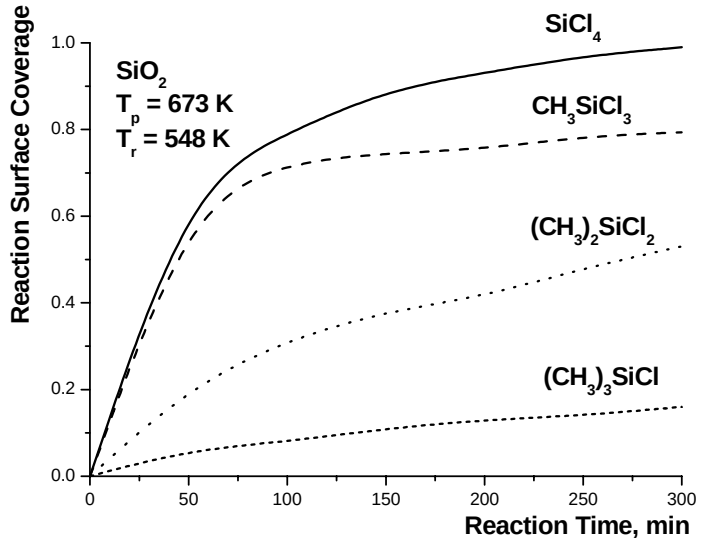

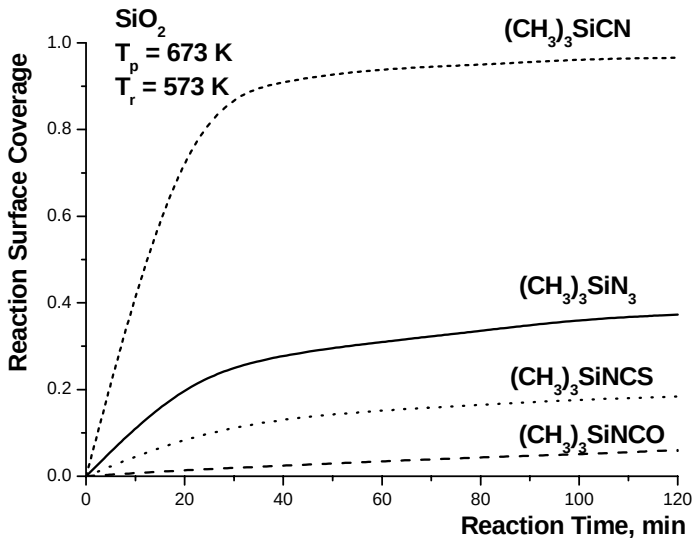

Chemisorption kinetics on amorphous surface

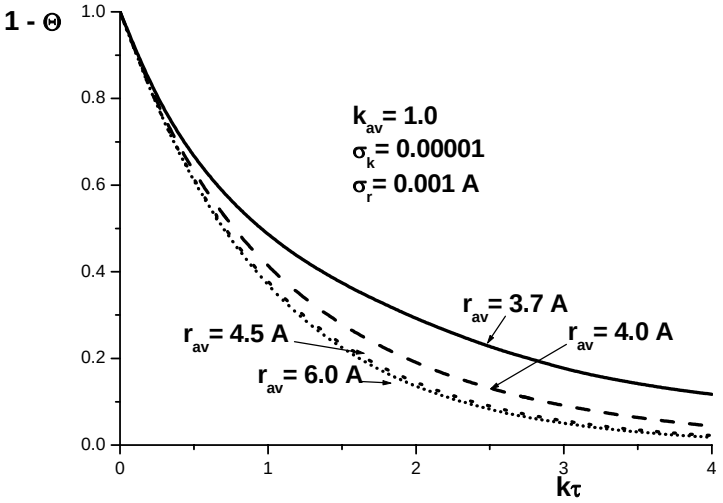

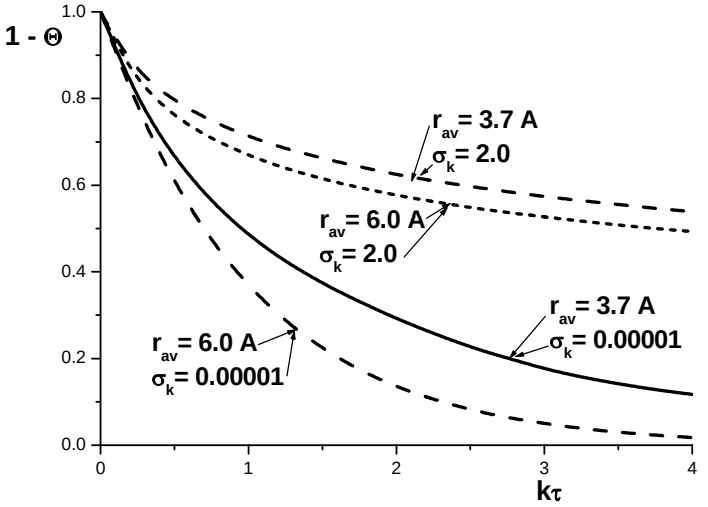

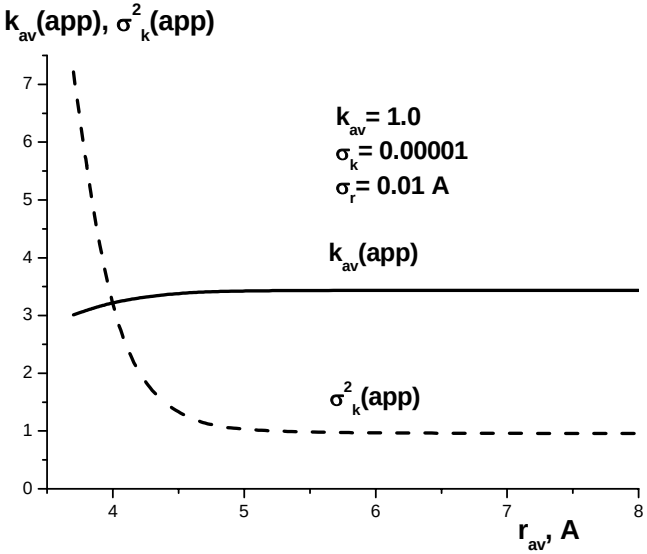

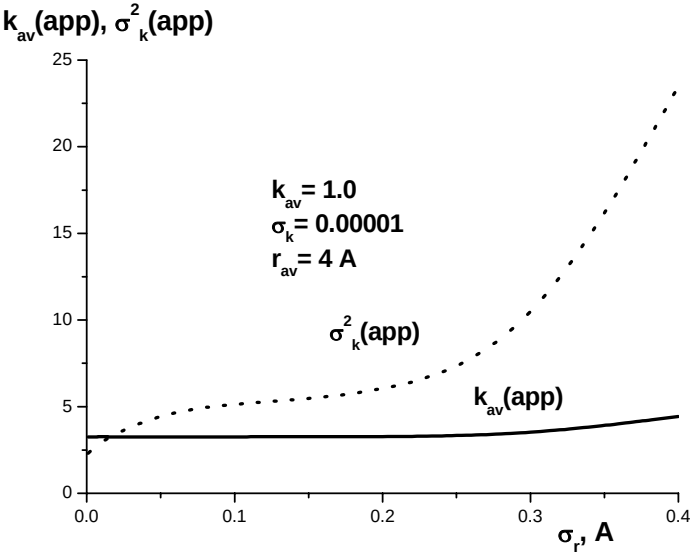

QSARs for chemisorption kinetics on metal oxide surfaces

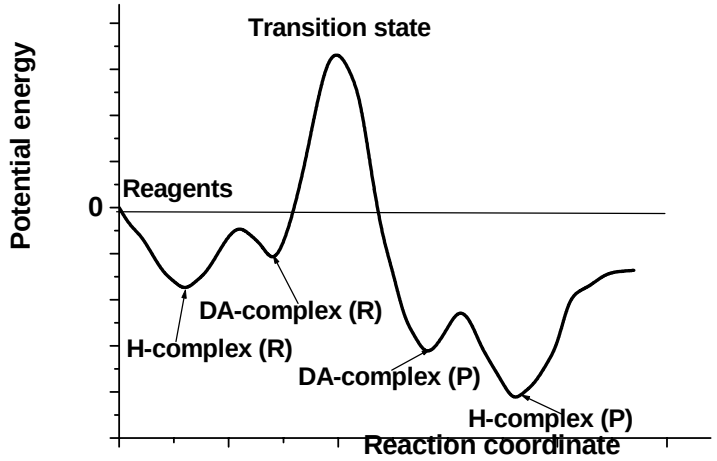

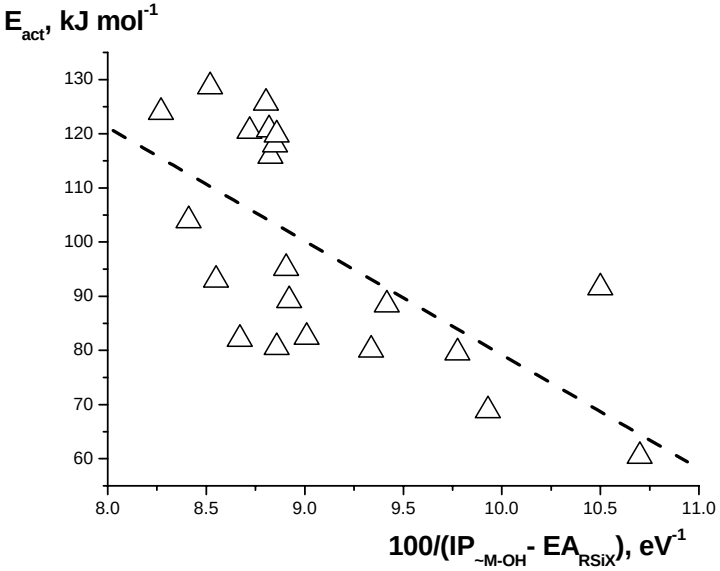

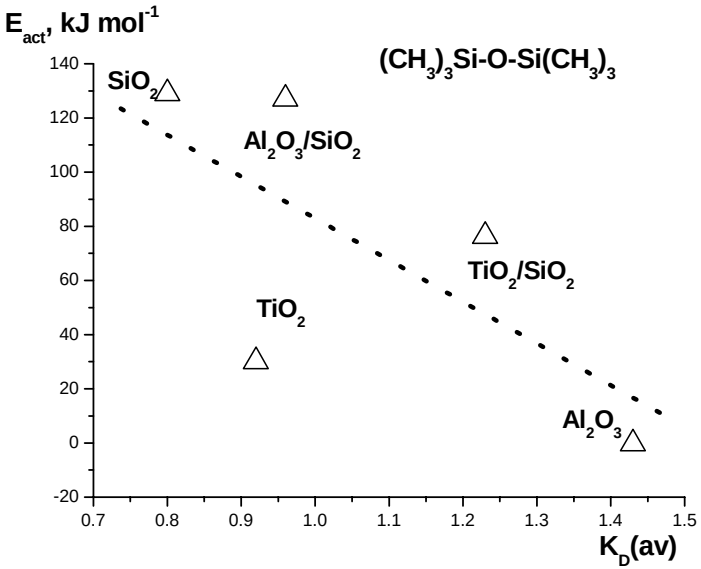

TPD kinetics of water from silica surface

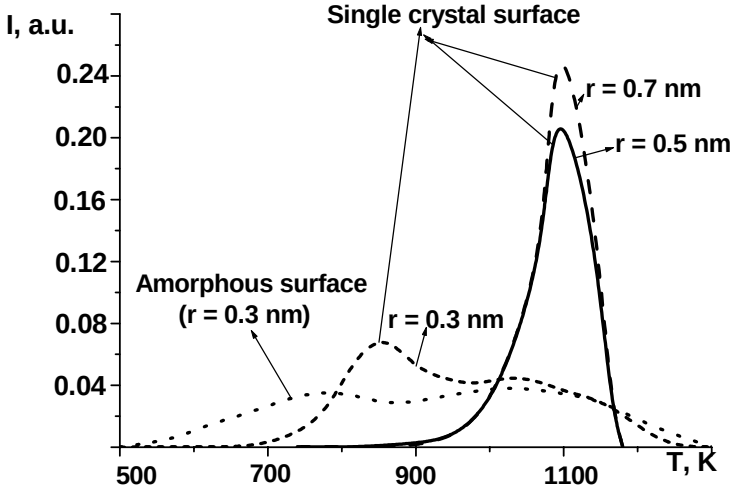

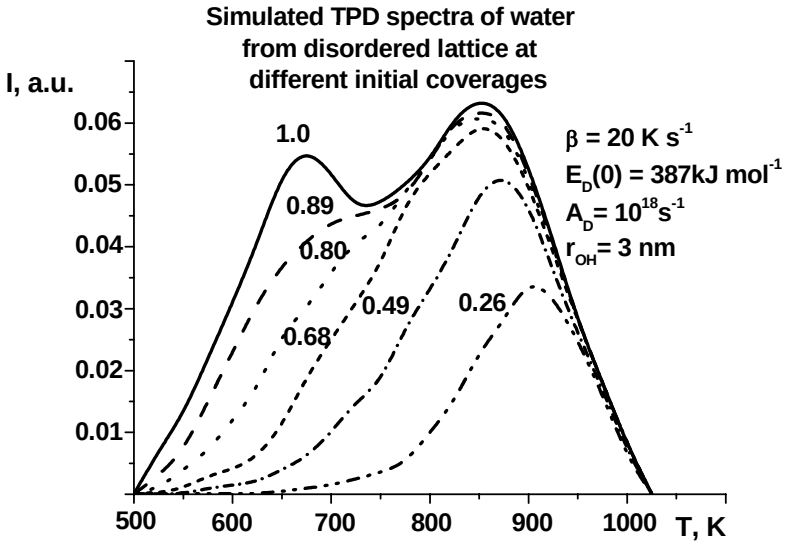

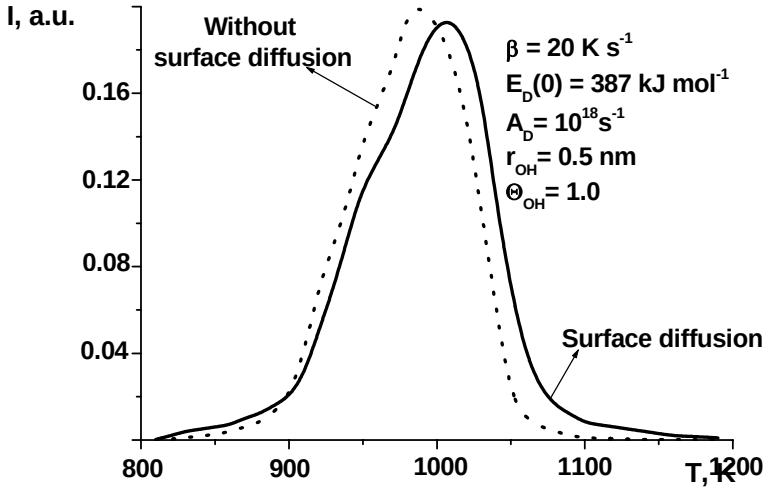

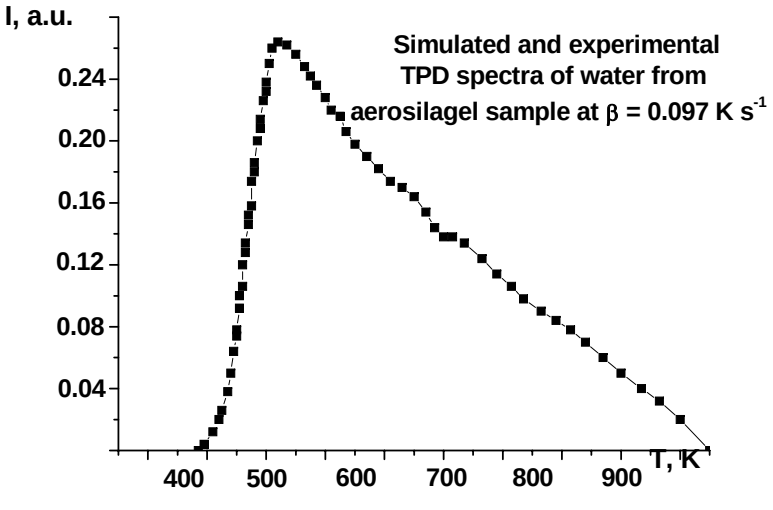

Determination of mesopores size distribution and desorption energy distribution from data of quasi-thermogravimetric analysis of solids

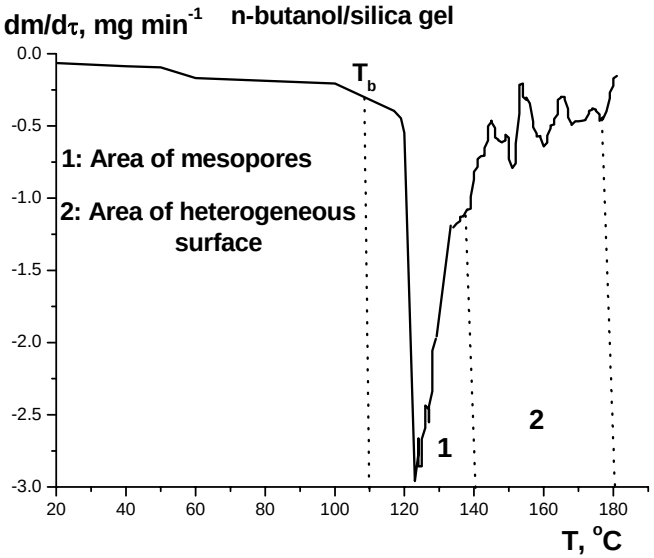

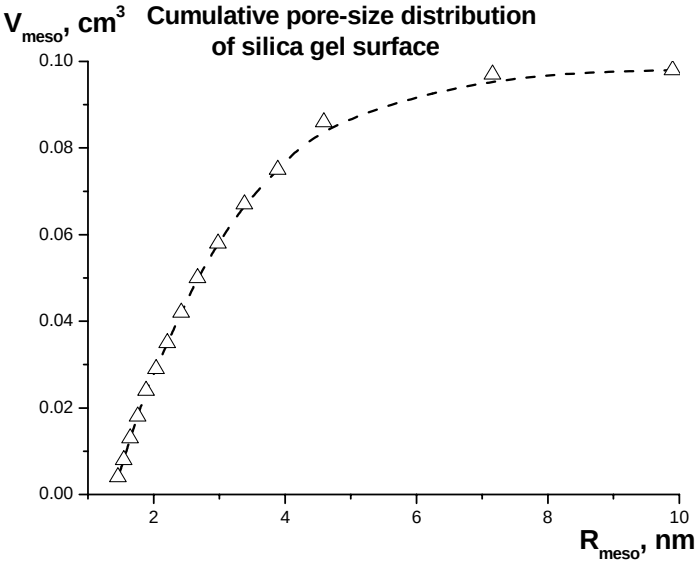

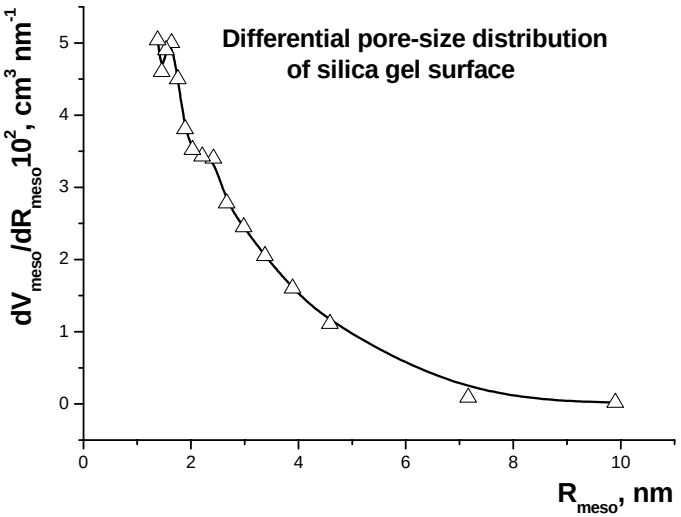

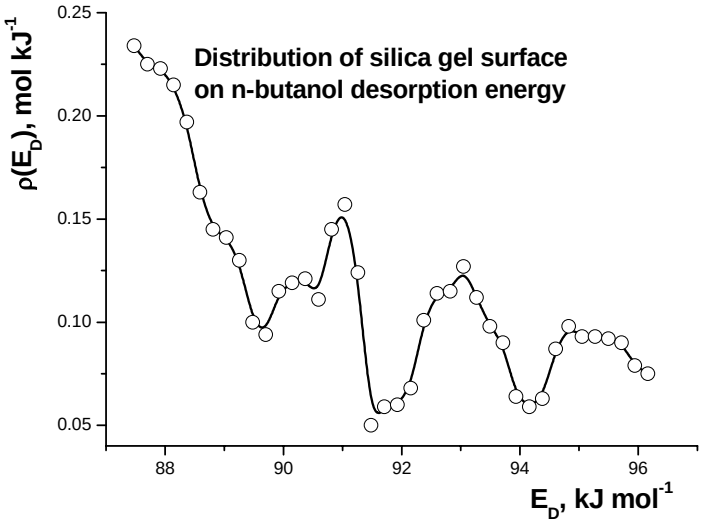

Kinetics of bimolecular photoreaction on silica surface (Py* + DMA)

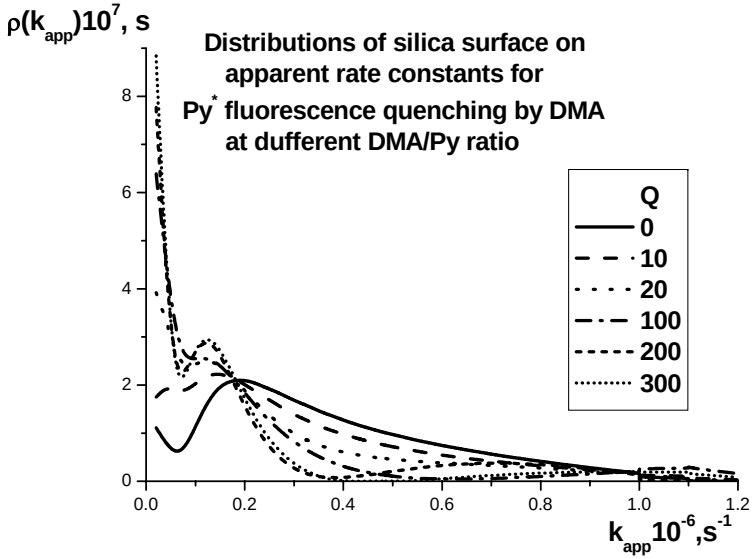

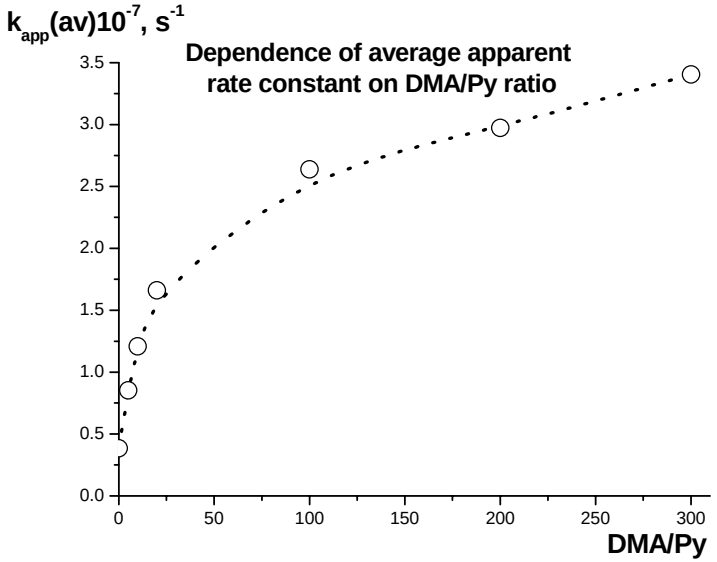

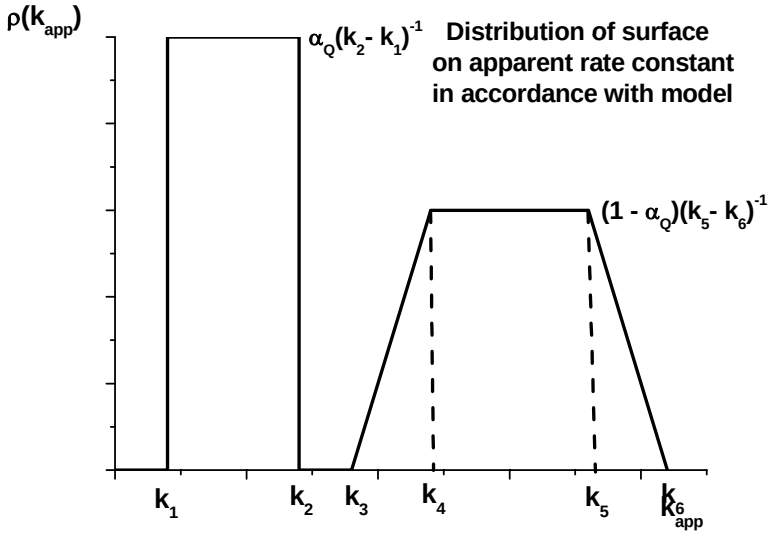

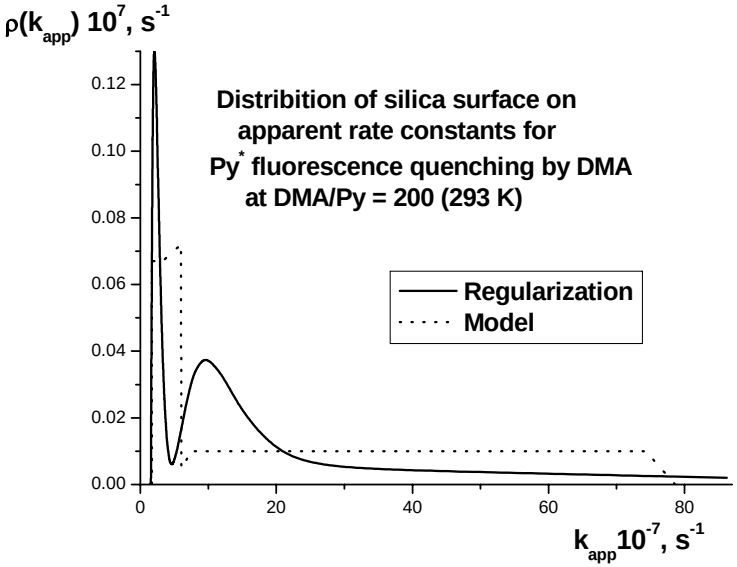

Conclusions

- **Parameters of compensation dependence are calculated for adsorption of VOCs series on the surface of 34 solids and liquids**
- **One-type QSARs for the gas/interface partitioning and its temperature dependencies are proposed and relations between the QSAR's coefficients and the surface characteristics determined by IGC are derived**
- **Coefficients in the QSAR's for 300 different surface components of atmospheric aerosols are calculated**
- **The relationships between experimental and theoretical acid-base descriptors of VOCs were established**
- **Proposed QSARs were extended to describe the VOCs gas/interface partitioning in region of finite surface concentrations for three solids**
- **Models for chemisorption, desorption and bimolecular reaction kinetics on heterogeneous aerosol surface are developed**
- **QSARs for chemisorption of organosilanes and organosiloxanes on the silica and other oxide surfaces are derived**

My acknowledgments:

- Center for Atmospheric Sciences, Cambridge University, UK
- Robert Scott Polar Institute, Cambridge University, UK